NOTICE

The quality of this microform is heavily dependent upon the quality of the original thesis submitted for microfilming. Every effort has been made to ensure the highest quality of reproduction possible.

If pages are missing, contact the university which granted the degree.

Some pages may have indistinct print especially if the original pages were typed with a poor typewriter ribbon or if the university sent us an inferior photocopy.

Previously copyrighted materials (journal articles, published tests, etc.) are not filmed.

Reproduction in full or in part of this microform is governed by the Canadian Copyright Act, R.S.C. 1970, c. C-30.

AVIS

La qualité de cette microforme dépend grandement de la qualité de la thèse soumise au microfilmage. Nous avons tout fait pour assurer une qualité supérieure de reproduction.

S'il manque des pages, veuillez communiquer avec l'université qui a conféré le grade.

La qualité d'impression de certaines pages peut laisser à désirer, surtout si les pages originales ont été dactylographiées à l'aide d'un ruban usé ou si l'université nous a fait parvenir une photocopie de qualité inférieure.

Les documents qui font déjà l'objet d'un droit d'auteur (articles de revue, tests publiés, etc.) ne sont pas microfilmés.

La reproduction, même partielle, de cette microforme est soumise à la Loi canadienne sur le droit d'auteur, SRC 1970, c. C-30.

Canada

A Laboratory Investigation of Local Scour Downstream of Box Culvert Outlets and an Alternative Measure for its Control.

By

Habib Abida

A thesis
presented to the University of Ottawa
in partial fulfillment of the
requirements for the degree of
Master of Applied Science
in
Civil Engineering

Department of Civil Engineering
University of Ottawa
Ottawa, Ontario, Canada, April 1988

ISBN 0-315-46706-1

UNIVERSITÉ D'OTTAWA
UNIVERSITY OF OTTAWA

Abstract

This laboratory study is divided into two main parts:

The first part investigates the local scouring phenomenon that occurs downstream of "box" culverts when the latter discharge their flows directly to sand-bed channels. While culvert hydraulics can include special cases, such as culverts on hydraulically steep slopes where special energy dissipators at outlet must be provided to handle supercritical culvert flows, this study was restricted to culverts on horizontal or mild slopes which operate freely and do not require special energy dissipators at outlet.

The principal factors governing this form of local scouring were found to be the discharge rate, the culvert width, the tailwater depth, the downstream channel width, and the bed material properties. Phase one of the experimental programme investigated the effects of these principal variables on the local scour hole characteristics. This part of the investigation also reviewed some well-known empirical formulas for the prediction of maximum scour depth, under a variety of hydraulic conditions. One of these (Chen's (1970) relationship for maximum scour depth in a stone bed downstream of a culvert outlet) was modified in this study to make it applicable to scour in a sand bed.

The second phase of the study examined a possible alternative means to reduce flow concentration at box culvert outlets with a view to reducing the severity and extent of local scouring in this area. In experiments employing model box culverts a special, pyramidal-shaped bed hump feature was added to the traditional culvert outlet geometry (flared wingwalls) to enhance the rate of spread of the jet-type flow issuing from the model culvert barrels.

The experimentation in this phase of the study was mainly concerned with optimizing the shape and location of the hump feature, such that its impact on near-capacity culvert flows was maximized, with minimal backwater effect. The preferred hump shape was then tested for a wide range of anticipated culvert operating conditions. The unit proved to be very effective in dealing with a "high culvert discharge-low tailwater depth" operating condition, which is clearly the worst scenario in regards to the local scouring phenomenon.

Acknowledgements

Special appreciation is expressed to Dr. D. R. Townsend for his assistance, guidance, and supervision of this research.

The author would also like to thank Mr. Robert Moore for his technical support and assistance with the experimental set-up.

Sincere appreciation is also expressed to the Tunisian Government and the National Science and Engineering Research Council of Canada (Grant # 7443) for providing financial support throughout the author's graduate programme.

Contents

List of Tables

List of Figures

Notations

a_1	=	hump leading length
a_2	=	hump downstream length
B	=	downstream channel width
b	=	vertical distance from the channel bottom to the point where the velocity is half the maximum
b_0	=	height of the jet at the culvert outlet
C_d	=	drag coefficient
C_e	=	the culvert entrance loss coefficient
C_l	=	lift coefficient
d_m	=	effective grain size
d_s	=	maximum depth of scour
d_{50}	=	sediment median grain size
f	=	sand friction factor
F_d	=	drag force
F_l	=	lift force
F_r	=	Froude number
g	=	acceleration due to gravity
H	=	culvert height
H_w	=	headwater depth
h	=	hump height
h_e	=	the culvert entrance loss
h_f	=	friction loss inside the culvert barrel
h_m	=	height of sediment mound
h_v	=	velocity head inside the barrel
H_w	=	headwater depth
K_s	=	"roughness" height of sand
l	=	distance from the downstream end of the culvert barrel to the hump
L	=	distance from culvert outlet to the downstream end of the sediment mound
L_c	=	culvert length
L_s	=	length of scour hole

n	=	pipe roughness coefficient
p	=	mean pressure
Q	=	culvert discharge
Q_i	=	volume rate of sediment being transported into the scour hole
Q_o	=	volume rate of sediment transport out of the scour hole
R	=	hydraulic radius
S	=	culvert slope
s	=	slope of the energy grade line
u	=	mean velocity in the x direction
$\acute{u}$	=	fluctuating velocity in the x direction
U_0	=	jet average velocity in the x direction
v	=	mean velocity in the y direction
$\acute{v}$	=	fluctuating velocity in the y direction
V_s	=	volume of the scour hole
w	=	mean velocity in the z direction
$\acute{w}$	=	fluctuating velocity in the z direction
W	=	culvert width
W_g	=	the weight of a sediment particle
w_h	=	hump width
w_j	=	width of the expanding jet
x	=	axis defining the axial direction of the wall jet
X_c	=	distance from the downstream end of the culvert barrel to the hump crest
X_d	=	distance from outlet to the point of deepest scour
X_w	=	distance from outlet to the point of widest scour
y	=	the axis normal to the horizontal plane
y_b	=	brink depth
y_m	=	vertical distance from the water surface to the point where the velocity is half the maximum
y_t	=	tailwater depth
z	=	the third axis of the coordinate system

ω = sediment fall velocity
ρ_s = the density of the bed material
ρ = the water density
γ_s = sediment specific gravity
γ = fluid specific gravity
μ = fluid dynamic viscosity
ν = fluid kinematic viscosity
σ = sediment gradation
τ_0 = wall or boundary shear stress
τ_l = laminar shear stress
τ_t = turbulent shear stress
δ = shear layer thickness of the vertical velocity profile
δ_1 = surface layer thickness of the vertical velocity profile

Chapter 1

INTRODUCTION

In open channel hydraulics, erosion is referred to as the detachment of sediment particles through the forces generated by flowing water. Generally, the process takes the form of layer erosion,in which a layer of soil over a sloping surface is removed and transported further downstream. This is known as "areal" erosion and the process may extend over large areas. Under special conditions, however, erosion can also be highly concentrated. This local erosion, known in engineering practice as "scouring", can be induced naturally (e.g. at the outside bank of river bends) or artificially (e.g. due to man-made structures such as bridge piers and highway culverts). With regard to the latter example, the local scouring associated with culvert outlet flows results from the unnatural flow concentration produced by the culvert structure (Fig.28(a)). This scouring process might lead to failure of the structure by the process of progressive undermining, especially if

the scour hole moves rapidly upstream. On the other hand, the lateral expansion of the scour hole may result in erosion of the channel banks which has important implications for any nearby properties. Furthermore, the formation of a scour hole can disrupt fish migration, and be a potential danger to small children.

There are basically two methods available to reduce the severity of local erosion downstream of culvert outlets:

1. Better flow distribution to decrease the flow concentration. This is usually attempted by means of a flared outlet section (i.e. using angled wingwalls).

2. Energy dissipation, that is the destruction of a major part of the kinetic energy to reduce the erosive potential of the flow. This is usually accomplished through the use of specially-designed stilling basin structures.

In problem situations both of these techniques might be combined for maximum effect.

The type of outlet structure to be used depends largely on the nature of the flow. For steep slopes the associated high (supercritical) velocities normally require the provision of costly energy dissipating structures which may include, in addition to a protective concrete apron, baffle piers and chute blocks.This, however, is the exception rather than the rule in highway

conduit design, in that mild slopes are normally encountered. As a result the flow is usually subcritical at the conduit outlet and consequently channel stabilization measures are generally less expensive.

It is worth mentioning here that large headwater depths upstream of hydraulically short culverts would also produce supercritical flows. However, again this is the exception rather than the rule for highway culverts.

The approach normally taken to protect against local scouring is to armour, or "rip-rap", those affected portions of the downstream channel's bed and banks. The provision of a layer of coarse granular material on the channel bed, immediately downstream of a culvert outlet, protects that portion of the bed from the concentrated flow issuing from the structure. Ideally this protective layer should either extend from the outlet to the downstream channel section where the expanding jet finally extends across the full width of the channel, or alternatively to a point where the flow concentration is reduced to an acceptable level. It should be emphasized, however, that while the armouring material protects the channel boundaries in the vicinity of the culvert outlet, it does little to lessen the flow concentration in this region.

At present there is no theoretical solution to describe scour satisfactorily. Because of the complexity of the turbulent flow patterns and the sophisticated mechanisms by which the flow entrains an erodible sediment, almost all studies in this area of research are based on experimentation and physical model testing. In the first part of the present study natural

scour in sand beds is investigated by means of a series of experimental tests with different culvert dimensions, sand properties, flow rates, and tailwater levels.

The second part of this research investigates the possible use of a low-profile, pyramidal-shaped bed hump to enhance the rate of expansion of the concentrated outflow. This feature, which is placed on the channel bed in the culvert's outlet section, produces an adverse pressure gradient on the stream's high velocity core region and this results in enhanced lateral spreading of the culvert outflow. The efficiency of such a feature in expanding the jet and reducing the flow velocities is expected to be a function of its geometric properties and its position relative to the outlet.

The principal goal of this research was to investigate the effectiveness of such a unit through experimental observations based on a wide range of flow and tailwater conditions. The bed feature described above was first examined by Dake and Francis (1965) to improve the expansion of a jet issuing from a circular-shaped spillway tunnel. The boundary conditions for the present study, however, are quite different. In this case the topic deals with the so-called "wall" jets emerging from box culverts, where usually the flow can be considered two-dimensional. Furthermore, a tailwater is frequently present in highway culvert operation and this feature tends to enhance the dissipation of kinetic energy of the culvert outflow.

Chapter 2

LITERATURE REVIEW

The scour phenomenon at culvert outlets, being an important consideration facing highway drainage engineers, has been studied extensively in the past. Investigators have attempted to reduce the erosive potential of the culvert outlet flow (and hence limit the severity and extent of local scour) by using channel stabilization measures such as pre-shaped scour holes and rip-rap protection (Smith, 1957 and Hállmark, 1955).

Before dealing with the scouring process in more detail, an understanding of the mechanism by which the bed sediment particles are entrained is required. In defining the starting or incipient motion of the particles, the ASCE committee on sedimentation (task committee, 1966) states that: *"...Water flowing over a bed of sediment exerts forces on the grains that tend to move or entrain them ... When the hydrodynamic force acting on*

a grain of sediment has reached a value that, if increased slightly will put the grain into motion, critical or threshold conditions are said to have been reached".

As was pointed out by Sarikelle and Simon (1980), many researchers attempted to analyze and study the incipient motion of channel bed material but very few have evaluated this effect at culvert outlets. Stevens (1969) described this case of local scouring as follows: *"At a culvert outfall, local scour begins when the flow field produces hydrodynamic forces which put the bed material into motion. Scour ceases when the scour hole has enlarged to such an extent that the hydrodynamic forces have neither sufficient strength nor further contact with the bed or sides of the hole. At this equilibrium scour depth, the material along the boundaries of the hole should be at the point of initiation of motion for a particular flow".*

Any detailed study of the process of local scouring should refer to the general characteristics describing this process as presented by Laursen (1952). The principal characteristics are as follows:

1. The rate of scour is the difference between the sediment rates into and out of the scour hole.
2. The rate of scour decreases as the flow section is enlarged.
3. There is a limiting extent of scour.
4. This limit is approached asymptotically.

Early experimenters investigating localized scour associated with two-dimensional flow field,including Doddiah (1950) and Hallmark (1955), related the depth of scour to the rate of flow, height of fall, tailwater depth, rate of scour, bed material size, sorting process, and "armouring". Firstly they found that scour increases with increasing discharge, since the erosive potential of the flow is associated with the ability of the rate of flow to penetrate or strike the bed material and continuously remove the grains out of the scour hole. An increase in the height of fall, which is related to the velocity and energy of the impinging jet, was found to increase the depth of scour. Regarding the tailwater depth effect, a critical value, for which scour is minimum, was observed. Any change of this optimum tailwater depth caused a greater depth of scour. Furthermore, Hallmark (1955) showed that the depth of scour increases directly with a geometric progression of time. On the other hand, he showed that the scour depth decreases with an increase in grain size. The same researcher also found that a wide variation in the size of bed material caused the bottom of the scour hole to be paved with a progressively coarser material, thereby decreasing the effective fall velocity of the sediment and reducing the scour rate. Finally, the depth of scour was found to decrease considerably with the use of armorplated well-graded materials.

Smith (1957) was one of the first to investigate local scouring below culvert outlets. He observed the development of scour holes below a cantilevered pipe outlet and produced relationships for the scour hole geometry in terms of outlet geometry and flow characteristics. Smith also presented

an analytical method to determine a standard pre-shaped scour hole for a given outlet geometry, design flow, and sediment characteristics. The method proceeded in two steps: (i) determination of the scour hole centre section, and (ii) determination of the other scour hole characteristics for a given set of boundary conditions. Finally, the author suggested the use of graded 'rip-rap' to protect against the local scouring phenomenon and, in connection with this, he supplied important design criteria in terms of size, amount and grading of the armorplate material.

Most research related to scour prevention at culvert outlets deals with non-cohesive bed material only. Very few studies, such as that performed by Abt, Jones and Ruff (1982) on sandy clays, consider cohesive bed material. The Abt et.al. study correlated the scour depth with a parameter, called the"inverted shear parameter", which can be determined by standard soil tests.

The effects of other physical properties of the bed material on scour resistance were also examined by others. Varga (1966) found that the angularity of the bed material increases its resistance to scour due to the interlocking of the particles. On the other hand, as a result of increased exposed surface area, angular bed material is more susceptible to scour. Doddiah (1950) and Hallmark (1955) showed that a well-graded and mixed material shows more resistance to scour than a uniform-sized material. To combine the effect of the material median size and gradation, Stevens (1969)

introduced a parameter, called " Effective grain size ", defined as:

$$d_m = \left[\frac{\sum_i^{10} d_i^3}{10}\right]^{\frac{1}{3}} \tag{2.1}$$

Where :

$$d_i = \frac{d_0 + d_{10}}{2}; i = 1 \tag{2.2}$$

$$d_i = \frac{d_{10} + d_{20}}{2}; i = 2 \tag{2.3}$$

$$\vdots$$

$$d_i = \frac{d_{90} + d_{100}}{2}; i = 10 \tag{2.4}$$

The d_0, d_{10}, ..., d_{100} terms are taken from the "percent finer by weight " vs. "sieve diameter" curve of the bed material.

Stevens proposed the use of the effective grain size as the parameter best describing the bed material properties because it accounts for two important material characteristics, namely the median grain size and gradation. On the other hand, the armouring process causes the finer particles to be removed by the flow and the bed material becomes progressively coarser during the scouring process. This would imply that finer grains in the original bed (before scour) are really not significant and hence the bed material has to be represented by a parameter greater than the median grain size namely the effective grain size. It is also worth noting that any increase in the stone density implies a direct increase in the scour resistance of the bed material. To account for different densities, Simons et al (1970) proposed the use of an "equivalent rock diameter " that can be computed by the ra-

tio $\left(\frac{\gamma_1}{\gamma_2}\right)^{\frac{1}{6}}$ where γ_1 equals 2.7 and γ_2 is the specific gravity of the available material.

The influence of culvert shape on scour development was examined by many researchers including Chen (1970), Ruff (1981) and Abt et al (1987), among others. After performing tests on circular, square, arch and rectangular culverts, the last group concluded that the culvert shape significantly influences the scour hole dimensions and geometry. The authors also observed that the dimensions of the scour hole downstream of circular pipe culverts vary significantly from the scour hole dimensions corresponding to arch, square and rectangular culverts. Mendoza (1980) and Ruff et al (1981) compared scour volumes downstream of circular and square culverts. Taking a diameter equal to the culvert height, they found that the volume of scour downstream of a square culvert is much higher than that for the equivalent circular section. Donnell and Abt (1983) introduced a parameter, called the "modified discharge intensity", (I'_d), to account for the variable flow field geometry associated with the different basic culvert shapes. They defined the modified discharge intensity as:

$$I'_d = \frac{Q}{A(gR)^{0.5}} \tag{2.5}$$

where Q is the discharge, A is the cross-sectional area of flow, g is the gravitational acceleration and R is the pipe hydraulic radius.

Mendoza et al (1983) studied the effect of headwall installation on scour. They found, based on experimentation and data analysis, that a headwall does not affect the maximum scour hole dimensions. They observed, how-

ever, that a headwall, if properly designed, can protect the embankment and prevent undermining of the structure. The authors also correlated the maximum scour hole dimensions to a parameter called the "discharge intensity", $I_d = \frac{Q}{g^{0.5} D^{2.5}}$, and presented a series of empirical equations for both "headwall" and "no headwall" conditions.

Rajaratnam and Diebel (1981) showed that a narrow downstream channel does not significantly affect the depth of scour but rather affects the distance from the outlet to the point where maximum erosion occurs. The effect of side walls on the diffusion of three-dimensional wall jets was also examined by Pani and Dash (1986). They distinguished two zones: zone 1 consisting of the initial portion of the jet, where the effect of lateral boundaries is negligible and zone 2, which is the two-dimensional "decay" zone. Isovel patterns for both zones were shown to be very different from each other.

Another important variable in the analysis of scour hole formation is the effect of repetitions of varying flow rates. Stevens (1969) showed that when scour is allowed at the design discharge, the lower flows can further increase the depth of scour. After a hydrograph sequence of a series of runs, he found that: *"(i) the scour hole depth was increased as the discharge was decreased and, for the sequence of tests, the final scour depth was 44 percent greater than for the initial flow condition. (ii) The scour hole was widened approximately 20 percent by the series of discharges. (iii) Only the highest flow could move rock from the hole onto the mound and the length of the*

hole decreased slightly".

Local scour caused by submerged wall jets was studied by Ali and Lim (1986). The authors studied mainly the effects of changing tailwater depth on scour. They confirmed the existence of a critical tailwater depth value for which scour is minimum and that a change in this depth causes an increase in the depth of scour. The authors also developed a simple method for estimating the boundary shear stress, using the floor velocities, which was found to give a good agreement with that obtained using turbulent boundary layer theory.

Compared with studies investigating scour below circular culverts, very few past studies have dealt with box culverts. One such study, however, was performed by Chen (1970) who correlated scour depth, as well as the other geometric elements of the scour hole with geometry, bed material properties, and flow conditions. Chen presented curves for estimating the geometric characteristics of the scour hole for mild-and steep-sloping rectangular culverts. He also modified Valentin's equation (Valentin, 1967), originally developed for scour downstream of sluice gates, to be applicable for the prediction of scour depths downstream of box culvert outlets.

Many methods have been proposed to control scour at culvert outlets. The purpose of such methods is either to expand the flow to achieve an acceptable velocity distribution, or alternatively to reduce its energy. the latter approach is usually achieved through the use of energy dissipators, either inside the culvert or at its outlet.

One of the well known internal energy dissipators is the "concrete ring" dissipator developed by Wiggert (1972). This unit consists of roughness elements in the form of circular rings placed at the downstream end of the culvert to increase friction and reduce flow velocities. The ring dissipator was found to be quite effective as a velocity reduction of up to 67% was realized in field applications (Wiggert,1972).

Scour control downstream of culvert outlets is generally achieved by riprap protection of the channel bed. The idea of lining the channel bed with a dense loose-placed (stable) material was first introduced by Schoklitsch (1937). Hallmark (1955) showed that a relatively small amount of riprap material substantially decreased the rate of scour.

Excess energy can also be dissipated using modular energy dissipators. Such structures are comprised of precast concrete units that interlock to form rigid stilling basins (Sarikelle and Simon, 1980). These stilling basins can be of different configurations and may be classified as subsurface, above surface and combination-type basins. The basin stability was found to be a function of flow properties, sediment characteristics and both basin and downstream channel dimensions.

Standard stilling basins, including those recommended by the U.S. Bureau of Reclamation (Peterka, 1974), are considered an efficient means of reducing the flow kinetic energy when highly erosive flows are encountered. These basins are developed utilizing the hydraulic jump principle and are designed for specific outlet conditions.

Another method of scour control at culvert outlets is the development of armorplated, pre-shaped stilling basins. This type of basin was first studied by Smith and Hallmark (1960) while investigating the problem of scour in an alluvial stream bed caused by a free-falling jet of water. The authors developed empirical relationships for the geometrical characteristics of the pre-shaped basin (basin diameters at the surface of the stream bed and the bottom of the basin as well as the basin height). Empirical relationships were also developed for the quantity of armorplate in terms of the scour volume and the maximum diameter of the armorplate.

Another factor studied was the influence of downstream channel width on the local scouring process. It was found that, assuming all other conditions remain fixed, local scouring is more severe for wider channels. This is because, for narrow channels, the energy of the eddy is destroyed through frictional resistance with the channel banks, leading to an increased energy transfer to small-scale turbulence which is then transformed into heat.

Chapter 3

THEORETICAL BACKGROUND

In this chapter the theoretical aspects related to the local scouring problem are briefly described. Firstly culvert flows are classified according to whether or not the flow is governed by "inlet" or "outlet" control, and six types of culvert flow are then identified. Following this section is a review of the theory of turbulent wall jets, which is applicable in the case of flows discharging from box culverts. Included in the latter section is a discussion of the constraints that might affect the validity of this theory when localized scour is encountered.

The third section of this chapter deals with incipient motion and the different criteria upon which this concept is based. Analysis of the scour

depth-time function is also described, based on the sediment continuity equation for a scour hole. In the last section a dimensional analysis incorporating all important variables governing the local scouring phenomenon is made to identify the appropriate dimensionless study parameters (i.e for the experimental program).

3.1 Culvert Hydraulics

A great variety of different types of flow can occur in a culvert. The culvert may flow with either a submerged or unsubmerged outlet; it might flow full or part-full over all or part of its length; and the flow can be subcritical, supercritical, or a combination of both, with one or more hydraulic jumps in the barrel. Culvert flow is affected by numerous physical factors, including the barrel length, size, slope, roughness, inlet and outlet geometry and also by hydraulic conditions, such as the depth of headwater, the culvert discharge and the downstream channel capacity. Under certain conditions some of these parameters are more important than others and therefore two major culvert flow categories are distinguished: flows with "inlet control" and flows with "outlet control".

3.1.1 flows with inlet control

Inlet control means that the culvert capacity is controlled at the entrance by the depth of headwater, the barrel cross-sectional area and the type of inlet geometry. Other factors, such as the culvert length, size and slope as well as the tailwater depth in the downstream channel are of less importance.

It is important to note here that the headwater depth (or depth of "ponding") is a very important factor in culvert design. It is equal to the vertical distance from the culvert invert at the entrance section to the energy line of the head pond (i.e. depth + velocity head). However, since velocities are usually low in entrance ponds, the water surface and the energy line are normally assumed to coincide.

3.1.2 flows with outlet control

Outlet control involves the additional consideration of the tailwater elevation in the discharge channel, the slope, roughness and length of the culvert barrel; in this instance the inlet geometry is of less importance. Culverts in outlet control can flow with the culvert barrel running full or part-full, for part of the barrel length or for all of it.

For "outlet control" condition the headwater depth (H_w) is equal to the

summation of the following terms:

$$H_w = h_v + h_e + h_f + h_o - LS \tag{3.1}$$

where h_v is the velocity head inside the barrel, h_e is the entrance loss, h_f is the friction loss, and L ans S are the culvert length and slope respectively. Regarding the parameter h_o, this is either equal to the tailwater depth for the "submerged outlet" condition, or either the tailwater depth or $\frac{(y_c+H)}{2}$ (in which y_c is the critical depth and H is the culvert height) whichever is greater for the "unsubmerged outlet" condition.

3.1.3 types of culvert flow

According to Chow (1987), culvert flow can be classified under 6 categories based on culvert slope, outlet submergence and tailwater level (Fig.(1)). Except for type-1 flow, which corresponds to the "submerged outlet" condition, the other 5 types of culvert flow are characterized by a "free-discharge" (i.e. unsubmerged outlet) condition and flow classification is based on the inlet being submerged. Chow stated that according to laboratory investigations the inlet can be submerged only if the headwater depth exceeds a critical value H^*, while the outlet is not submerged. The value of H^* varies from 1.2 to 1.5 times the height of the culvert, depending on the culvert entrance geometry, barrel characteristics and the approach condition, but is normally taken as 1.5 times the culvert height in preliminary analysis (Chow, 1987).

The following summarizes the main categories of culvert flow shown in Fig.(1):

- Type-1 flow: The outlet is submerged and the culvert barrel flows full.
- Type-2 flow: The headwater $H_w > H^*$ and the tailwater depth $y_t < H$, the culvert height. In this case the culvert barrel also flows full.
- Type-3 flow: Has the same headwater and tailwater conditions as type-2 flow except that the culvert flows partially full.
- Type-4 flow: Both inlet and outlet sections are unsubmerged. The flow is subcritical and the tailwater is relatively high ($y_t > y_c$).
- Type-5 flow: Same conditions as type-4 flow except that the tailwater depth is low ($y_t < y_c$) and the culvert slope is subcritical. The control section is at outlet in this instance.
- Type-6 flow: Same conditions as type-5 flow but the culvert slope is supercritical and therefore the control section is at the culvert inlet.

As this study was restricted to examining culvert operation based on subcritical culvert slopes and, since culvert flows are predominantly "free-surface" in practice, this study dealt, almost exclusively, with types 4 and 5 flows. However some model tests were, in fact, performed under submerged inlet/outlet conditions.

3.2 Turbulent Wall Jets

Wall jets are concentrated jet-type flows, which are encountered in practice, for example, below a sluice gate or downstream of a highway culvert. They can be discharged on a solid boundary, as is usually the case for the sluice gate flow, or on a loose boundary (i.e. channel bed) in the case of culvert flow. The wall jet can be thought of as a two-layer shear flow comprising a boundary layer occupying the lower or "wall" portion of the flow field and a "free mixing" region on top of the former. These fluid layers develop rapidly in the vertical direction and meet a short distance downstream from their point of initiation. Once the two layers meet, the potential core of the jet is consumed and beyond this section, the flow is said to be "fully-developed". In the fully developed region, assuming a uniform flow condition applies, the shape of the velocity profile is the same for all sections (see Fig.(2)).

3.2.1 Equations of motion

The Reynolds' equations in the cartesian system are written as:

$$\frac{\partial u}{\partial t} + u\frac{\partial u}{\partial x} + v\frac{\partial u}{\partial y} + w\frac{\partial u}{\partial z} = -\frac{1}{\rho}\frac{\partial p}{\partial x} + \nu\left[\frac{\partial^2 u}{\partial x^2} + \frac{\partial^2 u}{\partial y^2} + \frac{\partial^2 u}{\partial z^2}\right] - \left[\frac{\partial \overline{u^2}}{\partial x} + \frac{\partial \overline{uv}}{\partial y} + \frac{\partial \overline{uw}}{\partial z}\right] \quad (3.2)$$

$$\frac{\partial v}{\partial t} + u\frac{\partial v}{\partial x} + v\frac{\partial v}{\partial y} + w\frac{\partial v}{\partial z} = -\frac{1}{\rho}\frac{\partial p}{\partial y} + \nu\left[\frac{\partial^2 v}{\partial x^2} + \frac{\partial^2 v}{\partial y^2} + \frac{\partial^2 v}{\partial z^2}\right] - \left[\frac{\partial \overline{\acute{u}\acute{v}}}{\partial x} + \frac{\partial \overline{\acute{v}^2}}{\partial y} + \frac{\partial \overline{\acute{v}\acute{w}}}{\partial z}\right] \quad (3.3)$$

$$\frac{\partial w}{\partial t} + u\frac{\partial w}{\partial x} + v\frac{\partial w}{\partial y} + w\frac{\partial w}{\partial z} = -\frac{1}{\rho}\frac{\partial p}{\partial z} + \nu\left[\frac{\partial^2 w}{\partial x^2} + \frac{\partial^2 w}{\partial y^2} + \frac{\partial^2 w}{\partial z^2}\right] - \left[\frac{\partial \overline{\acute{w}\acute{w}}}{\partial x} + \frac{\partial \overline{\acute{v}\acute{w}}}{\partial y} + \frac{\partial \overline{\acute{w}^2}}{\partial z}\right] \quad (3.4)$$

where the x-axis defines the axial direction of the jet, the y-axis is normal to the horizontal plane, and the z-axis is the third axis of the coordinate system. u,v,w and $\acute{u}$, $\acute{v}$, $\acute{w}$ are the mean and fluctuating velocities in the x, y and z directions respectively, p is the mean pressure at any point, and ν and ρ are the fluid kinematic viscosity and density respectively. The continuity equation is written as:

$$\frac{\partial u}{\partial x} + \frac{\partial v}{\partial y} + \frac{\partial w}{\partial z} = 0 \quad (3.5)$$

To solve these equations, the following simplifying assumptions are introduced:

1. The flow is two-dimensional, i.e. $w = 0$ and $\frac{\partial}{\partial z}$ of any mean quantity is zero.
2. $\overline{\acute{u}\acute{w}} = 0$ and $\overline{\acute{v}\acute{w}} = 0$
3. The flow is steady, i.e. $\frac{\partial u}{\partial t} = 0$ and $\frac{\partial v}{\partial t} = 0$

4. The transverse extent of the flow is small. Thus, $u \gg v$ and velocity and stress gradients in the y-direction are much larger than those in the x-direction.

The equations of motion thus simplify to the following:

$$u\frac{\partial u}{\partial x} + v\frac{\partial u}{\partial y} = -\frac{1}{\rho}\frac{\partial p}{\partial x} + \nu\frac{\partial^2 u}{\partial y^2} - \frac{\partial \overline{\acute{u}\acute{v}}}{\partial y} - \frac{\partial \overline{\acute{u}^2}}{\partial x} \tag{3.6}$$

$$0 = -\frac{1}{\rho}\frac{\partial p}{\partial y} - \frac{\partial \overline{\acute{v}^2}}{\partial y} \tag{3.7}$$

$$\frac{\partial u}{\partial x} + \frac{\partial v}{\partial y} = 0 \tag{3.8}$$

Now, integrate equation (3.7) with respect to y from y to a point located outside the jet.

Thus : $\int_y^\infty \frac{\partial p}{\partial y} = -\rho \int \frac{\partial \overline{\acute{v}^2}}{\partial y}$ or : $p = p_\infty + \rho\overline{\acute{v}^2}$

Substituting into equation (3.6) gives :

$$u\frac{\partial u}{\partial x} + v\frac{\partial u}{\partial y} = -\frac{1}{\rho}\frac{dp_\infty}{dx} + \nu\frac{\partial^2 u}{\partial y^2} - \frac{\partial \overline{\acute{u}\acute{v}}}{\partial y} - \frac{\partial}{\partial x}\left(\overline{\acute{u}}^2 - \overline{\acute{v}}^2\right) \tag{3.9}$$

Now $\frac{\partial}{\partial x}\left(\overline{\acute{u}}^2 - \overline{\acute{v}}^2\right)$ is small compared to the other terms. Hence, it can be neglected and the following equation is obtained :

$$u\frac{\partial u}{\partial x} + v\frac{\partial u}{\partial y} = -\frac{1}{\rho}\frac{dp_\infty}{dx} + \nu\frac{\partial^2 u}{\partial y^2} - \frac{\partial \overline{\acute{u}\acute{v}}}{\partial y} \tag{3.10}$$

The turbulent shear stress $\tau_t = -\rho\overline{\acute{u}\acute{v}}$. Thus $\overline{\acute{u}\acute{v}} = -\frac{1}{\rho}\tau_t$. Substituting this in equation (3.10) gives :

$$u\frac{\partial u}{\partial x} + v\frac{\partial u}{\partial y} = -\frac{1}{\rho}\frac{dp_\infty}{dx} + \nu\frac{\partial^2 u}{\partial y^2} + \frac{1}{\rho}\frac{\partial \tau_t}{\partial y} \tag{3.11}$$

Neglecting the effect of any longitudinal pressure gradient equation (3.11) reduces to :

$$u\frac{\partial u}{\partial x}+v\frac{\partial u}{\partial y}=\nu\frac{\partial^2 u}{\partial y^2}+\frac{1}{\rho}\frac{\partial \tau_t}{\partial y} \tag{3.12}$$

On the basis of experimental observations (Forthmann, 1934), it was found that $\frac{u}{u_m}=f\left(\frac{y}{b}\right)=f(\eta)$ where $\eta=\frac{y}{b}$. Further, assume that: $\frac{\tau}{\rho u_m^2}=g(\eta)$. Now the continuity equation is expressed as : $\frac{\partial u}{\partial x}+\frac{\partial v}{\partial y}=0$. Or $\frac{\partial v}{\partial y}=-\frac{\partial u}{\partial x}$; hence $v=\int_0^y -\frac{\partial u}{\partial x}dy$. Since $\frac{\frac{\partial u}{u_m}}{\partial x}=\frac{u_m\frac{\partial u}{\partial x}+u\frac{\partial u_m}{\partial x}}{u_m{}^2}$, $\frac{\partial u}{\partial x}$ can be expressed as:

$$\frac{\partial u}{\partial x}=u_m\frac{\partial\left(\frac{u}{u_m}\right)}{\partial x}+\frac{u}{u_m}\frac{\partial u_m}{\partial x} \tag{3.13}$$

Or :

$$\frac{\partial u}{\partial x}=u_m\frac{\partial f\left(\frac{y}{b}\right)}{\partial x}+f\left(\frac{y}{b}\right)\frac{\partial u_m}{\partial x} \tag{3.14}$$

$\frac{\partial f\left(\frac{y}{b}\right)}{\partial x}$ can be written as :

$$\frac{\partial f\left(\frac{y}{b}\right)}{\partial x}=\frac{\partial f\left(\frac{y}{b}\right)}{\partial\left(\frac{y}{b}\right)}\times\frac{\partial\left(\frac{y}{b}\right)}{\partial x} \tag{3.15}$$

Thus :

$$\frac{\partial f\left(\frac{y}{b}\right)}{\partial x}=\frac{df}{d\eta}\times\frac{\left[b\left(\frac{dy}{dx}\right)-y\frac{db}{dx}\right]}{b^2} \tag{3.16}$$

But since $\frac{dy}{dx}=0$, this reduces to :

$$\frac{\partial f\left(\frac{y}{b}\right)}{\partial x}=-\left(\frac{y}{b^2}\right)\frac{db}{dx}\frac{df}{d\eta} \tag{3.17}$$

Substituting into equation (3.14) gives:

$$\frac{\partial u}{\partial x}=\frac{-yu_m}{b^2}\dot{b}\dot{f}+u'_m f(\eta) \tag{3.18}$$

Thus :

$$V = \int_0^y -\frac{\partial u}{\partial x} dy = \int_0^y \left[\frac{y u_m}{b^2} \dot{b} f' - u'_m f \right] dy \qquad (3.19)$$

Writing η for $\frac{y}{b}$ gives :

$$V = u_m \dot{b} \int_0^\eta \eta f' d\eta - b U'_m \int_0^\eta f d\eta \qquad (3.20)$$

Using these expressions the equation of motion reduces to the following form :

$$\dot{g} = \frac{b u'_m}{u_m} \left[f^2 - f' \int_0^\eta f d\eta \right] - \dot{b} \left(\eta f f' - f' \right) - \frac{\nu}{u_m b} f'' \qquad (3.21)$$

In most of the wall-jet problems of practical interest, $\frac{u_m b}{\nu}$ is large and therefore the last term in equation (3.21) can be neglected without adversely affecting overall accuracy.

For similarity, it is required that :

$$\frac{b u'_m}{u_m} \propto x^0 \qquad (3.22)$$

$$\dot{b} \propto x^0 \qquad (3.23)$$

If $u_m \propto x^p$,and $b \propto x^q$ then from equation (3.23) $q = 1$

To solve for the other exponent p, one more equation is needed.

3.2.2 Integral Momentum Equation

From equation (3.11) :

$$u \frac{\partial u}{\partial x} + v \frac{\partial u}{\partial y} = -\frac{1}{\rho} \frac{dp}{dx} + \frac{1}{\rho} \frac{\partial \tau_t}{\partial y} + \frac{1}{\rho} \frac{\partial}{\partial y} \left(\mu \frac{\partial u}{\partial y} \right) \qquad (3.24)$$

Substituting the laminar shear stress (τ_l) for $\mu\frac{\partial u}{\partial y}$ and neglecting the pressure gradient gives :

$$u\frac{\partial u}{\partial x}+v\frac{\partial u}{\partial y}=\frac{1}{\rho}\frac{\partial \tau_t}{\partial y}+\frac{1}{\rho}\frac{\partial \tau_l}{\partial y} \tag{3.25}$$

Note that in free turbulent flows τ_t is much larger than τ_l because of the absence of solid boundaries and hence it is reasonable to neglect τ_l. Thus :

$$u\frac{\partial u}{\partial x}+v\frac{\partial u}{\partial y}=\frac{1}{\rho}\frac{\partial \tau_t}{\partial y} \tag{3.26}$$

and therefore :

$$\int_0^\infty \rho u\frac{\partial u}{\partial x}dy+\int_0^\infty \rho v\frac{\partial u}{\partial y}dy=\int_0^\infty \frac{\partial \tau_t}{\partial y}dy \tag{3.27}$$

The first term of equation (3.27) can be written as :

$$\rho\int_0^\infty u\frac{\partial u}{\partial x}dy=\frac{1}{2}\int_0^\infty \frac{\partial}{\partial x}\left(\rho u^2\right)dy=\frac{1}{2}\frac{d}{dx}\int_0^\infty \rho u^2 dy \tag{3.28}$$

Regarding the second term :

$$\rho\int_0^\infty v\frac{\partial u}{\partial x}dy=\rho\left[|uv|_0^\infty-\int_0^\infty u\frac{\partial v}{\partial y}dy\right] \tag{3.29}$$

At $y=0$, $v=0$ and at $y=\infty$, $u=0$. Thus : $|uv|_0^\infty=0$.

On the other hand, from the continuity equation $\frac{\partial v}{\partial y}=-\frac{\partial u}{\partial x}$.

Making these substitutions in equation (3.29) gives:

$$\rho\int_0^\infty v\frac{\partial u}{\partial x}dy=\rho\int_0^\infty u\frac{\partial u}{\partial x}dy=\frac{1}{2}\frac{d}{dx}\int_0^\infty \rho u^2 dy \tag{3.30}$$

Considering the right hand side term of equation (3.26)

$$\int_0^\infty \frac{\partial \tau_t}{\partial y}dy=|\tau|_0^\infty=\tau(\infty)-\tau(0)=-\tau_0 \tag{3.31}$$

where τ_0 is the wall shear stress.

Substituting all the terms by their values in equation (3.27) gives :

$$\frac{d}{dx}\int_0^\infty \rho u^2 dy = -\tau_0 \qquad (3.32)$$

As a first approximation, if τ_0 is neglected equation (3.32) becomes :

$$\frac{d}{dx}\int_0^\infty \rho u^2 dy = 0 \qquad (3.33)$$

Equation (3.33) can also be written as :

$$\frac{d}{dx}\int_0^\infty \rho\left(\frac{u}{u_m}\right)^2 {u_m}^2 dy = \frac{d}{dx}\rho {u_m}^2 b\int_0^\infty f^2 d\eta \qquad (3.34)$$

which gives ${u_m}^2 b \propto x^0$. But as stated previously :$u_m \propto x^p$ and $b \propto x^q$. Thus $2p + q = 0$; and since $q = 1$ (equation 3.23), then $p = -0.5$.

Now, instead of neglecting τ_0 in equation (3.32), assume $\tau_0 \propto x^s$. Then $\frac{d}{dx}\rho {u_m}^2 b\int_0^\infty f^2 d\eta \propto x^s$, or $2p + q - 1 = s$, which gives $2p = s$.

If the first approximation $p = -0.5$ is accepted, then $s = -1$, which implies that τ_0 decreases inversely with x.

In conclusion for the plane turbulent wall jet : $u_m \propto \frac{1}{\sqrt{x}}$; $b \propto x$; and $\tau_0 \propto \frac{1}{x}$.

Based on experimental observations on the decay of the velocity scale by Rajaratnam and Subramanya (1967), it was found that : $\frac{u_m}{u_o} = \frac{3.5}{\sqrt{\frac{x}{b_o}}}$ for $\frac{x}{b_o}$ at least up to 100 and $b = 0.068x$

Finally, it is worth noting that for rough surfaces the velocity distribution follows the familiar "log" law in the boundary layer and is almost the same as for smooth walls in the free mixing region.

This "wall jet" theory however was developed for a "fixed boundary" condition, which is not the case when localized scour is encountered. In the latter case, the boundary is rather loose and irregular due to the continuous development of scour and deposition downstream. In addition, the existence of secondary currents at both sides of the channel and within the scour hole also affects the validity of this theory.

3.3 Incipient Motion

Consider a channel bed consisting of loose and cohesionless solid particles of uniform size. Because of the water flow on the bed, hydrodynamic forces, proportional to the flow intensity, are generated on the sand grains. Under these circumstances, a condition is eventually reached where the particles can no longer resist these hydrodynamic forces and therefore they start to move. This movement, however, is not instantaneous for all particles as some might move while others are still at rest. This is mainly explained by the stochastic nature of the problem and the structure of "wall" turbulence.

The incipient condition (i.e. initial movement of the bed) is determined by observations, which makes the definition very subjective. In fact, it can be defined in several ways:

1. With critical velocity equations determining the critical bottom velocity at which erosion first occurs. [This approach to define

incipient motion, however, was criticized by many researchers because of a lack of a good definition of the bottom velocity and the difficulties encountered in measuring it accurately].

2. With critical shear stress equations incorporating the frictional drag of the flow on the sediment particles.
3. Employing a lift force criterion; i.e. considering pressure differences generated across a sand grain due to the vertical velocity gradient.

Even though these approaches may appear to be different at first glance, they are not totally different from each other.

3.3.1 "Incipient motion" condition

The incipient motion condition for cohesionless, loose particles on a streambed is described by:

$$\tan\phi = \frac{F_t}{F_n} \tag{3.35}$$

where F_t and F_n are the forces parallel and normal to the angle of repose of the material ϕ respectively (see Fig.(3)). The particle is subjected to three forces: its submerged weight (W_g), the hydrodynamic drag (F_d) and the lift force (F_l).

Thus:

$$F_t = W_g \sin\alpha + F_d \tag{3.36}$$

and

$$F_n = W_g \cos\alpha - F_l \tag{3.37}$$

where α is the channel bed slope at which incipient sediment movement occurs. Hence equation (3.35) can be written as:

$$\tan\phi = \frac{W_g \sin\alpha + F_d}{W_g \cos\alpha - F_l} \tag{3.38}$$

Now the drag and lift forces can be expressed as :

$$F_d = C_d K_1 d^2 \rho \frac{{u_b}^2}{2} \tag{3.39}$$

$$F_l = C_l K_2 d^2 \rho \frac{{u_b}^2}{2} \tag{3.40}$$

where C_d and C_l are drag and lift coefficients respectively, K_1 and K_2 are particle shape factors, d is the particle diameter, ρ is the fluid density, and u_b is the fluid velocity near the channel bed.

Regarding the submerged weight (W_g), this can be expressed as:

$$W = K_3(\rho_s - \rho)gd^3 \tag{3.41}$$

Where K_3 is another particle shape factor and ρ_s is the dry sediment density.

Substituting equations (3.39) (3.40) and (3.41) into equation (3.38) yields the following:

$$\frac{{u_b}^2}{(\frac{\rho_s}{\rho} - 1)gd} = \frac{2K_3(\tan\phi\cos\alpha - \sin\alpha)}{C_d K_1 + C_l K_2 \tan\phi} \tag{3.42}$$

According to Forchheimer (1914), the tractive force per unit surface can be written as:

$$\tau_0 = \gamma R s = K_4 {u_b}^2 \tag{3.43}$$

where R is the hydraulic radius, s is the slope of the energy grade line and K_4 a constant.

Introducing equation (3.43) into equation (3.42) yields :

$$\frac{\tau_0}{(\gamma_s - \gamma)d} = \frac{K_4}{\rho}\frac{2K_3(\tan\phi\cos\phi - \sin\alpha)}{C_d K_1 + C_l K_2 \tan\phi} = A \qquad (3.44)$$

where A is a sediment coefficient.

For the special case of uniform-sized grains on a flat bed, this sediment coefficient is a function of the so-called "shear Reynolds number" $R_{e_*} = \frac{du_*}{\nu}$, in which u_* is the shear velocity and ν is the fluid kinematic viscosity.

Hence equation (3.44) can be written as:

$$\frac{\tau_0}{(\gamma_s - \gamma)d} = \Phi\left(\frac{du_*}{\nu}\right) \qquad (3.45)$$

3.3.2 Shields' diagram

Equation (3.45) was established by Shields in 1936 and is represented graphically as Fig.(4).

This figure may be divided into three zones:

- (i) A zone characterized by a shear Reynolds number less than two, where the particle diameter d is less than the laminar sub-layer. The movement in this region is mainly due to viscous action and is independent of turbulent forces.

- (ii) A transition zone, where the particle diameter is approximately equal to the laminar sublayer. The transition portion of the curve has a minimum $\frac{\tau_0}{(\gamma_s-\gamma)d} = 0.03$, which occurs at $R_{*} = 10$. According to the diagram, no particle movement below this value can ever occur.

- (iii) In the third zone the particle diameter is much larger than the laminar sublayer. The dimensionless shear stress $\frac{\tau_0}{(\gamma_s-\gamma)d}$ is independent of the shear Reynolds number and is found to be approximately 0.06. The shear Reynolds number associated with this zone exceeds 400, which implies a particle diameter of at least 0.26 inches to ensure stability.

Shields' relationship has been checked by many experimenters in the past and is generally considered to be reliable. Very recently, however, it was shown that the so-called "threshold" condition does not in fact exist, even for a uniform-sized material (Lavelle and Mofjeld, 1987). Experiments have been performed which demonstrate that occasional transport can occur at very low Shields stress values providing that a sufficient test duration is allowed. The conclusion, therefore, is that there is no stress below which all particles are at rest and the threshold condition corresponds to a small but finite value of transport. Accordingly, it is suggested that particle erosion and transport should be viewed as a probabilistic phenomenon where the bed stresses are considered as distributed properties and an instantaneous stress in the turbulent flow can set individual particles in motion.

3.4 Analysis of the Scour Depth-Time Function

The aim of any study of the local scouring problem is to solve the sediment continuity equation:

$$\frac{dV_s}{dt} = Q_s - Q_i \tag{3.46}$$

Where $\frac{dV_s}{dt}$ is the rate of change of the volume of sand removed from the scour hole, Q_s is the volume rate of sediment transport out of the scour hole and Q_i is the volume rate of sediment being transported into the scour hole.

The problem, however, is very hard to solve analytically because of the complexity of the non-steady flow patterns and the mechanisms by which an erodible sediment is entrained. Rather the problem is examined experimentally, which leads to empirical relationships between the significant variables affecting the flow, the bed properties and the scour hole characteristics. Altinbilek and Basmaci (1980) suggested an empirical relationship for Q_s. They showed experimentally that the volume of the scour hole can be closely approximated by a triangular profile function which gives the scour volume as:

$$V_s = \frac{2Bd_s^2}{\tan\phi} \tag{3.47}$$

Where B is the inlet width of a two-dimensional channel, d_s is the maximum depth of scour and ϕ is the angle of repose of the sediment.

They also determined an empirical relationship for the scour depth, as the time approaches infinity.

$$\frac{d_{s\infty}}{b} = \left(\frac{\tan\phi}{\frac{d_{50}}{b}}\right)^{\frac{1}{2}} \left(\frac{U_0}{gb(\gamma_s - 1)^{\frac{1}{2}}}\right)^{\frac{3}{2}} \tag{3.48}$$

Where b is the wall jet thickness at the section of the vena contracta d_{50} is the median size of the sediment, g is the acceleration due to gravity, U_0 is the jet mean velocity, and γ_s is the sediment specific gravity.

The sediment transport rate Q_s is given by:

$$\frac{Q_s}{U_0 d_{50} B} = f\left(\frac{C_d N_s^2}{8.2} - \tan\phi\right) \tag{3.49}$$

where C_d is the drag coefficient of a particle falling in a quiescent fluid, N_s is a sediment number equal to $\left[\frac{U_0}{(gd_{50}(\gamma_s-1))^{\frac{1}{2}}}\right]$ and f is a function of $\frac{d_m}{b}$, N_s, $\frac{d_{50}}{b}$ and $\tan\phi$.

Once the function f is determined, Q_s can be found or calculated and a relationship for the time of scour action can be obtained using equation (3.46).

3.5 Dimensional Analysis

Scour geometry depends on many variables characterizing the culvert, the bed material and the flow. These variables are: the culvert width W, the downstream channel width B, the tailwater depth y_t, the culvert slope S, the culvert length L, the culvert height H, the

pipe roughness coefficient n, the brink depth y_b, the effective particle size of the bed material d_m, the volume flow rate Q, the entrance loss coefficient C_e, the density of the bed material ρ_s, the water density ρ, the dynamic viscosity of the water μ, and the acceleration due to gravity g. Thus if X represents any dimension of the scour hole then:

$$X = \Phi(W, B, y_t, S, L, H, n, y_b, d_m, Q, C_e, \rho_s, \rho, \mu, g) \qquad (3.50)$$

However, for the purpose of this study some of these variables can be disregarded and only the most significant ones are preserved. First, S=0 since the culvert is horizontal. Furthermore, the entrance coefficient C_e is not included because the study is limited to only one type of pipe entrance. The culvert length is eliminated since the model culvert length is too short to affect the flow and the water viscosity, μ, is also disregarded since it is constant. Since both water and sand densities are also constant, they too can be dropped. Finally, the same pipe material is used for all experiments and thus the roughness coefficient n can be eliminated in the analysis.

As a result of these decisions, equation (3.50) simplifies to:

$$X = \Phi(W, B, y_t, H, y_b, d_m, Q, g) \qquad (3.51)$$

Upon performing dimensional analysis on equation (3.51), the following non-dimensional terms are obtained:

$$X = \Phi(\frac{B}{W}, \frac{y_t}{H}, \frac{y_b}{H}, \frac{d_m}{H}, \frac{Q}{g^{\frac{1}{2}} W H^{\frac{5}{2}}}) \qquad (3.52)$$

In the last term, however, g is dropped for convenience and thus:

$$X = \Phi\left(\frac{B}{W}, \frac{y_t}{H}, \frac{y_b}{H}, \frac{d_m}{H}, \frac{Q}{WH^{\frac{3}{2}}}\right) \qquad (3.53)$$

Chapter 4

EXPERIMENTAL PROGRAM

This chapter consists of four parts. The first section contains descriptions and results of tests performed to determine the physical properties of the four types of sand (W,X,Y,Z) used in the experimental program. The physical properties determined were: average particle size (d_{50}), effective grain size (d_m), gradation (σ), specific gravity (γ), fall velocity (ω), and angle of repose (ϕ). The second section of this chapter describes the experimental apparatus used. The third section is devoted to the weir and velocity current meter calibration and the final section describes the experimental procedure adopted.

4.1 Material Physical Properties

4.1.1 Description of material

The sand used in most of the experiments was uniform white silica sand. For comparison purposes, however, several additional experiments were performed using a well-graded grey sand (type X in Table 1). It was decided to use a uniform-sized material in the experimental program because this is known to cause a more severe scour condition than well-graded sand would produce under the same hydraulic conditions (Doddiah, 1950 and Hallmark, 1955). Accordingly, in this study, any design criteria established to reduce the local scouring associated with culvert outlet flows, would tend to err on the conservative side.

4.1.2 Average particle size

Mechanical sieving was performed on samples of the four types of sand and representative grain size distribution curves ("percentage finer by weight" vs."sieve opening") were obtained for each type of material (Fig.(5)). From these curves the average particle sizes (d_{50}), defined as the size for which 50% is finer by weight, were determined.

4.1.3 Effective grain size

As will be shown later, this parameter is adopted in most studies dealing with the investigation of scour because it is believed to be better correlated to the scour hole geometric properties than the average particle size, (d_{50}) (Stevens,1969).

As can be seen from Table 4.1, which summarizes all sand properties, the effective grain size (d_m) is usually larger than the average particle size (d_{50}). This is explained by the fact that during the scouring process, the fine particles are transported downstream and the bed material becomes progressively coarser, which in turn makes its representative grain size greater than the original average particle size. This natural process is referred to as "bed armouring".

4.1.4 Gradation

The parameter σ, which is a measure of the sand gradation, was estimated as : $\sigma = \frac{1}{2}\left[\frac{d_{84}}{d_{50}} + \frac{d_{50}}{d_{16}}\right]$ where d_{84}, d_{50} and d_{16} are the sizes for which 84, 50 and 16% respectively are finer by weight and are determined from the grain size distribution curves.

4.1.5 Specific gravity

The specific gravity for each type of sand was determined as follows : a sand sample was weighed and then poured into a known volume of water in a graded cylinder. This resulted in a rise in the water surface elevation within the cylinder, thereby allowing the volume of the sand sample to be estimated. Knowing the mass and volume, the specific gravity for sands W,X,Y and Z was calculated to be 2.52, 2.48, 2.71 and 2.67 respectively.

4.1.6 Fall velocity

"Representative" particles of each sand type were allowed to fall, under the effect of their own weight, in a column of still water. Knowing the height of uniform rate of fall (measured as 1 meter) and the time of travel (determined by stopwatch) the corresponding fall velocity was estimated. This experiment was repeated several times and the average fall velocity was determined.

4.1.7 Angle of repose

A sample of sand was poured in a conical container placed on a horizontal surface. The container was then lifted causing the particles to slip and slide down the slope to establish a new slope angle, known as the "angle of

repose". The angle of repose was determined from the average height and base width of the newly formed conical mound of sand.

4.2 Experimental Apparatus

The experimental programme was performed in the University of Ottawa Hydraulics Laboratory and the general arrangement of the apparatus used is shown in Fig.(6). The experimental program investigated clear water scour produced by the concentrated jet-type flow emerging from culverts of rectangular cross-section. The model conduits used were all 7.6 cm high × 1.2 m long but had the following different widths :5.1, 15.2, 20.3 and 25.4 cm.

The experiments were performed in a fixed-bed flume 60 cm high × 50 cm wide × 7.6 m long. Water entered the flume through a supply line located at the former's upstream end and an adjustable-height gate was installed at the downstream end to control the water surface elevation in the flume's test section. Screens were installed immediately downstream of the entrance section to destroy any large-scale secondary currents that might be present in the entrance flow and a calibrated triangular weir was placed a short distance downstream of the screens to determine the flow used in each experiment.

The model culverts were placed at a horizontal slope on a 20.3 cm high

wooden platform so that their inverts were at the same elevation as the "test section" sand bed that extended immediately downstream of the culvert outlets. This 1.2 m long sand bed had a uniform thickness of 20.3 cm, which was generally sufficient to allow full horizontal and vertical development of the scour profiles produced during the various tests.

Eight piezometers, each 12.7 cm apart, were connected to the model box culvert inverts to measure for each experiment the corresponding internal water surface profile. A depth gauge, mounted on an instrument carriage capable of moving in both the longitudinal and transverse directions, measured the depth of scour at any desired location in the sand bed.

4.3 Weir and Current meter calibration

The flow was determined using a 30° triangular weir. The calibration was performed as follows: The weir was mounted on a tank and a wide range of flows was discharged over the weir. The height above the weir crest was determined by means of a piezometer connected to the bottom of the tank and the corresponding discharge was measured using another collecting tank resting on a weighscale.

Since the fundamental equation for all triangular weirs can be represented in the form $Q = KH_c^n$, the logarithm of the data was taken and a linear regression analysis was performed to yield the equation $Q =$

$0.296H_c^{2.41}$, where H_c is the head above the weir crest in meters and Q is the corresponding discharge in cubic meters per second. This relationship is shown in Fig.(7).

For the second part of the experimental program, where the use of the pyramidal hump feature was investigated, velocities were measured using a streamflo current meter manufactured by Nixon Instrumentation Limited. The probe frequency readings (in Hz) were recorded which were then transformed into velocity readings by means of a given linear relationship between the two variables. This relationship was checked experimentally as follows: For a particular set of discharge conditions , point velocities were measured at six different sections in the test flume using both the streamflo current meter and a standard pitot tube. The experimental data were plotted together on the calibration curve provided by the manufacturer (Fig.(8)) and a good agreement was noted. Accordingly, the calibration curve for the meter was adopted in the experimental programme.

4.4 Experimental Procedure

Prior to each test the sand bed was evened and levelled to the same elevation as the model conduit invert. The bed was then gently and thoroughly saturated to remove air from the voids in the sand bed in order to produce a reasonably uniform density of sand in the test section. The saturation process, however, caused the bed surface to drop slightly as the material

settled and sand had to be added to bring the surface once again to the correct level. Next, a small flow was introduced in the model culvert and the outlet control gate adjusted so as to produce the desired tailwater elevation. The discharge was then smoothly increased to the required (test) value (with corresponding adjustments being made to the control gate setting) and measurements of the tailwater and brink depths, as well as the model culvert piezometric heads were then taken.

An important consideration in the experimental program was the presumption that a steady state scour condition had been reached in each experiment before recording the principal dimensions of the corresponding scour profiles. In regards to this consideration, a preliminary series of experiments was performed, in which the scour hole development process was carefully monitored for the given range of flows. It was observed that, for all practical purposes, the local scour ceased after a duration of about one hour. Accordingly, to ensure that an equilibrium state had indeed been reached in all subsequent tests, a standard two-hour test duration was adopted for all experiments.

At the end of each test, the supply was turned off and the sand bed carefully drained to permit a detailed survey to be taken of the exposed scour hole. During the local scouring process, the finer particles of the exposed sand bed were transported downstream, leaving more and more of the coarser fractions within the scour hole. Thus, in order to preserve the original sand homogeneity condition, the sand was thoroughly mixed

Table 4.1: Test Series Classification Based on Culvert Width and Sand Properties

Model Culvert		Sand Characteristics					
Series	Width (cm)	Series	$d_{50}(mm)$	$d_m(mm)$	σ	$\omega(m/s)$	ϕ
A	5.1	W	0.47	0.72	1.64	0.07	31.8
B	15.3	X	0.54	1.20	2.24	0.09	27.5
C	20.3	Y	1.08	1.17	1.24	0.14	30.0
D	25.4	Z	1.35	1.56	1.22	0.19	27.6

before starting the next experiment.

For reference purposes, the experiments were catalogued according to the model culvert dimensions and the sand grain sizes used. Table 4.1 summarizes both the sand properties and model culvert dimensions used in the experimental program. Thus, according to the notation in Table 4.1, experiment BW20 was the twentieth test of the program in which a 15.3 cm wide model culvert and sand type W were used.

Chapter 5

RESULTS AND DISCUSSION: NATURAL SCOUR

The purpose of this part of the experimental program was to relate the geometric properties of the local scour profile with the culvert dimensions, bed material properties and flow conditions. The experimental data was analyzed based on a parametric study. The principal factors affecting scour, such as: discharge, downstream channel width and tailwater elevation, were expressed in terms of dimensionless ratios to examine their separate and combined effect on local scour.

The observed scour data are reported in Table A.1 and the parameters

(expressed in dimensionless form) are listed in Table A.2. As indicated in Table A.1, the distance from the outlet to the downstream limit of sediment deposition (L), as well as the local deposition mound height (h_m) were often not measured. This was due to the fact that, when relatively little scour occurred, the related downstream deposition could hardly be observed. On the other hand, when local scour was excessive, the material deposition extended beyond the total length of the sand bed and thus the ridge's height and extent could not be accurately determined. A detailed survey was taken of the local scour pattern for particular flow condition (run BX26).The resulting scour contours for this particular flow condition are shown in Fig.(9). Similar contour maps were reported in other studies investigating local scour (e.g. Stevens, 1969). These studies, however, usually show the deposition mound downstream of the scour hole, which is not present in this study. This is due to the fact that the scour duration was too long, which caused the ridge to flatten out as was stated by Ali and Lim (1986).

5.1 Validation of the Dimensionless Study Parameters

Dimensional analysis performed in chapter 3 provided the principal dimensionless parameters affecting scour downstream of culvert outlets. Prior to any data analysis it is important to check if these dimensionless study parameters are satisfactory, from a physical modelling viewpoint. As noted

in Figs.(10) to (12), for example, the local bed scour generally increases with an increase in the dimensionless parameter $\frac{Q}{WH^{\frac{5}{2}}}$. The variation in this parameter can be due to variations in the culvert flow and/or the culvert dimensions. Either way, an increase in $\frac{Q}{WH^{\frac{5}{2}}}$ generally results in an increase in local scour. Furthermore, it can be seen from the recorded data that similar scour hole geometric properties (d_s,L_s,W_s,..) were obtained for experiments having the same dimensionless parameter $\frac{Q}{WH^{\frac{5}{2}}}$, but different test conditions (discharge, culvert dimensions,..). This can be noted, for instance, by comparing runs BW19 and DW60 (Tables A.1 and A.2). The scour hole geometric properties for these particular runs are almost the same even though different culverts and different discharges were considered. This is explained by the fact that both runs have the same dimensionless discharge parameter ($\frac{Q}{WH^{\frac{5}{2}}}$), which shows the validity of the latter in representing different discharges and culvert dimensions.

5.2 Variables Affecting Scour Depth

5.2.1 Culvert discharge

Fig.(10) shows, for a given culvert size, the variation of local scour with tailwater depth for a range of culvert flows. Figs.(11) and (12) show the same thing but for different culvert sizes and the same discharge (1.25 and 3.87l/s respectively). The local scour depth was observed to increase with

an increase in the discharge parameter $\frac{Q}{WH^{\frac{5}{2}}}$. This result was anticipated, as an increase in flow rate, assuming all other variables remain constant, implies an increase in the flow velocities and hence an increase in the flow's erosive power.

5.2.2 Tailwater depth

Referring again to Figs.(10),(11) and (12), it is clear that scour depth decreases with increasing tailwater depth. This is largely due to the reduced velocities, flow concentration and enhanced energy dissipation at outlet that results from an increase in tailwater depth. Moreover, the water jet issuing from the culvert is more buoyant in the deeper tailwater channel and so the former rises off the floor of the channel much earlier than would occur if the tailwater depth were shallow. This also contributes to lower velocities near the bed and hence reduced local scouring. On the other hand, the curves presented in the aforementioned figures generally reach a"lower limit" at a $\frac{y_t}{H}$ value of around unity. This would imply that for high tailwater elevations (near "submerged outlet" condition) the scour depth (d_s) becomes independent of the tailwater depth (y_t).

Finally, when the tailwater depth is very shallow ($\frac{y_t}{H} < 0.25$), local scouring was found to decrease with a decrease in the tailwater depth. The same phenomenon was also observed by Stevens (1969) while investigating local scour downstream of circular culverts. He explained that: *"the de-*

crease in scour depth for low tailwater levels is believed to be caused by the formation of a high mound over which the flow can not discharge material, even though it has the rock in motion".

5.2.3 Downstream channel width

As indicated in Fig.(14), for the same hydraulic conditions, scour depth is much smaller when the downstream channel is narrow. This is partly due to the fact that the energy of the turbulent eddies is destroyed through frictional resistance with the channel banks. However, for confined downstream channel conditions, scour usually develops over the entire width of the downstream channel and so it may represent a potentially more dangerous situation from the "bank stability" viewpoint. Furthermore, the scour hole length was observed to be generally larger in the case of narrow channels. This results from the fact that the jet lateral expansion is restricted and so the eddies in the expanding flow field tend to erode further in the longitudinal direction. This fact can be demonstrated by comparing the three experimental runs AW44, AW49 and AW53 in Table A.2.

In summary it can be stated that decreasing the width of the downstream channel, to a point where it limits the normal flow expansion and scour development processes, results in a decrease in both the width and maximum depth of scour and a slight increase in the overall length of scour. On the other hand Stevens (1969) showed that, in cases where the down-

stream channel may be considered "wide" (i.e. no lateral restriction on flow expansion and local scour development), varying the channel width has no influence on the scour profile generated.

5.2.4 Effective grain size

Fig.(13) shows, for a given discharge condition, the variation of scour depth with tailwater level for different types of sand (properties given in table 4.1). It can be seen that scour decreases as the particle median grain size (d_{50}) increases. This is due to the fact that the stabilizing force due to particle weight is increased with an increase in d_{50}. An increase in grain size, however, does not necessarily imply a decrease in scour because, under certain conditions, the increase in weight is counterbalanced by an increase in the particle's circumferential pressure forces which, when integrated around the particle surface, results in higher drag and/or lift forces. On the other hand, Stevens (1969) found that the scour depth (d_s) was proportional to $\frac{1}{d_m{}^a}$, where d_m is some representative grain size diameter and 'a' is a constant ranging from 0.30 to 0.55. (i.e. $d_s \propto \frac{1}{d_m{}^a}$). This relationship shows that, for large scour depths, increasing the particle size is not an efficient way of reducing local scour.

The median grain size is not the only bed material property affecting scour. As indicated in Fig.(13) scour behaviour is very different for two types of sand (W and X) of approximately the same d_{50} grain size (d_{50} =

0.465 and 0.54mm respectively). The difference is due to the fact that these two sands have different gradations. Scour is observed to be much more severe for the more uniform material ($\sigma = 1.64$) than for the well-graded sand ($\sigma = 2.24$). This is explained by the fact that the fine particles in the well-graded mixture are rapidly removed during the scouring process and carried downstream. This results in a progressively coarser residual bed material, which becomes more and more resistant to the scouring action.

However, in the case of the more uniform sand, after the fine particles are removed the residual bed material is still relatively fine and therefore more susceptible to large-scale degradation. Therefore, scour is observed to be dependent not only on the representative grain size (d_{50}) but also on the material gradation (σ). These two sediment properties can be combined into one parameter called the "effective grain size", which is believed to be better correlated to the scour hole geometric characteristics (Stevens, 1969).

Nevertheless, even though sands X and Y have the same effective grain size, the corresponding scour patterns (generated under the same flow conditions) were observed to be quite different. This was especially true for a "shallow tailwater depth" condition where, excessive local scouring occurred. In fact, sand X showed more conservative scour depths under these conditions. This was mainly due to the presence of very coarse grains (fine gravel) in sand X which helped to minimize scour compared to sand Y, which was practically uniform ($\sigma = 1.24$).

In conclusion, the effective grain size can be viewed as being an important representative parameter of the bed material as it combines, to a certain extent, the median grain size with the material gradation. For this reason, it is generally adopted in studies dealing with scour and sediment transport.

5.3 Related Scour Hole Characteristics

5.3.1 Length of scour hole

The length of scour hole, defined as the longitudinal distance from the culvert outlet to the downstream limit of scour, was observed to vary in the same way as the scour depth (Figs.(16) and (18)). That is, it was found to increase with an increase in flow, a decrease in effective grain size and a decrease in tailwater depth (Figs.(15) and (17)). However, for the "very shallow tailwater" condition ($\frac{y_t}{H} < 0.25$) the tailwater depth has little or no effect on the length of scour. On the other hand, the scour hole was found to be much longer when the tailwater depth is relatively high compared to another experimental run of the same maximum scour depth. This can be noted, for example, when experimental runs BW8 and BW15 are compared (Table A.2). In these cases the scour length almost doubled when the dimensionless tailwater ratio $\frac{y_t}{H}$ was increased from 0.05 to 0.38.

5.3.2 Maximum scour width

Scour width is expected to be a function of scour depth and the initial outlet jet width. Thus, to investigate the scour width and its variation with other parameters, the ratio $\frac{W_s}{d_m}$ was plotted against the dimensionless scour depth parameter $\frac{d_s}{d_m}$, for different culvert widths (Fig.(19)). It is worth mentioning here that the effective grain size d_m was used to non-dimensionlize the parameters because it is believed to affect scour width (W_s) more than the culvert height (H). For this reason, d_m was also adopted by previous researchers (e.g. Stevens, 1969) to non-dimensionlize their experimental data. According to the aforementioned figure, it can be noted that the scour width increases as the scour depth and the culvert width (and hence the outlet jet width) increase. The same data, for one culvert width ($\frac{W}{H} = 2.0$), is compared with results from other studies (Smith, 1957 and Stevens, 1969),see Fig.(20). The experimental data of this present work extended over a wider range of values and showed a reasonably good agreement with the other reported data.

5.3.3 Sediment mound height

The height of the sediment mound, located immediately downstream of the scour hole, is expected to be mainly a function of the depth of scour. In fact, the greater the scour, the greater the deposition downstream. The relationship of $\frac{h_m}{H}$ versus $\frac{d_s}{H}$ is shown in Fig.(21). The height of the mound

is shown to be directly proportional to the depth of scour. The relationship obtained from the experiments, even though polynomial in nature, can be represented by a linear relationship $h_m = 0.3d_s$ where the only disagreement is shown to be near the origin, which is a region of not much importance in practice as it represents very small scour depth values.

The relationship $H = 0.3d_s$ however, has a slope much lower than that obtained by Tse (1977). This is due mainly to the fact that, in the present study, measurements relating to the scour profiles were performed only after the equilibrium state of scour was reached. For this condition the mound is more streamlined (i.e. flatter), which results in lower H values. This fact was also observed by Ali and Lim (1986); they state that: " ... *the ridge tends to flatten out with a decrease in tailwater depth and is minimal or totally absent at long scouring durations, especially for the two-dimensional jets*".

5.3.4 Distance from outlet to the downstream end of the mound

As mentioned earlier, this parameter is often not recorded because local deposition immediately downstream of the scour hole is difficult to observe for the case of little scour. Furthermore, in studies of this type where scouring is excessive, this zone usually extends beyond the downstream limit of the test section sand bed. However, where possible, the distance

to the end of the mound (L) was correlated with the scour length (L_s) and the bed material grain size (d_m). The relationship obtained is shown in Fig.(22). The plot contains significant scatter of the data points, which is largely due to the difficulty of defining the downstream limit of both the scour and deposition zones in many of the experiments. Nevertheless, the suggested relationship, namely: $\frac{L}{d_m} \Rightarrow 2.2\frac{L_s}{d_m}$, corresponds closely to that obtained by Stevens (1969) for circular culverts, even though the latter study involved smaller $\frac{L}{d_m}$ and $\frac{L_s}{d_m}$ values.

5.3.5 Distance from outlet to the point of deepest scour

The measurement of X_d was often difficult because the bottom of the scour hole was practically flat in the region of deepest scour. $\frac{X_d}{d_m}$ was plotted against $\frac{L_s}{d_m}$ in Fig.(23) and from this the relationship $\frac{X_d}{d_m} = 0.4\frac{L_s}{d_m}$ was obtained. A similar relationship, developed by Chen (1970), is included in the figure for the purpose of comparison.

5.3.6 Distance from outlet to the point of widest scour

This parameter was also correlated with the scour hole length (see Fig.(24)). Note that d_m, rather than H, was used to non-dimensionlize the parameters because X_w is believed to be more dependent on the bed material rather

than the culvert height (Stevens,1969 and Chen, 1970). The plot obtained represent a power relationship of the form: $\frac{X_w}{d_m} = a\left(\frac{L_s}{d_m}\right)^b$ where $a = 1.61$ and $b = 0.76$. Chen (1970) obtained a linear relationship between X_w and L_s, namely: $\frac{X_w}{d_m} = 0.5\frac{L_s}{d_m}$, however it should be noted that his $\frac{X_w}{d_m}$ and $\frac{L_s}{d_m}$ values were much smaller than those observed in the present study.

5.4 Prediction of the Maximum Depth of Scour

Local scouring is a phenomenon that frequently accompanies "fluid-structure" interaction in alluvial channel flows. Since the severity and areal extent of local scouring are usually critically important factors in design, this phenomenon is a much-researched topic in area of river engineering.

In addition to examining the complex transport mechanisms governing, for example, scour in alluvial channel bends (Friedkin, 1945 and Suga, 1965), past studies have also dealt with scour in the vicinity of bridge piers (Dargahi, 1982), downstream of spillway structures (Bilashevsky, 1967), and other types of river structure .

Empirical expressions, relating the maximum depth of scour to the bed material properties, discharge, and local depth of flow, have been proposed as a result of these studies and some notable examples are given below:

1. Schoklitsch (1935), studying local scour in an unprotected river bed below a free overfall, developed the following equation:

$$d_s = k d_{90}^{-0.32} h_t^{0.2} q^{0.57} \tag{5.1}$$

where d_s is the maximum depth of scour measured from the water surface, k is a constant which depends on the system of units used, d_{90} is the particle grain size by which 90% is finer by weight, h_t is the difference between the upstream and downstream water surface elevations, and q is the discharge per unit width.

2. Laursen (1963) reported his equation for scour in a long contraction as:

$$\frac{d_s}{y_1} = 0.13\left[\frac{Q}{d^{\frac{1}{3}} y_1^{\frac{7}{6}} B}\right]^{\frac{6}{7}} - 1 \tag{5.2}$$

where d_s is the depth of local scour in the contraction (ft), y_1 is the flow depth upstream of the contraction (ft), Q is the discharge (cfs), d is a representative sediment grain size (ft), and B is the contraction width (ft).

3. Valentin (1967) studied scour in a sand bed downstream of model sluice gates and developed the following empirical relationship:

$$\frac{d_s}{y} = \left(\exp \frac{F_r - 2}{2.03}\right)\left(\frac{d_{90}}{y}\right)^{-0.55} \tag{5.3}$$

where d_s is the depth of scour measured from the original bed elevation, y is the flow depth below the sluice gate, and F_r is the flow Froude number below the sluice gate.

Chen (1970) modified equation (5.3) to make it applicable to culvert flows. Essentially, he added to the original Valentin equation a constant so that scour depth is zero when the velocity is zero. His modified equation took the form:

$$\frac{d_s}{H} = \left(\exp \frac{F_r - 2}{2.03} - 0.373\right)\left(\frac{d_{90}}{H}\right)^{-0.50} \tag{5.4}$$

where H is the culvert height and d_m is the bed material effective grain size. This equation, however, is only valid when the culvert flows full (or near full) and the tailwater depth is equal to the flow depth inside the barrel. Under this condition all streamlines are straight and parallel at the culvert outlet and the flow can then be considered one-dimensional. It should be noted that this is the condition for which the original (Valentin's) equation was developed. Furthermore, for this equation to be valid, $\frac{d_s}{d_m}$ should be relatively large. This is because the power law equation $d_s \propto {d_m}^{0.5}$ is applicable only when $\frac{d_s}{d_m} \geq 5$ (Stevens, 1969).

The modified Valentin's equation was proved to be valid as a fairly good agreement was obtained when compared with Chen's data (Chen, 1970). However, the equation was tested for a stone bed, where the stone median grain size was roughly 2.0 cm. For sand beds, the grain size is much smaller and scour depth might change differently with $\frac{d_m}{H}$. Indeed, Valentin's equation was modified again to predict the maximum depth of scour in sand beds. The range $0.3 \leq \frac{y_t}{H} \leq 0.7$ was selected as the most appropriate "design range" for this exercise. Firstly, this range is the most common operating range in practice. Secondly, as pointed out earlier in this chapter, at very shallow tailwater depths ($\frac{y_t}{H} \leq 0.3$) the scour depth

varies in a completely different manner with the tailwater depth. The experimental data used in this part of the analysis was representative of a wide range of hydraulic conditions and culvert sizes. In each case, however, the tailwater depth (y_t) was made equal to the flow depth inside the barrel (y_b),as was the case in Valentin's original work.

In the analysis equation (5.4) was modified by systematically changing the value of the exponent of $\left(\frac{d_m}{H_0}\right)$ until the discrepancy between the observed and computed values was minimal. This exercise produced the value -0.275 for the exponent of $\left(\frac{d_m}{H_0}\right)$ and the resulting comparison of observed and computed data is shown in Fig.(25). Accordingly the recommended form of equation (5.4) for a freely discharging culvert in a sand bed, in which $y_t = y_b$, is :

$$\frac{d_s}{H} = \left(\exp \frac{F_r - 2}{2.03} - 0.373\right)\left(\frac{d_m}{H}\right)^{-0.275} \tag{5.5}$$

The exponent (-0.275) in equation (5.5) shows that scour depth in sand beds is less sensitive to the effective grain size than it is for a stone bed, (where the exponent is -0.5).

5.5 Similarity of Vertical Velocity Profiles

As noted in chapter 3, the shape of the vertical velocity profiles is the same for all sections in the fully-developed flow region. All velocity profiles in

this region can be represented by the following relationship:

$$\frac{u}{u_m} = \exp\left[-0.693\left(\frac{y-\delta}{y_m-\delta_1}\right)^2\right] \tag{5.6}$$

where y is the depth of flow measured from the water surface, y_m is the normal distance to the point where $u = \frac{u_m}{2}$, u_m is the maximum velocity and δ_1 and δ are the surface and shear layer thicknesses of the velocity profile respectively. This similarity of velocity profiles was verified experimentally in one particular experiment ($\frac{Q}{WH^{\frac{3}{2}}} = 0.97$; $\frac{y_1}{H} = 0.50$) where vertical velocity distributions were measured at 5 successive channel sections at 5 cm spacings. The measured velocities were plotted in dimensionless form with the above relationship and a reasonably good agreement was obtained (see Fig.(26))

5.6 Boundary Shear Stress Measurement

The boundary shear stress along the centerline of the scour hole was estimated using the method of Melville and Raudviki (1977), which is based on bottom velocity measurement, namely:

$$\tau_0 = \rho f \frac{{u_b}^2}{8} \tag{5.7}$$

where ρ is the fluid density, u_b is the bottom velocity and f is the friction factor. The friction factor was estimated using the Colebrook-White equation:

$$\frac{1}{f^{\frac{1}{2}}} = -2\log\left[\frac{K_s}{14.83H_t} + \frac{2.52}{f^{\frac{1}{2}}R_h}\right] \tag{5.8}$$

Where H_t is the depth of flow above the scoured bed, $R_h = \frac{u_* H_t}{\nu}$, and K_s, being the "roughness height" of sand, was related to the d_{90} grain size by the formula $K_s = 3d_{90}$ (Rijn, 1984).

This method for calculating the boundary shear stress in a scour hole was compared with that obtained using turbulent boundary layer theory, (Ali and Lim, 1986) and a reasonably good agreement between the two methods was obtained.

The test in which detailed shear stress measurements were performed, was the one used to verify similarity of velocity distributions in the fully developed flow region,i.e. $\frac{Q}{WH^{\frac{3}{2}}} = 0.97$ and $\frac{y_t}{H} = 0.50$. Boundary shear stress was calculated and plotted against the longitudinal distance from the culvert outlet (Fig.(27)). According to this plot, the boundary shear stress is a minimum at the bottom of the scour hole and gradually increases in value along the up-slope of the scour profile to reach a maximum value as the bed profile approaches the original flat-bed condition.

Chapter 6

THE "PYRAMIDAL HUMP" FEATURE: EFFICIENCY ANALYSIS

Earlier in this thesis (chapter 1), it was stated that, depending on the nature of the culvert flow, there are generally two methods available to reduce the severity of local erosion downstream of culvert outlets. If the flow is supercritical, this certainly requires some form of energy dissipator (e.g. baffle piers and end sill) immediately downstream of the culvert outlet. On the other hand, if the flow is subcritical, the usual approach is to redistribute the outlet velocity distribution through an improved outlet geometry.

In the majority of cases the usual practice is to simply reverse the inlet

wingwall arrangement at the outlet i.e. provide flared wingwalls that gradually increase the section width in the flow direction. However unlike the entrance geometry, which is effective in terms of reducing entrance head loss, the outlet wingwall flare is so large that it is ineffective , re: redistribution of mean flow velocity along the outlet section. As a result, the concentrated "jet-type" flow issuing from the structure can lead to severe local scouring of the channel bed and banks (Fig.(28.a)). In these situations the usual preventive measure taken is to stabilize the affected portions of the channel with either a rock lining ('rip-rap") or vegetative cover. While these measures usually provide adequate protection for the natural channel boundaries, they do little to reduce the aforementioned flow concentration at the outlet.

If the traditional outlet expansion section was made more effective in regards to flow redistribution, this would contribute to reduced local scouring of the downstream channel bed. Therefore, the purpose of this phase of the study was to improve the efficiency of the traditional culvert outlet section. The method proposed is based on the flow redistribution principle, namely enhancing the jet expansion to reduce the otherwise concentrated "jet-type" flow issuing from a rectangular-shaped ("box") culvert. This can be achieved by imposing an adverse pressure gradient on the high velocity core region of the culvert flow as the latter traverses the outlet section. From hydraulics theory, this would require an adverse slope on the central portion of the bed in the direction of flow. This local bed feature, however, must be smoothly integrated with its surroundings otherwise flow

separation would occur and this would produce unwanted secondary currents. The appropriate bed geometry is therefore a smooth, streamlined, pyramidal-shaped hump located on the conduit centerline (with its major axis superimposed on the conduit centerline). Such an arrangement is shown in Fig.(28b). The efficiency of such a feature, in terms of expanding the jet and reducing the flow concentration, is expected to be a function of its geometric properties and its location relative to the outlet section.

In this chapter the effects of the hump's shape and location on its hydraulic performance are examined for a wide range of hydraulic conditions.

Most of the experiments performed in this phase of the study used the 15.2 cm and 20.3 cm-wide model culvert. Flared wingwalls, angled at 45 degrees to the culvert alignment, were installed to reflect the normal outlet arrangement for box culverts. Eight hump units of different geometric properties (Table 6.1) were considered in this phase of the investigation.

A detailed preliminary experiment was performed, in which cross-stream velocity distributions were measured near the water surface, at mid-depth and near the channel bottom for a "fixed bed" condition (see Fig.(29)). Since the three velocity distributions were observed to be approximately the same for all sections (with the mid-depth values being slightly higher than the others), only mid-depth velocities were measured in subsequent tests.

Table 6.1: Hump Dimensions

Hump #	a_1 (cm)	a_2 (cm)	w_h	h
1	10.0	5.0	15.0	2.5
2	10.0	5.0	10.0	2.5
3	10.0	5.0	15.0	3.7
4	10.0	5.0	15.0	5.0
5	5.0	10.0	15.0	2.5
6	15.0	10.0	20.0	2.5
7	20.0	10.0	20.0	2.5
8	25.0	10.0	20.0	2.5

6.1 Flow Characteristics-Boundary Conditions

Preliminary tests were performed to examine if the proposed "pyramidal hump" feature has some beneficial effect on the jet expansion and hence on the cross-stream velocity distribution in the downstream channel. These tests were conducted with a "mobile bed" and using the 15.2 cm-wide model culvert. The tests were performed using a wide range of culvert flows ($0.39 \leq \frac{Q}{WH^{\frac{3}{2}}} \leq 1.21$) and tailwater depths ($0.33 \leq \frac{y_t}{H} \leq 0.92$). These limits, although chosen arbitrarily, were considered reasonable as they represent a wide range of possible (subcritical flow) culvert operation. Firstly,

the maximum flow rate (3.87 l/s) was close to the culvert capacity, based on a "free surface" operating condition. Secondly, the tailwater depth to culvert height ratio ($\frac{y_t}{H}$) varied from 0.33, which represents a " relatively shallow tailwater" condition, to 0.92, which corresponds to a " nearly submerged outlet" condition. Therefore, the adopted range covered most of the possible operating tailwater depths for highway culverts. $\frac{y_t}{H}$ values less than 0.33 were not considered because culverts discharging into natural channels that are only marginally wider than the culvert itself normally operate with some tailwater present.

Average jet velocities (U_0) for the model culvert ranged from 0.5 to 0.9 m/s. Consider, for example, a prototype culvert 2m high by 2m wide. Then the corresponding "linear" scale, based on the present model culvert width, is $y_s = \frac{0.152}{2} = 0.076$. Since free surface culvert flows are largely governed by "gravity" effects, then, for modelling purposes: $F_{rm} = F_{rp}$, where F_{rm} and F_{rp} are the model and prototype Froude numbers respectively. Therefore:

$$\frac{U_{0m}}{\sqrt{g_m y_m}} = \frac{U_{0p}}{\sqrt{g_p y_p}} \tag{6.1}$$

Now, assuming gravity is a constant then equation (6.1) reduces to:

$$\frac{U_{0m}}{\sqrt{y_m}} = \frac{U_{0p}}{\sqrt{y_p}} \tag{6.2}$$

or:

$$\frac{U_{0m}}{U_{0p}} = \sqrt{\frac{y_m}{y_p}} = \sqrt{y_s} \tag{6.3}$$

that is:

$$U_{0p} = \frac{U_{0m}}{\sqrt{y_s}} = \frac{U_{0m}}{\sqrt{0.076}} \tag{6.4}$$

Since $0.5 \leq U_{0m} \leq 0.9$, then:

$$\frac{0.5}{\sqrt{0.076}} \leq U_{0p} \leq \frac{0.9}{\sqrt{0.076}} \qquad (6.5)$$

or: $1.8 \leq U_{0p} \leq 3.3$ m/s. therefore the model velocity range (0.5 to 0.9 m/s) is considered reasonable from a practical viewpoint as it covers the highest prototype velocities that would normally occur in practice (1.8 to 3.3 m/s). In fact, it is for these high velocities that scour control measures are usually required.

Fig.(30) and other subsequent figures (Figs.(30) to (43) for the "mobile bed" condition and (47) to (55) and (57) to (68) for the "fixed bed" condition) show , by means of the observed mid-depth velocity profile development along the test section, the expansion of the jet as it moves into the unconfined flow region downstream of the culvert outlet. The figures show cross-stream velocity distributions at the culvert outlet and at four downstream sections (spaced at 17.8 cm intervals) for both "with hump" (dashed line) and "without hump" (solid line) conditions.

These figures are representative of the many more experiment conducted in this phase of the programme. It should be emphasized, at this point, that outflow jet characteristics (jet width and average velocity) at the four sections considered, for all experiments performed, are reported in tables A.3 ("mobile bed" condition) and A.4 ("fixed bed" condition).

The tests were performed using the same hump (hump # 1), but for different hump locations relative to the culvert outlet. Since the effect of the

hump's position on its efficiency is examined in a subsequent section, only the hump's relative performance at a given location, based on different flow conditions, is considered here. Figs.(30) to (32) show the velocity profile development for the dimensionless flow parameter $\frac{Q}{WH^{\frac{3}{2}}} = 1.21$ and the dimensionless tailwater depth parameter $\frac{y_t}{H} = 0.42$. In this particular case the flow is close to the conduit's capacity, based on a free-surface operating condition, while the tailwater depth represents the smallest possible value in the experimental facility at this particular flow rate. The effectiveness of the hump in expanding the jet is immediately apparent from a comparison of the velocity distributions at section 2, for the hump in place and without the hump. The jet expansion angle, without the hump, was observed to be roughly 4 degrees. With the hump in place, however, the width of the jet was found to be 32.5 cm ($\frac{w_1}{B} = 0.65$), which corresponds to a jet expansion angle of roughly 26 degrees. This enhanced value is more than 6 times the initial jet expansion angle, which is a significant improvement in terms of flow (and hence velocity) redistribution. This increased rate of spread of the jet continued up to section (4), after which velocity is more or less evenly distributed across the entire channel width.

With regard to reduction of velocities, in general, some overall improvement is noted at section 3 in this instance, where the velocity ratio $\frac{u}{U_0}$ was reduced from 1.0 for the unaided jet to 0.8 when the hump is in place. Some additional velocity reduction was noted at section 4 where $\frac{u}{U_0}$ approached 62% with the hump in place.

In the next set of experiments the culvert flow was reduced, so that $\frac{Q}{WH^{\frac{3}{2}}} = 0.7$, but the tailwater depth was kept the same (i.e. $\frac{y_t}{H} = 0.42$). As can be seen in Figs(33) to (35), in this instance the hump's performance was improved over the previous case ($\frac{Q}{WH^{\frac{3}{2}}} = 1.21$). Starting from section 3 significant velocity reduction (around 50 % in the case where $l = -4.5$ cm) was achieved in the central flow region. Moreover, the jet expansion rate was improved slightly, such that the jet eventually occupied the entire width of the channel just downstream of section 4.

When the culvert flow was reduced still further ($\frac{Q}{WH^{\frac{3}{2}}} = 0.53$), again keeping the same tailwater depth as before, the impact of the hump on the outlet flow was lessened considerably (Figs.(36) to (38)). In fact, with regard to jet expansion, almost no improvement was observed at sections 2 and 3. Furthermore, the cross-stream velocity distribution was more or less even for most of the channel width at sections 4 and 5, even without hump. This is evidenced in Fig.(39), where $\frac{Q}{WH^{\frac{3}{2}}} = 0.39$ and $\frac{y_t}{H} = 0.33$. For this particular situation the natural jet (without hump) spread over the entire channel width starting at section 4.

The fact that the hump performs better for the case of relatively high discharge becomes clear when one examines Figs.(44) and (45), where the jet expansion rate is shown to be much greater compared to the case of low flows. Similarly, as evidenced in Fig.(46) compared to the "without hump" condition the reduction in flow velocities is generally greater for the "high discharge" case.

Fig.(44) shows a comparison of the rate of jet expansion with and without the hump for two flow conditions. For the lower flow ($\frac{Q}{WH^{\frac{3}{2}}} = 0.39$) placing the hump did not cause any improvement. However, when $\frac{Q}{WH^{\frac{3}{2}}} = 1.21$ the hump was observed to be quite efficient in terms of enhancing the jet expansion. Therefore, the hump's performance is much better for relatively high flows than for low culvert discharges. This conclusion can be confirmed by examining Figs.(45) and (46), which show the rates of jet expansion and velocity reduction respectively again for two different flows but for a "fixed bed" condition.

Nevertheless, the hump's efficiency was observed to decrease not only with decreasing culvert flow, but also with increasing tailwater depth. Consider, for instance, the case where $\frac{Q}{WH^{\frac{3}{2}}} = 1.21$ and $\frac{y_t}{H} = 0.73$ (Fig.(40)). Under these conditions, the hump had almost no effect, re: enhancing the jet expansion, as velocity distributions for the "with hump" and "without hump" conditions, were almost identical. The same observation was made in those tests where the tailwater depth (y_t) exceeded 50% of the culvert height (H), irrespective of whether the flow was small or large (Figs.(41) to (43)).

In conclusion, it can be stated that the hump's best performance, in terms of jet expansion rate, is achieved when the culvert is operating under a " relatively high discharge-low tailwater" condition but where $\frac{Q}{WH^{\frac{3}{2}}}$ does not exceed unity. This particular condition is also the worst situation in terms of local scouring because, without the hump unit, high (central)

flow concentrations normally occur downstream of the outlet. Therefore an effective scour control measure (such as the proposed pyramidal hump feature) is clearly necessary in such instances.

In the case of small culvert flows the velocities are so low that they do not represent a problem in terms of localized scouring. Similarly, when high tailwater depths are encountered, much of the flow's associated kinetic energy is quickly dissipated in the ponded channel reach immediately downstream of the outlet. Therefore, in this instance the need for scour control measures is not as crucial as for the case of shallow tailwater depths.

6.2 Hump Location

In all experiments the hump feature was positioned in the flared outlet section of the model box culvert, but the exact location with respect to the downstream end of the culvert barrel was varied throughout the series of tests. According to Table (A.3), which summarizes jet parameters ($\frac{w_j}{B}$; $\frac{u}{U_0}$) for both "with hump" and "without hump" conditions, the hump performed equally well for different positions although it performed slightly better when placed partially inside the barrel (i.e. when $l = -4.5$ and -2.5 cm). The experimental results for the "mobile bed" condition, however, were not consistent enough to clearly establish the optimum hump position. Accordingly, it was decided to repeat some of the experiments once again, but this time for a "fixed bed" condition. The same hump (hump # 1) was

used in this series of tests, in which the distance from the downstream end of the barrel to the beginning of the hump (l) was varied from 0 to 10 cm.

In Figs.(47) and (48) the dimensionless discharge parameter $\frac{Q}{WH^{\frac{3}{2}}} = 0.70$, the tailwater depth to the culvert height ratio $\frac{y_t}{H} = 0.42$, and $l = 0$ and 5cm respectively. Comparing these two figures, there is almost no difference in the respective cross-stream velocity distributions, especially for sections 4 and 5, where the jet parameters ($\frac{w_j}{B}$, $\frac{u}{U_0}$) are almost the same.

When the hump location was increased to 10 cm (i.e. twice that for Fig.(48)), in a test that had reasonably similar flow conditions ($\frac{Q}{WH^{\frac{3}{2}}} = 0.53$; $\frac{y_t}{H} = 0.42$), the hump had almost no impact on the jet expansion as the velocity distributions were almost the same for both "with hump" and "without hump" conditions (Fig.(49)).

In conclusion, there was a wide range of positions where the hump performed equally well irrespective of whether it was placed partially inside the culvert barrel (see data for "mobile bed" condition) or a relatively short distance downstream. However, from an operation and maintenance viewpoint, the hump should not be placed much further inside the barrel section as this might result in clogging by debris during flood events. On the other hand, the unit should not be placed too far downstream of the culvert outlet, as its impact on the jet (and hence its efficiency) would be considerably reduced. Therefore, placing the hump a short distance downstream of the barrel but at the same time within the flared outlet

section, would appear to be the most suitable location.

6.3 Hump Width

As was mentioned earlier in this chapter some improvement re: enhancing the jet expansion and reducing the flow velocities, was achieved using hump # 1, which was 15 cm wide. For comparison purposes, the hump's width was reduced to 10 cm (hump # 2) and the tests repeated. For this series of tests, the hump was placed partially inside the culvert barrel, at a position considered acceptable from a hydraulics viewpoint (i.e. $l = -2.5$ cm.)

The dimensionless flow parameter $\frac{Q}{WH^{\frac{3}{2}}}$ was varied between 0.39 and 0.97, however the tailwater depth was kept the same as before (i.e. $\frac{y_t}{H} = 0.42$) for all tests. According to Figs.(50) to (52) hump # 2 had only a marginal effect in terms of expanding the jet and reducing local velocities. In fact, the cross-stream velocity distributions were almost the same for both "with hump" and "without hump" conditions. This would appear to suggest that a desirable width for the hump is at least one culvert width and the wider the hump is the better. On the other hand, the hump should not be made overly wide otherwise maintenance problems, such as clogging by debris, might occur.

6.4 Hump Height

Hump # 1, which had a height of 2.5 cm, was shown to perform reasonably well for a wide range of flows. In most of the cases studied the hump unit was submerged. For comparison purposes (i.e. to determine the effect of hump height on hydraulic performance), two other humps (# 3 and # 4) which were 3.7 and 5.0 cm-high respectively were also examined.

Figs.(53) to (55) show the cross-stream velocity distributions obtained using hump # 3. Firstly, the divided outflow jet spans the entire channel width as early as section 2, which is only one culvert width downstream of the outlet. In addition, a well-defined "wake" zone (flow recirculation through large eddy formation) developed in the central part of the channel directly behind the hump unit. The two high-velocity jets that developed on either side of the hump unit are clearly not acceptable from a practical viewpoint. For example, in the case of narrow downstream channel, these separate jets would result in rapid erosion of the "toe" region of the channel banks, which could lead to their collapse.

A backwater effect also occurred in this series of tests, when the hump was not fully submerged (Fig.(56)). Another test was performed with the same hump (# 3) but for a higher tailwater depth ($\frac{y_t}{H} = 0.58$) that ensured that the hump was indeed submerged. The results for this test are reported in Fig.(55). Under the submerged hump condition the two separate jets were avoided, however the hump did not show any improvement in terms

of enhancing the jet expansion. This confirms the previous finding, namely that the hump does not improve the situation if high tailwater depths are encountered-even if the hump itself is made relatively high.

Hump # 4 (height = 5.0 cm) was also found to perform very poorly. As was the case for hump #3, two high-velocity jets, whose velocities exceeded the original (without hump) velocities, were generated on either side of the hump (see Figs.(57) to (59)).

clearly, therefore, if the hump unit is not submerged, the jet expansion is excessive and results in: (i)two high-velocity jets directed towards the channel banks, and (ii) a dead zone (wake region) in the central part of the channel immediately downstream of the hump unit. This particular mode of operation is deemed unacceptable as it would result in severe local erosion of the channel boundaries in the case of a "narrow downstream channel" condition. Therefore, for the hump to be effective, in terms of acceptable flow redistribution downstream of the culvert outlet, it must be designed to operate submerged for the most part. However, the hump height should not be so small as to minimize its impact on the culvert outflow.

Finally, it is worth mentioning that, based on the experimental data, the hump is most effective when its height is approximately 80% of the tailwater depth.

6.5 Hump Leading Length

While most of the experiments were performed using hump # 1 ($a_1 = 10.0$ cm), some experiments used hump # 5, for which $a_1 = 5.0$ cm. In the latter experiments the hump was placed immediately downstream of the culvert barrel (i.e $l = 0$). Comparing the results of these tests with the data obtained using hump # 1, it is clear that the performance of hump # 5 is much better for the same hump position ($l = 0$). Consider, for instance, Figs.(47) and (60), which display unit performance (under the same flow conditions) using humps # 1 and # 5 respectively. For hump # 1, the jet expansion is less efficient. In fact, the jet does not span the entire channel width even at section 5. In the case of hump # 5, however, the jet spreads over the entire channel width starting from section 2. Also, for hump # 1, there is almost no reduction in flow velocities until section 4 is reached whereas, in the case of hump # 5, $\frac{u}{U_0}$ is reduced to 0.55, 0.50 and 0.45 for sections 3, 4 and 5 respectively.

If the results for hump # 5, for $l \neq 0$, are compared with the data for hump # 1, for $l = -4.5$ cm, almost the same jet expansion rate and reduction in flow velocities are achieved. This is evident when comparing Figs.(60) and (61) in which $\frac{w_l}{B}$ and $\frac{u}{U_0}$ are almost the same for both humps. Hump performance was essentially the same for these two conditions mainly because the distance from the barrel outlet to the hump crest (X_c) was about the same in both cases. In fact, since hump # 5 was placed exactly at the barrel outlet, $X_c = a_1 = 5.0$ cm. On the other hand, for hump # 1,

$X_c = l + a_1 = -4.5 + 10.0 = 5.5$ cm. In other words parameter X_c, which combines the hump's position with its leading length (a_1), is an important design parameter in that it should be kept relatively small for improved performance.

Similar tests were performed using the 20.3 cm wide model culvert and three humps of different leading lengths (humps # 6, 7 and 8). In all tests the humps were placed at the barrel outlet ($l = 0$) and two flow ratios were considered, namely: $\frac{Q}{WH^{\frac{3}{2}}} = 0.53$ and $\frac{Q}{WH^{\frac{3}{2}}} = 0.97$. The cross-stream velocity distributions for this set of experiments are reported in Figs.(62) to (67). Velocity measurements were not taken at section 2 for the "with hump" condition. This was because the hump unit extended too far downstream, making it very difficult to measure velocities at that particular section. With regard to performance, for both flow conditions examined, hump # 6 ($a_1 = 15.0$ cm.) performed better than the other two units. This is especially apparent when the results for $\frac{Q}{WH^{\frac{3}{2}}} = 0.53$ are compared (see Figs.(62) to (64)). Under these conditions, when hump # 6 ($a_1 = 15.0$ cm) was used, the jet occupied the entire width of channel by section 3. However, when hump # 8 ($a_1 = 25.0$ cm) was employed, since the rate of jet expansion was only marginally improved, almost no reduction was observed in the flow velocities (all sections). This supports the earlier conclusion that the "leading length" parameter (a_1) should be kept reasonably small. On the other hand, a_1 should not be so short that the hump steepness ($\frac{h}{a_1}$) becomes large, as this would lead to increased backwater effects.

6.6 Bed Hump Unit versus Guide Vanes

In recent laboratory studies dealing with scour in alluvial channel bends, submerged guide vanes were investigated as one possible means of solving the local scouring problems (Odgaard,1986). Since, from an 'economics' viewpoint, a simple vane arrangement would appear at first glance to be an attractive alternative to the proposed hump unit, a test incorporating submerged directional vanes was performed and the results compared with those obtained using the bed hump feature.

Three vanes, each 15 cm long × 2.5 cm high × 0.3 cm thick, were placed in the flared outlet section in the symmetrical arrangement shown in Fig.(68). This 'vanes' test used the 20.3 cm wide model culvert and the following flow conditions: $\frac{Q}{WH^{\frac{3}{2}}} = 0.97$ and $\frac{y_1}{H} = 0.42$. The results for the test are reported in Fig.(68). Fig.(65) shows the corresponding data (i.e. for the same flow conditions) for hump unit # 6 in place of the vanes. From a 'hydraulics' viewpoint, the results for the vanes test are only marginally better than those for the hump unit. However, from a practical (i.e. operation and maintenance) viewpoint, the submerged vane arrangement was considered potentially problematic as the upstream end of the vanes would tend to promote clogging of the outlet by large debris fractions during flood events. The submerged streamlined hump profile, on the other hand, creates negligeable loss of flow area at its upstream end and promotes smooth flow deceleration across the outlet transition section, both of which contribute to an effective self-cleaning mode of operation.

A limited series of experiments using simulated debris fractions supported the above conclusions.

6.7 Effect of the Pyramidal Hump on Scour Pattern

All experiments performed to evaluate the hump's efficiency were based on cross-stream velocity measurements. In addition to these tests some experiments were performed to illustrate the effect of the hump on the downstream local scour configuration. These tests were performed using the 20.3 cm-wide model culvert and two flow conditions namely: $\frac{Q}{WH^{\frac{3}{2}}} = 0.97$, $\frac{y_t}{H} = 0.42$, and $\frac{Q}{WH^{\frac{3}{2}}} = 0.97$, $\frac{y_t}{H} = 0.17$.

According to the observed cross-stream velocity distributions, by adding the hump feature the severity of local scouring is reduced, starting mainly from section 3. Upstream of this section, a difference between the velocity distributions for "with" and "without hump" conditions is difficult to observe. This would imply that no improvement is achieved by introducing the hump for the area just downstream of the culvert barrel. However, this region is the most critical with regard to scour formation since the flow is highly concentrated. Therefore, even with the hump in place, some protection of the region just downstream of the culvert barrel is still required.

The usual practice is to protect the channel bed and banks using "rip-

rap" along five culvert "diameters" downstream of the outlet (Ontario Ministry of Transport and Communication, 1982)

Since, in this research, we are dealing with "box" rather than "circular" culverts, an equivalent diameter principle was adopted. This equivalent diameter was determined as: $D_e = 4 \times R$; where $R = \frac{W \cdot H}{W+2H}$ in which R is the hydraulic radius and W and H are the culvert width and height respectively. Accordingly, the equivalent diameter (D_e), for the 20.3 cm wide-model culvert used, was 17.4 cm.

A plexiglas sheet, of length 34.8 cm (i.e. $2D_e$), was placed downstream of the culvert barrel, hump # 6 was installed and the resulting scour pattern was compared with the "natural scour" case.

With the hump in place the maximum depth of scour was reduced from 6.2 to 3.6 cm, for $\frac{y_t}{H} = 0.42$ and from 12.0 to 9.1 cm, for $\frac{y_t}{H} = 0.17$. In general, the scour configuration was observed to be very different compared to the case of natural scour. In the latter case, a relatively wide, centrally located scour hole is obtained. However, with the hump in place, 2 smaller scour holes were observed at both sides of the channel with not much local erosion occurring in the central region of the channel.

Therefore, the use of the hump does not eliminate all local scouring; it just lessens its severity and shifts it towards the channel sides. This might imply some reduction in the overall amount of "rip-rap" required and greater need to safeguard the "toe" region of the channel banks, where

"narrow" receiving channels are encountered.

Chapter 7

CONCLUSIONS AND RECOMMENDATIONS

7.1 General Conclusions

Based on the first phase of the study, namely the investigation of natural scour, the following are the principal conclusions:

1. The maximum depth of scour depends mainly on discharge, tailwater depth, culvert width, downstream channel width and bed material properties.

2. Scour depth generally increases with decreasing tailwater depth. However, for a "very shallow tailwater" condition ($\frac{y_t}{H} < 0.3$), local scouring was found to decrease with a further decrease in tailwater depth.

3. The maximum depth of scour depends not only on the sand median grain size (d_{50}) but also on its gradation σ. In fact, uniform sands were found to be more susceptible to scour than a well-graded mixture. A parameter, called "effective grain size" (d_m), which combines both d_{50} and σ, was found to be better correlated to the depth of scour.

4. Scour depth was found to increase with an increase in flow or a decrease in culvert width. Both of these variables are accounted for in the dimensionless flow parameter $\frac{Q}{WH^{\frac{3}{2}}}$.

5. If the downstream channel is sufficiently wide that its banks do not limit the scour hole development, the bed width does not have any effect on the scour hole produced. On the other hand, decreasing the width of the downstream channel to a point where it limits the normal flow expansion and scour development processes results in a decrease in both the maximum width and depth of scour and a slight increase in the overall length of scour.

6. Scour hole characteristics (scour length, maximum scour width, etc...) were found to be a function of the maximum depth of scour. That is, they generally increase with an increase in scour depth.

7. An empirical relationship for the prediction of the maximum depth of scour was developed. This is basically Valentin's equation (Valentin,

1967) modified to be applicable for the prediction of scour in sand beds downstream of culverts operating under an "unsubmerged outlet" condition. The equation was calibrated using the experimental data obtained in this study, for which the dimensionless tailwater parameter $\frac{y_t}{H}$ ranged between 0.3 and 0.7.

The following conclusions refer to the second phase of the study, which dealt with the efficiency of the bed hump unit:

1. The hump was found to be effective in enhancing the jet expansion and reducing the central region flow velocities in the downstream receiving channel. The feature was found to be most efficient for "high discharge-low tailwater" operating conditions. Using the hump feature for the case of small culvert flows and/or high tailwater levels did not lead to any significant improvement, in terms of reduced flow concentrations.

2. The hump's efficiency depends mainly on its principal dimensions (i.e. width, height and steepness) and its location, relative to the culvert outlet section.

3. The hump was tested for different positions in the flared culvert outlet section. It was found that the feature performs reasonably well for a range of positions relative to the downstream end of the culvert barrel. However, placing the hump too far downstream reduces its effectiveness and placing it too close to or partially inside the culvert

barrel could lead to maintenance problems (clogging might occur).

4. The hump width has an important effect on its hydraulic performance. The wider the hump, the better the flow redistribution and the faster the jet expansion. However, in order to avoid possible clogging by debris, the hump width should not exceed the culvert width.

5. The hump should be high enough to ensure reasonable jet expansion and reduction of "core" flow velocities. However, increasing the hump height to an extent where the hump is not submerged results in a dead zone (almost zero velocities) in the central part of the channel and two highly concentrated jets directed towards the sides of the downstream channel. This may affect the channel bank stability, especially if the downstream channel is relatively narrow.

6. Best hydraulic performance is achieved by making the leading length of the hump unit (a_1) as short as possible. However, a high hump "steepness" value $\frac{h}{a_1}$ results in backwater effects. On the other hand, a small steepness tends to make the hump less effective, particularly for the higher culvert discharges.

7.2 Recommendations for Future Research

1. This study concentrated mainly on detailed velocity measurements to assess hump efficiency. Furthermore, most of the experiments were performed based on a "fixed bed" condition. An obvious extention to

this work would be a similar study based on a "mobile bed" condition, in which local scour development is investigated for both "clear" water flow and "sediment transport" conditions.

2. In this study the hump unit was tested for box culvert sections only. A similar study should be performed to test the effectiveness of the pyramidal hump to expand jets emerging from circular culverts, where the flows would be more three-dimensional.

3. Besides the suggested pyramidal hump feature, there might be other methods such as "guide vanes" that could be used to enhance the expansion of the outflow jet. A detailed comparison study, incorporating other such features, would be helpful in terms of selecting the most appropriate method.

Chapter 8

BIBLIOGRAPHY

Bibliography

[1] Abida, H. and Townsend, D.R. (1988),"*On the Reduction of Flow Concentration at Box Culvert Outlets*", Sixth IWRA World Congress on Water Resources, Ottawa, Canada.

[2] Abt, S.R., et al (1987),"*Influence of Culvert Shape on Outlet Scour*", Journal of Hydraulic Engineering, ASCE, Vol.113, No.3.

[3] Abt, S.R., et al (1985),"*Culvert Slope and Shape Effects on Outlet Scour*", Transportation Research Record, No.1017.

[4] Abt, S.R. and Donnel, C.A. (1983), "*Culvert Shape Effects on Localized Scour*", Hydr. Engineering Publication, Colorado State University, CER 82-83-CAD-SRA 42.

[5] Abt, S.R., et al (1983),"*Headwall Influence on Scour at Culvert Outlets*", Journal of Hydraulic Engineering ASCE, Vol.109, No. 7.

[6] Abt, S.R., et al (1981), "*Scour at Culvert Outlets in Mixed Bed Materials*", Report for the Office of Research and Development, Fed-

eral Highway administration, U.S. DOT, Contract DOT-FH-11-922-7,Washington,D.C.

[7] Abt, S.R., et al (1982), *"Scour at Culvert Outlets in a Sandy-Clay Material"*, Public Roads, Vol.46, No. 1.

[8] Ali, K.H.M. and Lim, S.Y. (1986), *"Local Scour Caused by Submerged Wall Jets"*, Proceedings of the Institution of Civil Engineers, Part 2 Research and Theory, Vol.81.

[9] Altinbilek, H.D. and Basmaci,Y. (1980), *"Localized Scour Below Submerged Vertical Gates"*, Proc. Speciality Conf., Computer and Physical Modelling in Hydraulic Engineering, Chicago.

[10] Anderson, C.L., et al (1981), *"Ultimate Dimensions of Local Scour"*, Journal of the Hydraulic division ,ASCE, Vol.107, No. HY3.

[11] Basak,S. and Ramamurthy, A.S. (1973), *"Control of Flow Separation in a Wide Channel Expansion "*, Canadian Hydraulics Conference, The University of Alberta, Edmonton.

[12] Bilashevsky, N. (1967), *"The Mechanism of the Local Scour Behind the Spillway Structures with the Aprons and the Influence of the Macro Turbulence Upon the Scour"*, Proceedings of The Twelfth Congress of the International Association for Hydraulic Research, Colorado State University, Fort collins, Colorado.

[13] Chee,S.P. and Kung, T. (1973), *"Stream Geometry of Water Jet Basins"*, Canadian Hydraulics Conference, The University of Alberta,

Edmonton.

[14] Chen, Y.H. (1970), *"Scour at Outlets of Box Culverts"*, M.S. Thesis, Colorado State University, Fort Collins, Colorado.

[15] Chow, V.T. (1987), *"Open Channel Hydraulics"*, McGraw Hill.

[16] Dargahi, B. (1982), *"Local Scour at Bridge Piers. A review of Theory and Practice"* , Bul. No. 114, Hydraulics Laboratory, Royal Institute of Technology, Stockholm.

[17] Dash, R.N. and Pani, B.S. (1986), *"Diffusion of a Three Dimensional Wall Jet in a Conveyence Channel of Limited Width"* , Proceedings of the Institution of Civil Engineers, Part 2 Research and Theory, Vol.81.

[18] Diebel, M. and Rajaratnam, N. (1981), *"Erosion Below Culvert-Like Structures"*, Canadian Society for Civil Engineering, 5th Canadian Hydrotechnical Conference, May 26 and 27, Fredericton, New brunswick.

[19] Doddiah,D. (1950), *"Comparison of Scour Caused by Hollow and Solid Jet of water"*, Master's Thesis , Colorado A and M college, Fort Collins, Colorado.

[20] Erfle, P.D. and Wiggert, J.M. (1972), *"Culvert Velocity Reduction by Internal Energy Dissipators"* , Concrete Pipe News, American Concrete Pipe Association, Arlington, Va.

[21] Erfle, P.D. and Wiggert, J.M. (1972), *"Roughness Elements as Energy Dissipators of Free-Surface Flow in Circular Pipes"* , Highway Research Board, Record No. 373, Wahington, D.C.

[22] Friedkin, J.F. (1945), *"A Laboratory Study of the Meandering of Alluvial Rivers"* , Waterways Experiment Station, Corps of Engineers, U.S. Army, Vicksburg, Miss.

[23] Graf, W.H. (1971), *"Hydraulics of Sediment Transport"* , McGraw Hill.

[24] Halliwell, A.R. and Johnston, A.J. (1986), *"Jet Behaviour in Shallow Receiving Water"* , Proceedings of the Institution of Civil Engineers, Part2 Research and Theory, Vol. 81.

[25] Hallmark, D.E. (1955), *"Scour at the Base of a Free Overfall"* , Masters Thesis, Fort Collins, Colorado.

[26] Hallmark, D.E. and Smith, G.L. (1960), *"New Developments for Erosion Control at Culvert Outlets"* , Highway Research Board, Bulletin No. 286, Washington, D.C.

[27] Johnson,S.R. (1979), *"Scour Protection Below Overhanging Culvert Outlets"* , Master's Thesis, University of Saskatchewan, Saskatoon, Saskatchewan.

[28] Karim, M., et al (1971), *"Design Criteria for Controlled Scour and Energy Dissipation at Culvert Outlets Using Rock and a Sill"* , Highway Research Record, Number 373, National Research Council.

[29] Lavelle, J.W. and Mofjeld, H.O. (1987), *"Do Critical Stresses for Incipient Motion Really Exist?"* , Journal of Hydraulic Engineering, ASCE, Vol.113, No. 3.

[30] Macdougall, R.K. and Rajaratnam, N. (1983), *"Erosion by Plane Wall Jets With Minimum Tailwater"* , Journal of Hydraulic Engineering, ASCE, Vol. 109, No. 7.

[31] McCorquodale, J.A. and Zaghloul, N. (1973), *"A Numerical Model for Flow past a Spur-Dike"* , Canadian Hydraulics Conference, The University of Alberta, Edmonton.

[32] Melville, B.W. and Raudviki, A.J. (1977), *"Flow Characteristics in Local Scour at Bridge Piers"* , Journal of Hydraulic Research , 15, No 4, pp 373-380.

[33] Mendoza, C. (1980), *"Headwall Influence on Scour at Culvert Outlets"*, M.S. Thesis, Colorado State University, Fort Collins, Colorado.

[34] Odgaard, A.J. (1986), *"Streambank Protection by Iowa Vanes"* , River Sedimentation, Volume III. Proc. of the Third International Symposium of Sedimentation, University of Mississippi, Mississippi, U.S.A.

[35] Ontario Ministry of Transportation and Communication (1982), *"MTC Drainage Manual"* , Downsview , Ontario.

[36] Peterka, A.J. (1974), *"Hydraulic Design of Stilling Basins and Energy Dissipators"* , United States Government Printing Office, Washington.

[37] Portland Cement Association (1975), *"Concrete Culverts and Conduits"*, Hydraulic Structures Reference Series, Illinois.

[38] Portland Cement Association (1964), *"Handbook of Concrete Culvert Pipe Hydraulics"* , Illinois.

[39] Rajaratnam, N. (1976), *"Turbulent Jets"* , Elsevier Scientific Publishing Company, Amsterdam.

[40] Rajaratnam, N. and Subramanya, K. (1968), *"Plane Turbulent Reattached Wall Jets"* , Journal of the Hydraulic Division, ASCE, Vol. 94, No. HY1.

[41] Rijn, L.C. Von (1984), *"Sediment Transport, Part I: Bed Load Transport"*, Journal of Hydraulic Engineering, vol. 110, No 10.

[42] Sarikelle,S. and Simon, A.L. (1980), *"Field and Laboratory Evaluation of Energy dissipators for Culvert and Storm Drain Outlets"* , Volume 1, University of Akron, Akron, Ohio.

[43] Schilling, M.G. (1974), *"Culvert Outlet Protection Design: Computer Program Documentation"* , Federal Highway Administration, Report No. FHWA-RD-74-501, Washington, D.C.

[44] Schoklitsch, A. (1937), *"Hydraulic Structures"* , ASME, Vol. II.

[45] Schoklitsch, A. (1937), *"Prevention of Scour and Energy Dissipation"*, Translated by Edward, F., Colorado.

[46] Seaburn, G.E. (1962), *"Incipient Motion Caused by a Jet"* , M.S. Thesis, University of Cincinnati, Cincinnati, Ohio.

[47] Simons, D.B.et al (1970), *"Flood Protection at Culvert Outlets"* , Research Report, Colorado State University, Fort Collins, Colorado.

[48] Simons, D.B.et al (1971), *"Riprapped Basins for Culvert Outfalls"*, Highway Research Record number 373, National Research Council.

[49] Smith, C.D. (1973), *"Culvert Velocity Reduction with an Outlet Expansion"* , Concrete Pipe News, American Concrete Pipe Association, Volume 25, No. 5.

[50] Smith, G.L.(1957), *"An Analysis of Scour Below Culvert Outlets"* M.S. Thesis, Colorado A and M College, Fort Collins, Colorado.

[51] Smith, G.L.(1957), *"Scour and Energy Dissipation Below Culvert Outlets"* , Colorado Agricultural and Mechanical College, Fort Collins, Colorado.

[52] Stevens, M.A. (1969), *"Scour in Riprap at Culvert Outlets"* ,Ph.D. Dissertation, Colorado State University, Fort Collins, Colorado.

[53] Suga, K. (1965), *"Stable Shape of Bed in Curved Open Channels"* , Symposium of Hydraulic Research, Japanese Society of Civil Engineers.

[54] Task Committee (1966), *"Sediment Transportation Mechanics: Initiation of Motion"* , Journal of the Hydraulics Division, ASCE, Vol. 92, No. HY2.

[55] Tse, W.L. (1979), *"A Study of Scour at Culvert Outlets"* , Master's Thesis, The University of New Brunswick, Fredericton, New Brunswick.

[56] United States Bureau of Reclamation (1964), *"Hydraulic Design of Stilling Basins and Energy Dissipators"*, A Water Resources Technical Publication, Engineering Monograph No. 25.

[57] Valentin,F. (1967), *"Considerations Concerning Scour in the Case of Flow Under gates"*, Proceedings of the Twelfth Congress of the IAHR, vol.3, Colorado State University, Fort Collins, Colorado.

[58] Vanoni, V. (1964), *"Transportation of Suspended Sediment bt Water"*, Trans. ASCE, vol. 111.

[59] Varga, L. (1966), *"Effect of Tailwater on Oncipient Erosion at Culvert Outlets"*, M.S. Thesis, University of Cincinnati, Cincinnati, Ohio.

Appendix A: Tables

Table A.1: Scour Data

Run	Q	B	y_b	y_t	d_s	X_d	L_s	W_s	X_w	L	H_m
	(l/s)	(cm)	(cm)	(cm)	(cm)	(cm)	(cm)	(cm)	(cm)	(cm)	(cm)
BW1	1.25	50	-	1.1	12.7	21.6	42	45.2	-	-	-
BW2	1.25	50	-	3.2	5.6	13.3	28	27.9	-	53.3	-
BW3	1.25	50	1.9	1.9	6.4	8.9	22.9	29.2	15.2	91.5	1
BW4	1.25	50	-	0.5	10.7	-	38.1	35.6	15.2	50.8	0.5
BW5	1.25	50	9.9	9.9	1.5	4.6	6.4	16.5	5.1	25.4	0.4
BW6	1.25	50	5.7	5.7	1.3	2.5	6.4	20.3	4.6	35.6	0.3
BW7	0.6	50	1.7	1.9	2.2	-	20.3	20.3	8.6	-	0.9
BW8	0.6	50	1.2	0.4	8.1	-	21.6	31	8.9	-	1.3
BW9	0.6	50	0.7	0.6	9.7	-	22.9	38.1	10.2	-	1.1
BW10	0.6	50	0.7	0.8	10.2	-	22.9	38.6	10.2	-	1.8
BW11	0.6	50	1.1	1.5	3.6	4.1	17.8	22.9	6.4	53.3	1.3
BW12	0.6	50	0.7	0.3	9.4	-	25.4	41.9	9.7	-	1.3
BW13	0.6	50	2.4	3	2	2.3	10.7	15.2	2.5	-	-
BW14	2.39	50	3.8	3.8	7.2	17.8	36.8	33	20.3	122	2.2
BW15	2.39	50	2.9	2.9	8.1	14	38.1	33	16.5	99	2.8
BW16	2.39	50	2.4	1.8	12	-	61	34.3	15.2	-	-
BW17	2.39	50	2.3	0.8	18.3	-	61	-	20.3	-	-
BW18	2.39	50	9.1	9	2.5	3.6	11.4	15.2	4.6	45.7	0.6
BW19	2.39	50	5.6	5.7	2.8	15.2	32.3	22.9	16.5	61	0.8
BW20	3.87	50	3.5	3.6	10.8	-	58.4	34.3	24.1	-	3.9
BW21	3.87	50	3.2	3.1	14.6	-	83.8	34.3	20.3	-	-
BW22	3.87	50	3	2.3	20.3	36.8	77.5	-	33	-	-
BW23	3.87	50	12	11.8	6.4	15.2	55.9	28	25.4	72.4	3.3
BW24	3.87	50	5.1	5.5	8.6	15.2	45.7	34.3	19.1	122	2.8
BW25	3.87	50	7.3	7.6	6.9	19	48.3	29.2	20.3	76.2	3.2

Table A.1: Scour Data (continued)

Run	Q	B	y_b	y_t	d_s	X_d	L_s	W_s	X_w	L	H_m
	(l/s)	(cm)	(cm)	(cm)	(cm)	(cm)	(cm)	(cm)	(cm)	(cm)	(cm)
BX26	1.25	50	1.8	1.2	9.7	-	71.1	-	-	-	-
BX27	1.25	50	-	2	4.1	-	40.6	20.3	-	-	-
BX28	1.25	50	-	2.8	2.3	17.8	50.8	17.3	-	-	-
BX29	1.25	50	-	0.9	6.1	-	38.1	33	-	-	-
BY30	1.25	50	2.1	1.6	5.5	8.1	26.7	30.5	13.7	-	2.2
BY31	1.25	50	1.8	1	12	19.1	33	50.8	19.1	-	-
BY32	1.25	50	1.8	0.8	12.2	19.1	35.6	-	15.2	-	-
BY33	1.25	50	3.8	2.9	2	3	8.4	7.6	3	-	-
BY34	1.25	50	1.9	0.5	11.7	19.1	34.3	50.8	14	-	-
BZ35	1.25	50	2	0.8	5.1	-	24.1	24.1	8.9	-	0.9
BZ36	1.25	50	3.1	1.8	4.6	7.6	30.5	22.9	10.2	-	0.9.
BZ37	1.25	50	3	2.5	0	-	-	-	-	-	-
BZ38	1.25	50	2.2	2	2.5	-	28	17.8	12	-	0.8
BZ39	1.25	50	2	1.3	9.7	20.3	31.8	50.8	11	-	-
BZ40	1.25	50	1.9	1.4	8.9	-	35.6	35.6	14.2	-	-
AW41	1.25	50	2.5	0.6	16.5	25.4	59.7	-	25.4	-	-
AW42	1.25	50	2.5	0.9	15	22.9	60.2	30.5	22.9	-	-
AW43	1.25	50	2.4	1.3	10.2	-	69.9	25.4	21.6	-	1.8
AW44	1.25	50	2.5	1.7	9.7	-	62.2	24.1	24.1	-	1.8
AW45	1.25	50	2.6	2.5	8.6	-	71.1	27.9	15.2	119	2.9
AW46	1.25	50	5.3	5.3	7.4	19.1	52.1	27.9	17.8	95.3	3.3
AW47	1.25	50	10.1	10.2	4.3	-	41.9	19.1	12.7	64.8	5.5
AW48	1.25	30	2.4	0.6	14.7	-	50.8	30.5	15.2	-	-
AW49	1.25	30	2.5	1.8	9.7	27.9	66	21.6	19.1	-	1.5
AW50	1.25	30	5.4	5.3	5.1	12.7	55.9	15.2	17.8	76.2	2.8

Table A.1: Scour Data (continued)

Run	Q	B	y_b	y_t	d_s	X_d	L_s	W_s	X_w	L	H_m
	(l/s)	(cm)	(cm)	(cm)	(cm)	(cm)	(cm)	(cm)	(cm)	(cm)	(cm)
AW51	1.25	30	10.2	10.2	4.6	19.1	44.5	17.8	22.9	61	2.8
AW52	1.25	30	2.7	2.8	7.1	12.7	61	21.6	19.1	-	-
AW53	1.25	11	2.7	1.8	10.2	39.4	73.7	11.4	-	-	-
AW54	1.25	11	2.5	2	11.9	44.5	73.7	11.4	-	-	-
AW55	1.25	11	5.3	5.3	3.6	5.1	11.4	8.4	6.4	112	1.5
AW56	1.25	11	10.2	10.2	1.5	7.6	17.8	7.6	6.4	52.1	0.8
DW57	3.87	50	1.8	1.1	10.4	10.2	66	34.3	19.1	-	-
DW58	3.87	50	2.5	2.5	7.6	14	58.4	38.1	17.8	-	-
DW59	3.87	50	3.8	3.8	6.1	11.4	63.5	36.8	15.2	114	2.5
DW60	3.87	50	5.8	5.8	2.3	8.9	30.5	35.6	20.3	105	-
DW61	3.87	50	10.2	10.2	0	-	-	-	-	-	-
DW62	1.25	50	1.1	0.8	8.9	2.5	30.5	40.6	11.4	-	-
DW63	1.25	50	1.1	1.1	4.6	5.1	43.2	43.2	10.2	-	-
DW64	1.25	50	1.7	1.7	3.6	3.8	45.7	33	15.2	88.9	1.3
DW65	1.25	50	2.5	2.5	1	2.5	11.4	24.1	7.6	58.4	0.3
CW66	1.25	50	3.8	3.8	0	-	-	-	-	-	-
CW67	1.25	50	2.5	2.5	4.8	7.6	27.9	30.5	19.1	94	1
CW68	1.25	50	1.8	1.8	6.1	6.4	53.3	40.6	11.4	-	-
CW69	1.25	50	1.3	1.3	9.7	5.1	43.2	36.8	12.7	-	-
CW70	3.87	50	9.1	9.1	0	-	-	-	-	-	-
CW71	3.87	50	5.8	5.8	5.6	11.4	44.5	33	24.1	96.5	2.3
CW72	3.87	50	5.1	5.1	6.4	11.4	34.3	36.8	15.2	88.9	3.8
CW73	3.87	50	2.8	2.8	8.1	15.7	73.7	36.8	16.5	-	-
CW74	3.87	50	1.7	1.7	11.9	19.1	69.9	36.8	14	-	-
CW75	3.87	50	-	0.8	16.3	25.4	74.9	38.1	16.5	-	-

Table A.2: Dimensionless Parameters

Run	$\frac{Q}{WH\sqrt{gH}}$	$\frac{u_1}{v_b}$	$\frac{y_1}{H}$	$\frac{d_s}{H}$	$\frac{L_s}{H}$	$\frac{W_s}{H}$	$\frac{H_m}{H}$	$\frac{d_s}{d_m}$	$\frac{W_s}{d_m}$	$\frac{L_s}{d_m}$	$\frac{L_r}{d_m}$	$\frac{X_d}{d_m}$	$\frac{X_m}{d_m}$
BW1	0.39	-	0.14	1.67	5.51	5.93	-	175.9	626.0	581.7	-	299.2	-
BW2	0.39	-	0.42	0.73	3.67	3.66	-	77.6	386.4	387.8	738.2	184.2	-
BW3	0.39	1	0.25	0.84	3.01	3.83	0.13	88.6	404.4	317.2	1267	123.3	210.5
BW4	0.39	-	0.07	1.40	5.00	4.67	0.07	148.2	493.1	527.7	703.6	-	210.5
BW5	0.39	1	1.30	0.20	0.84	2.16	0.05	20.8	228.5	88.6	351.8	63.7	70.6
BW6	0.39	1	0.75	0.17	0.84	2.66	0.03	18.0	281.2	88.6	493.1	34.6	63.7
BW7	0.19	1.12	0.25	0.29	2.66	2.66	0.12	30.5	281.2	281.2	-	-	119.1
BW8	0.19	0.33	0.05	1.06	2.83	4.07	0.17	112.2	429.4	299.2	-	-	123.3
BW9	0.19	0.86	0.08	1.27	3.01	5.00	0.15	134.3	527.7	317.2	-	-	141.3
BW10	0.19	1.14	0.10	1.34	3.01	5.07	0.23	141.3	534.6	317.2	-	-	141.3
BW11	0.19	1.36	0.20	0.47	2.34	3.01	0.17	49.9	317.2	246.5	738.2	56.8	88.6
BW12	0.19	0.43	0.04	1.23	3.33	4.50	0.17	130.2	580.3	351.8	-	-	134.3
BW13	0.19	1.25	0.39	0.26	1.40	1.99	-	27.7	210.5	148.2	-	31.9	34.6
BW14	0.75	1	0.50	0.94	4.83	4.33	0.29	99.7	457.0	509.7	1690	246.5	281.2
BW15	0.75	1	0.38	1.06	5.00	4.33	0.37	112.2	457.0	527.7	1371	193.9	228.5
BW16	0.75	0.75	0.24	1.57	8.01	4.50	-	166.2	475.0	844.9	-	-	210.5
BW17	0.75	0.35	0.1	2.40	8.01	-	-	253.5	-	844.9	-	-	281.2
BW18	0.75	0.99	1.18	0.33	1.50	1.99	0.08	34.6	210.5	157.9	633	49.9	63.7
BW19	0.75	1.02	0.75	0.37	4.24	3.01	0.11	38.8	317.2	447.4	845	210.5	228.5
BW20	1.21	1.02	0.47	1.42	7.66	4.50	0.51	149.6	475.0	808.9	-	-	333.8
BW21	1.21	0.97	0.41	1.92	11.00	4.50	-	202.2	475.0	1161	-	-	281.2
BW22	1.21	0.77	0.30	2.66	10.17	0.00	-	281.2	-	1073	-	509.7	457.1
BW23	1.21	0.98	1.55	0.84	7.34	3.67	0.43	88.6	387.8	774.2	1003	210.5	351.8
BW24	1.21	1.08	0.72	1.13	6.00	4.50	0.37	119.1	475.0	633.0	1690	210.5	264.5
BW25	1.21	1.04	1.00	0.91	6.34	3.83	0.42	95.6	404.4	669.0	1055	263.2	281.2

Table A.2 Dimensionless Parameters (Continued)

Run	$\frac{Q}{WH\sqrt{}}$	$\frac{u_t}{v_t}$	$\frac{y_t}{H}$	$\frac{d_s}{H}$	$\frac{L_s}{H}$	$\frac{W_s}{H}$	$\frac{H_m}{H}$	$\frac{d_s}{d_m}$	$\frac{W_s}{d_m}$	$\frac{L_s}{d_m}$	$\frac{L_r}{d_m}$	$\frac{X_d}{d_m}$	$\frac{X_m}{d_m}$
BX26	0.39	0.67	0.16	1.27	9.33	0.00	-	80.8	-	592.5	-	-	-
BX27	0.39	-	0.26	0.54	5.33	2.66	-	34.2	169.2	338.3	-	-	-
BX28	0.39	-	0.36	0.30	6.67	2.27	-	19.2	144.2	423.3	-	148.3	-
BX29	0.39	-	0.12	0.80	5.00	4.33	-	50.8	275.0	317.5	-	-	-
BY30	0.39	0.76	0.20	0.72	3.50	4.00	0.28	47.2	261.8	229.2	-	69.5	117.6
BY31	0.39	0.56	0.13	1.57	4.33	6.67	-	103.0	436.0	283.3	-	163.9	163.9
BY32	0.39	0.44	0.10	1.60	4.67	0.00	-	104.7	-	305.6	-	163.9	130.5
BY33	0.39	0.76	0.38	0.26	1.10	1.00	-	17.2	65.2	72.1	-	25.8	25.8
BY34	0.39	0.26	0.07	1.54	4.50	6.67	-	100.4	436.0	294.4	-	163.9	120.2
BZ35	0.39	0.4	0.10	0.67	3.16	3.16	0.12	32.6	154.1	154.1	-	-	56.9
BZ36	0.39	0.58	0.24	0.60	4.00	3.01	0.12	29.4	146.4	195.0	-	48.6	65.2
BZ37	0.39	0.83	0.33	0	0.00	0.00	-	0.0	-	-	-	-	-
BZ38	0.39	0.91	0.26	0.32	3.67	2.34	0.10	16.0	113.8	179.0	-	-	76.7
BZ39	0.39	0.65	0.17	1.27	4.17	6.67	-	62.0	324.8	203.3	-	129.8	70.3
BZ40	0.39	0.74	0.18	1.17	4.67	4.67	-	56.9	227.6	227.6	-	-	90.8
AW41	1.17	0.25	0.08	2.17	7.83	-	-	228.7	-	826.7	-	351.8	351.8
AW42	1.17	0.36	0.12	1.97	7.90	4.00	-	207.6	422.2	833.8	-	316.6	316.6
AW43	1.17	0.53	0.17	1.33	9.17	3.33	0.23	140.7	351.8	967.5	-	-	299.0
AW44	1.17	0.66	0.22	1.27	8.17	3.17	0.23	133.7	334.2	861.9	-	-	334.2
AW45	1.17	0.98	0.33	1.13	9.33	3.67	0.38	119.6	387.0	985.0	1653	-	211.1
AW46	1.17	1.01	0.70	0.97	6.83	3.67	0.43	102.0	387.0	721.2	1319	263.9	246.3
AW47	1.17	1.01	1.33	0.57	5.50	2.50	0.72	59.8	263.8	580.5	897.0	-	175.9
AW48	1.17	0.26	0.08	1.93	6.67	4.00	0.00	204.0	422.2	703.6	-	-	211.1
AW49	1.17	0.71	0.23	1.27	8.67	2.83	0.20	133.7	299.0	914.7	-	387.0	263.9
AW50	1.17	0.99	0.70	0.67	7.33	2.00	0.37	70.4	211.1	774.0	1055	175.9	246.3

Table A.2 Dimensionless Parameters (Continued)

Run	$\frac{Q}{\sqrt{g}H^{\frac{5}{2}}}$	$\frac{u_1}{u_0}$	$\frac{y_1}{H}$	$\frac{d_s}{H}$	$\frac{L_s}{H}$	$\frac{W_s}{H}$	$\frac{H_m}{H}$	$\frac{d_s}{d_m}$	$\frac{W_s}{d_m}$	$\frac{L_s}{d_m}$	$\frac{L}{d_m}$	$\frac{X_d}{d_m}$	$\frac{X_m}{d_m}$
AW51	1.17	0.99	1.33	0.60	5.83	2.83	0.37	63.3	246.3	615.7	844.3	263.9	316.6
AW52	1.17	1.04	0.37	0.93	8.00	2.83	-	98.5	299.0	844.3	-	-	263.9
AW53	1.17	0.66	0.23	1.33	9.67	1.50	-	140.7	158.3	1020	-	-	-
AW54	1.17	0.81	0.27	1.57	9.67	1.50	-	165.3	158.3	1020	-	-	-
AW55	1.17	1.01	0.70	0.47	1.50	1.10	0.20	49.3	116.1	158.3	1548	70.4	88.0
AW56	1.17	1.01	1.33	0.20	2.33	1.00	0.10	21.1	105.5	246.3	721.2	105.5	88.0
DW57	0.72	0.64	0.15	1.37	8.67	4.50	-	144.2	474.9	914.7	-	-	263.9
DW58	0.72	1.02	0.33	1.00	7.67	5	-	105.5	527.7	809.1	-	-	246.3
DW59	0.72	1	0.50	0.80	8.33	4.83	0.33	84.4	510.1	879.5	1583	-	211.1
DW60	0.72	1.01	0.77	0.37	4.00	4.67	-	38.7	492.5	422.2	1460	123.1	281.4
DW61	0.72	1	1.33	0.00	0.00	0.00	-	-	-	-	-	-	-
DW62	0.23	0.69	0.10	1.17	4.00	5.33	-	123.1	562.9	422.2	-	-	158.3
DW63	0.23	1.04	0.15	0.60	5.67	5.67	-	63.3	598.1	598.0	-	-	140.7
DW64	0.23	0.97	0.22	0.47	6.00	4.33	0.17	49.3	457.3	633.2	1231	-	211.1
DW65	0.23	1.02	0.33	0.13	1.50	3.17	0.03	14.1	334.2	158.3	809.1	-	105.5
CW66	0.29	1	0.50	.00	0.00	0.00	-	-	-	-	-	-	-
CW67	0.29	1.02	0.33	0.63	3.67	4.00	0.13	66.8	422.2	387.0	1032	105.5	263.9
CW68	0.29	0.99	0.23	0.80	7.00	5.33	-	84.4	562.9	738.8	-	-	158.3
CW69	0.29	0.98	0.17	1.27	5.67	4.83	-	133.7	510.1	598.1	-	-	175.9
CW70	0.91	1	1.20	0.00	0.00	0.00	-	-	-	-	-	-	-
CW71	0.91	1	0.77	0.73	5.83	4.33	0.30	77.4	457.3	615.7	1337	158.3	334.2
CW72	0.91	1	0.67	0.83	4.50	4.83	0.50	88.0	510.1	475.0	1231	158.3	211.1
CW73	0.91	1	0.37	1.07	9.67	4.83	-	112.6	510.1	1020	-	-	228.7
CW74	0.91	1	0.22	1.57	9.17	4.83	-	165.3	510.1	967.5	-	-	193.5
CW75	0.91	-	0.10	2.13	9.83	5.00	-	225.2	527.7	1038	-	351.8	228.7

Table A.3: Jet Parameters ($\frac{w_i}{B}$; $\frac{u}{U_0}$) for a "mobile bed" condition

hump #	l (cm)	$\frac{Q}{WH^{\frac{3}{2}}}$	$\frac{y_i}{H}$	$\frac{w_i}{B}$	with hump			$\frac{u}{U_0}$	with hump		
					without hump				without hump		
				(2)	(3)	(4)	(5)	(2)	(3)	(4)	(5)
1	-4.5	0.39	0.33	0.51	0.69	1.00	1.00	1.10	0.65	0.50	0.35
				0.40	0.79	1.00	1.00	1.00	1.00	0.95	0.95
		0.53	0.42	0.36	0.36	1.00	1.00	0.85	0.55	0.55	0.20
				0.43	0.43	0.45	0.45	1.00	1.00	0.75	0.50
		0.70	0.42	0.51	0.54	0.93	1.00	0.82	0.67	0.50	0.40
				0.47	0.60	0.60	0.60	1.00	1.00	0.75	0.45
		0.70	0.58	0.34	0.40	0.70	1.00	1.00	0.95	0.78	0.62
				0.45	0.64	0.69	0.69	0.80	0.85	0.82	0.80
		0.97	0.42	0.76	0.77	1.00	1.00	0.90	0.70	0.55	0.50
				0.43	0.38	0.47	0.50	1.05	1.10	0.80	0.70
		1.21	0.42	0.65	0.82	1.00	1.00	1.05	0.80	0.62	0.50
				0.34	0.34	0.43	0.43	1.05	1.00	0.80	0.50
		1.21	0.73	0.40	0.43	0.47	0.51	0.80	0.85	0.70	0.45
				0.47	0.47	0.46	0.45	1.15	0.95	0.80	0.65

Table A.3: (...Continued)

hump #	l (cm)	$\frac{Q}{WH^{\frac{3}{2}}}$	$\frac{y_t}{H}$	$\frac{w_j}{B}$	with hump			$\frac{u}{U_0}$	with hump		
					without hump				without hump		
				(2)	(3)	(4)	(5)	(2)	(3)	(4)	(5)
1	-2.5	0.39	0.33	0.59	0.93	1.00	1.00	0.60	0.70	0.70	0.62
				0.40	0.79	1.00	1.00	1.00	1.00	0.95	0.95
		0.39	0.50	0.45	0.59	0.64	0.74	1.00	0.90	0.80	0.75
				0.45	0.53	0.64	0.69	1.00	0.90	0.80	0.75
		0.70	0.42	0.64	0.78	1.00	1.00	1.00	0.75	0.55	0.45
				0.47	0.60	0.60	0.60	1.00	1.00	0.75	0.45
		0.70	0.58	0.54	0.51	1.00	1.00	0.85	0.75	0.70	0.50
				0.45	0.64	0.69	0.69	0.80	0.85	0.82	0.80
		0.70	0.75	0.44	0.54	0.53	0.59	1.20	1.20	1.00	0.87
				0.40	0.59	0.59	0.54	1.10	1.10	1.00	0.90
		0.97	0.42	0.51	0.42	0.50	0.51	1.05	0.95	0.55	0.55
				0.43	0.38	0.47	0.50	1.05	1.10	0.80	0.70
		1.21	0.73	0.38	0.42	0.52	0.50	1.15	1.10	0.73	0.50
				0.47	0.47	0.46	0.45	1.15	0.95	0.80	0.65
		1.21	0.93	0.44	0.64	0.64	0.93	0.85	0.90	0.85	0.75
				0.44	0.51	1.00	1.00	0.80	0.75	0.80	0.82

Table A.3: (...Continued)

hump #	l (cm)	$\frac{Q}{WH^{\frac{3}{2}}}$	$\frac{y_1}{H}$	$\frac{w_i}{B}$	with hump			$\frac{u}{U_0}$	with hump		
					without hump				without hump		
				(2)	(3)	(4)	(5)	(2)	(3)	(4)	(5)
1	0.0	0.39	0.33	0.45	0.55	1.00	1.00	0.80	0.55	0.50	0.35
				0.40	0.79	1.00	1.00	1.00	1.00	0.95	0.95
		0.53	0.42	0.42	0.51	1.00	1.00	0.85	0.60	0.50	0.30
				0.43	0.43	0.45	0.45	1.00	1.00	0.75	0.50
		0.70	0.42	0.48	0.53	0.73	1.00	1.00	0.70	0.55	0.40
				0.47	0.60	0.60	0.60	1.00	1.00	0.75	0.45
		0.70	0.58	0.35	0.40	0.60	1.00	1.00	0.80	0.55	0.45
				0.45	0.64	0.69	0.69	0.80	0.85	0.82	0.80
		0.97	0.42	0.63	0.71	1.00	1.00	1.05	0.80	0.50	0.45
				0.43	0.38	0.47	0.50	1.05	1.10	0.80	0.70
		1.21	0.42	0.56	0.56	0.75	1.00	1.05	1.00	0.55	0.40
				0.34	0.34	0.43	0.43	1.05	1.00	0.80	0.50
		1.21	0.73	0.46	0.50	0.61	1.00	1.15	0.90	0.65	0.50
				0.47	0.47	0.46	0.45	1.15	0.95	0.80	0.65

Table A.3: (...Continued)

hump #	l (cm)	$\frac{Q}{WH^{\frac{3}{2}}}$	$\frac{y_1}{H}$	$\frac{w_1}{B}$	with hump			$\frac{u}{U_0}$	with hump		
					without hump				without hump		
				(2)	(3)	(4)	(5)	(2)	(3)	(4)	(5)
1	5.0	0.39	0.33	0.41	1.00	1.00	1.00	1.00	0.50	0.50	0.40
				0.40	0.79	1.00	1.00	1.00	1.00	0.95	0.95
		0.53	0.42	0.47	0.45	-	1.00	0.95	0.75	-	0.30
				0.43	0.43	0.45	0.45	1.00	1.00	0.75	0.50
		0.70	0.42	0.47	0.53	0.56	0.63	1.00	0.68	0.47	0.42
				0.47	0.60	0.60	0.60	1.00	1.00	0.75	0.45
		0.70	0.58	0.48	0.41	0.47	0.74	0.95	0.80	0.78	0.50
				0.45	0.64	0.69	0.69	0.80	0.85	0.82	0.80
		0.70	0.75	0.43	0.42	0.58	0.64	1.10	0.95	0.95	0.80
				0.40	0.59	0.59	0.54	1.10	1.10	1.00	0.90
		0.97	0.42	0.44	0.58	0.53	0.67	0.95	0.75	0.55	0.45
				0.43	0.38	0.47	0.50	1.05	1.10	0.80	0.70
		1.21	0.42	0.47	0.56	0.60	0.67	1.05	0.80	0.50	0.30
				0.34	0.34	0.43	0.43	1.05	1.00	0.80	0.50
		1.21	0.73	0.40	0.50	0.55	0.72	1.15	0.95	0.80	0.45
				0.47	0.47	0.46	0.45	1.15	0.95	0.80	0.65

Table A.3: (...Continued)

hump #	l (cm)	$\frac{Q}{WH^{\frac{3}{2}}}$	$\frac{y_t}{H}$	$\frac{w_i}{B}$	with hump / without hump			$\frac{u}{U_0}$	with hump / without hump		
				(2)	(3)	(4)	(5)	(2)	(3)	(4)	(5)
2	-2.5	0.39	0.33	0.43	0.47	1.00	1.00	1.20	0.95	0.80	0.55
				0.39	0.79	1.00	1.00	1.00	1.00	1.00	1.00
		0.53	0.42	0.61	0.61	0.73	1.00	1.00	0.78	0.65	0.50
				0.43	0.43	0.46	0.56	1.00	1.00	0.75	0.50
		0.70	0.42	0.37	0.38	0.40	0.46	1.00	1.00	0.80	0.75
				0.48	0.50	0.55	0.60	1.00	1.00	0.75	0.50
		0.97	0.42	0.61	0.61	0.73	1.00	1.10	1.00	0.55	0.50
				0.43	0.38	0.47	0.50	1.10	1.10	0.90	0.60
		0.70	0.58	0.35	0.40	0.55	0.60	1.30	1.30	1.05	1.05
				0.46	0.46	0.50	0.70	0.95	0.85	0.85	0.80

Table A.4: Jet Parameters ($\frac{w_j}{B}$; $\frac{u}{U_0}$) for a "Fixed Bed" Condition

hump #	l (cm)	$\frac{Q}{WH^{\frac{3}{2}}}$	$\frac{y_t}{H}$	$\frac{w_j}{B}$	with hump			$\frac{u}{U_0}$	with hump		
					without hump				without hump		
				(2)	(3)	(4)	(5)	(2)	(3)	(4)	(5)
1	-4.5	0.53	0.42	0.62	0.65	0.73	0.75	1.00	0.95	0.70	0.70
				0.40	0.48	0.50	0.55	1.00	1.00	0.95	0.95
		0.70	0.42	1.00	1.00	1.00	1.00	0.60	0.50	0.50	0.45
				0.57	0.60	0.65	0.68	1.05	1.00	0.80	0.80
		0.97	0.42	0.75	0.93	1.00	1.00	0.80	0.45	0.40	0.35
				0.53	0.61	0.68	0.73	0.95	0.95	0.95	0.95
		1.21	0.42	1.00	1.00	1.00	1.00	1.00	0.80	0.80	0.70
				1.00	1.00	1.00	1.00	1.00	0.95	0.80	0.75
1	0	0.53	0.42	0.67	0.73	0.75	0.71	1.00	0.90	0.75	0.70
				0.40	0.48	0.50	0.55	1.00	1.00	0.95	0.95
		0.70	0.42	0.65	0.65	0.67	0.69	0.95	0.75	0.62	0.55
				0.57	0.60	0.65	0.68	1.05	1.00	0.80	0.80
		0.97	0.42	0.65	0.65	0.82	0.77	1.20	1.00	0.80	0.70
				0.53	0.61	0.68	0.73	0.95	0.95	0.95	0.95
1	5.0	0.53	0.42	0.54	0.54	0.60	0.68	1.10	0.80	0.70	0.62
				0.40	0.48	0.50	0.55	1.00	1.00	0.95	0.95
		0.70	0.42	0.54	0.59	0.75	0.79	1.00	0.80	0.70	0.65
				0.57	0.60	0.65	0.68	1.05	1.00	0.80	0.80

Table A.4 (...Continued)

hump #	l (cm)	$\frac{Q}{WH^{\frac{3}{2}}}$	$\frac{y_t}{H}$	$\frac{w_i}{B}$	with hump			$\frac{u}{U_0}$	with hump		
				without hump				without hump			
				(2)	(3)	(4)	(5)	(2)	(3)	(4)	(5)
		0.97	0.42	0.63	0.61	0.65	0.74	1.00	0.95	0.75	0.70
				0.53	0.61	0.68	0.73	0.95	0.95	0.95	0.95
1	10.0	0.53	0.42	0.48	0.58	0.58	0.58	1.00	1.00	0.90	0.85
				0.40	0.48	0.50	0.55	1.00	1.00	0.95	0.95
3	-4.5	0.70	0.42	1.00	1.00	1.00	1.00	0.70	0.70	0.70	0.70
				0.57	0.60	0.65	0.68	1.05	1.00	0.80	0.80
		0.97	0.42	1.00	1.00	1.00	1.00	0.70	0.50	0.50	0.45
				0.53	0.61	0.68	0.73	0.95	0.95	0.95	0.95
		0.70	0.58	0.60	0.62	0.70	0.70	1.05	0.85	0.65	0.65
				0.45	0.58	0.63	0.68	0.90	0.85	0.70	0.70
4	-4.5	0.70	0.42	1.00	1.00	1.00	1.00	0.90	1.05	1.05	1.00
				0.57	0.60	0.65	0.68	1.05	1.00	0.80	0.80
		0.97	0.42	1.00	1.00	1.00	1.00	0.65	0.70	0.70	0.70
				0.53	0.61	0.68	0.73	0.95	0.95	0.95	0.95
		0.70	0.58	0.90	1.00	1.00	1.00	1.00	0.80	0.65	0.55
				0.45	0.58	0.63	0.68	0.90	0.85	0.70	0.70
5	0	0.53	0.42	0.68	0.72	0.74	0.75	1.00	0.85	0.75	0.70
				0.40	0.48	0.50	0.55	1.00	1.00	0.95	0.95

Table A.4: (...Continued)

hump #	l (cm)	$\frac{Q}{WH^{\frac{3}{2}}}$	$\frac{y_t}{H}$	$\frac{w_i}{B}$	with hump / without hump			$\frac{u}{U_0}$	with hump / without hump		
				(2)	(3)	(4)	(5)	(2)	(3)	(4)	(5)
		0.70	0.42	1.00	1.00	1.00	1.00	0.70	0.55	0.50	0.45
				0.57	0.60	0.65	0.68	1.05	1.00	0.80	0.80
		0.97	0.42	1.00	1.00	1.00	1.00	0.85	0.75	0.50	0.50
				0.53	0.61	0.68	0.73	0.95	0.95	0.95	0.95
6	0	0.53	0.42	-	1.00	1.00	1.00	-	1.05	0.85	0.70
				0.50	0.55	0.64	0.69	1.25	1.25	1.25	1.25
		0.97	0.42	-	0.88	0.88	0.88	-	0.80	0.60	0.55
				0.77	0.77	0.72	0.70	1.10	1.10	0.75	0.90
7	0	0.53	0.42	-	0.69	0.73	0.80	-	0.95	0.80	0.70
				0.50	0.55	0.64	0.69	1.25	1.25	1.25	1.25
		0.97	0.42	-	1.00	1.00	1.00	-	0.90	0.75	0.60
				0.77	0.77	0.72	0.70	1.10	1.10	0.75	0.90
8	0	0.53	0.42	-	0.70	0.74	0.85	-	0.80	0.70	0.65
				0.50	0.55	0.64	0.69	1.25	1.25	1.25	1.25
		0.97	0.42	-	0.86	0.88	0.88	-	0.80	0.80	0.70
				0.77	0.77	0.72	0.70	1.10	1.10	0.75	0.90

Appendix B: Figures

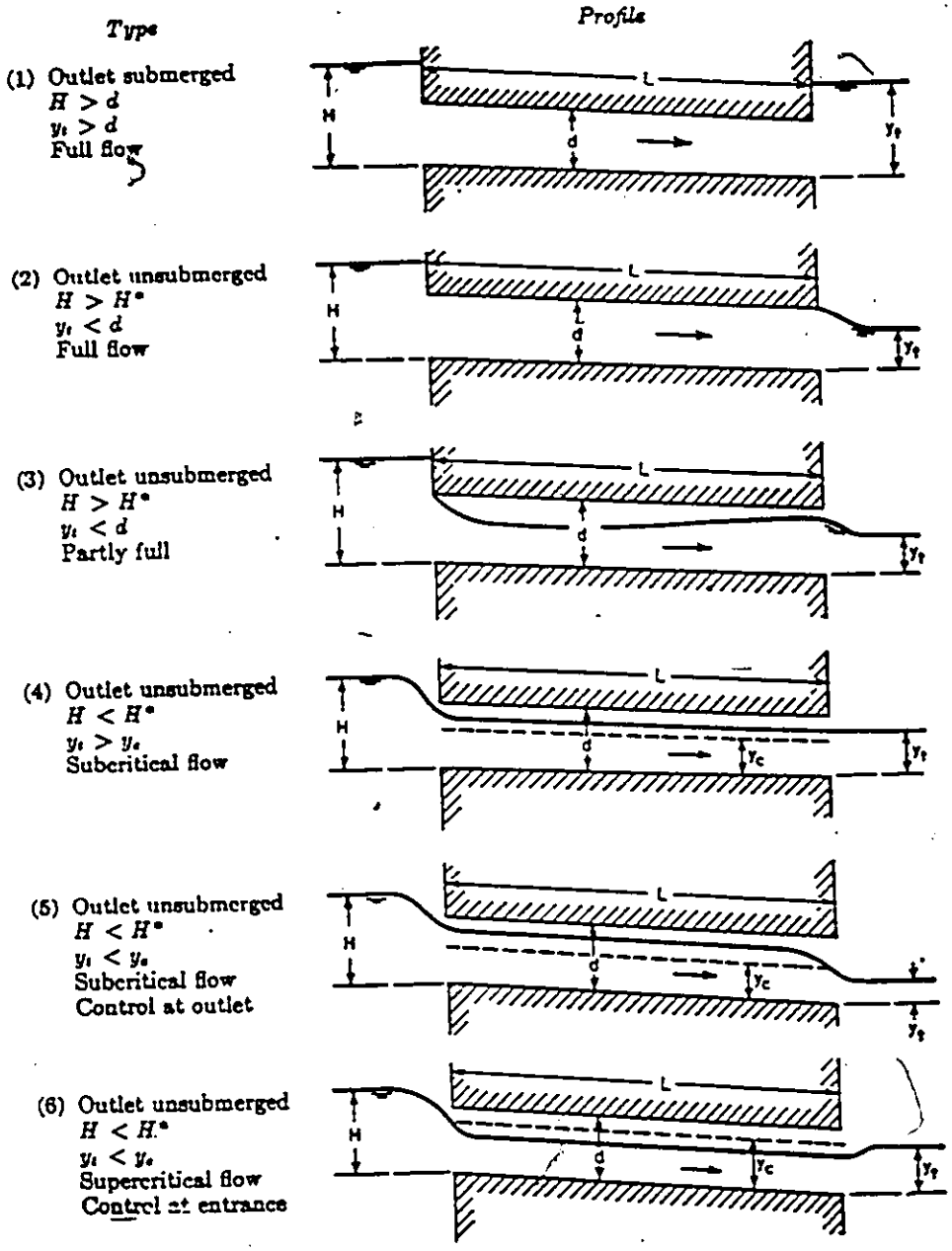

Fig.1: Types of Culvert Flow (after Chow, 1987).

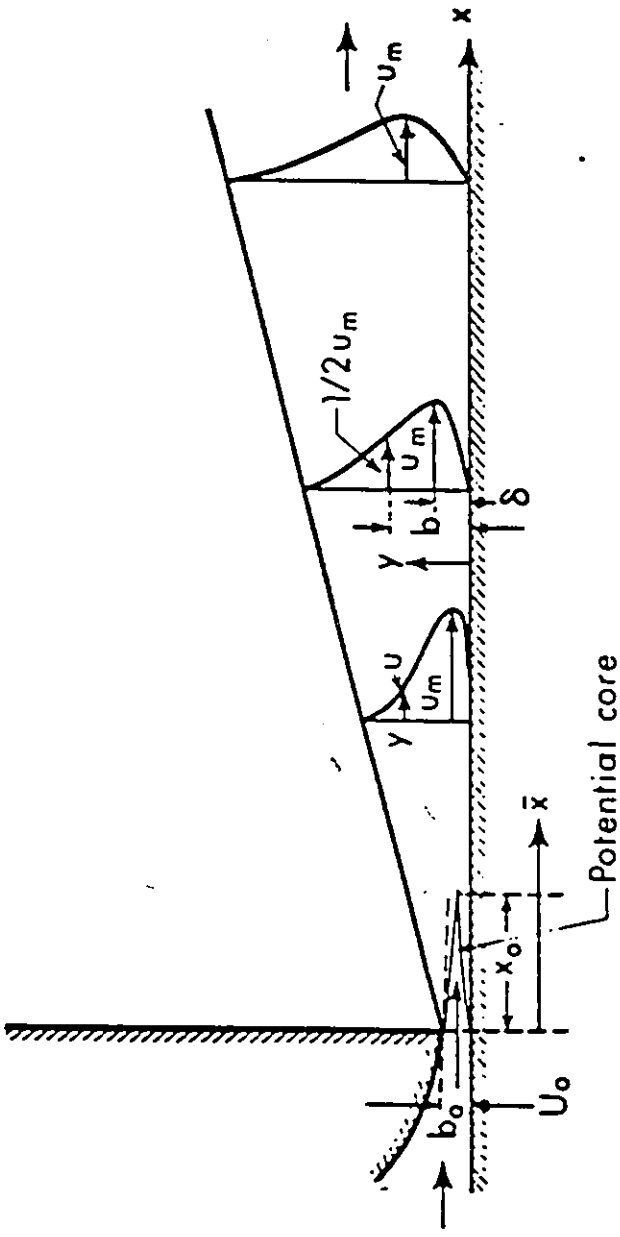

Fig.2: Definition Sketch of Plane Turbulent Wall Jets.

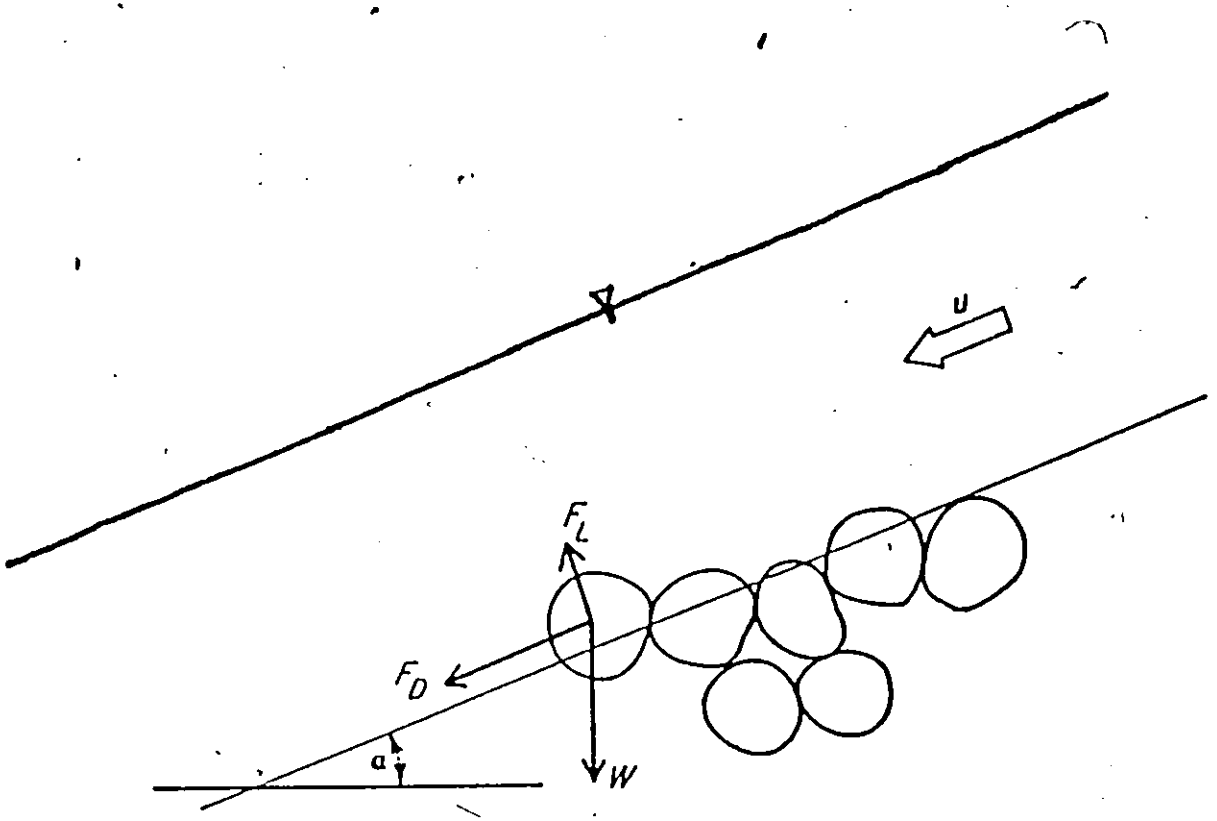

Fig.3: Principal Forces Acting on a Particle in a Cohesionless Loose Bed

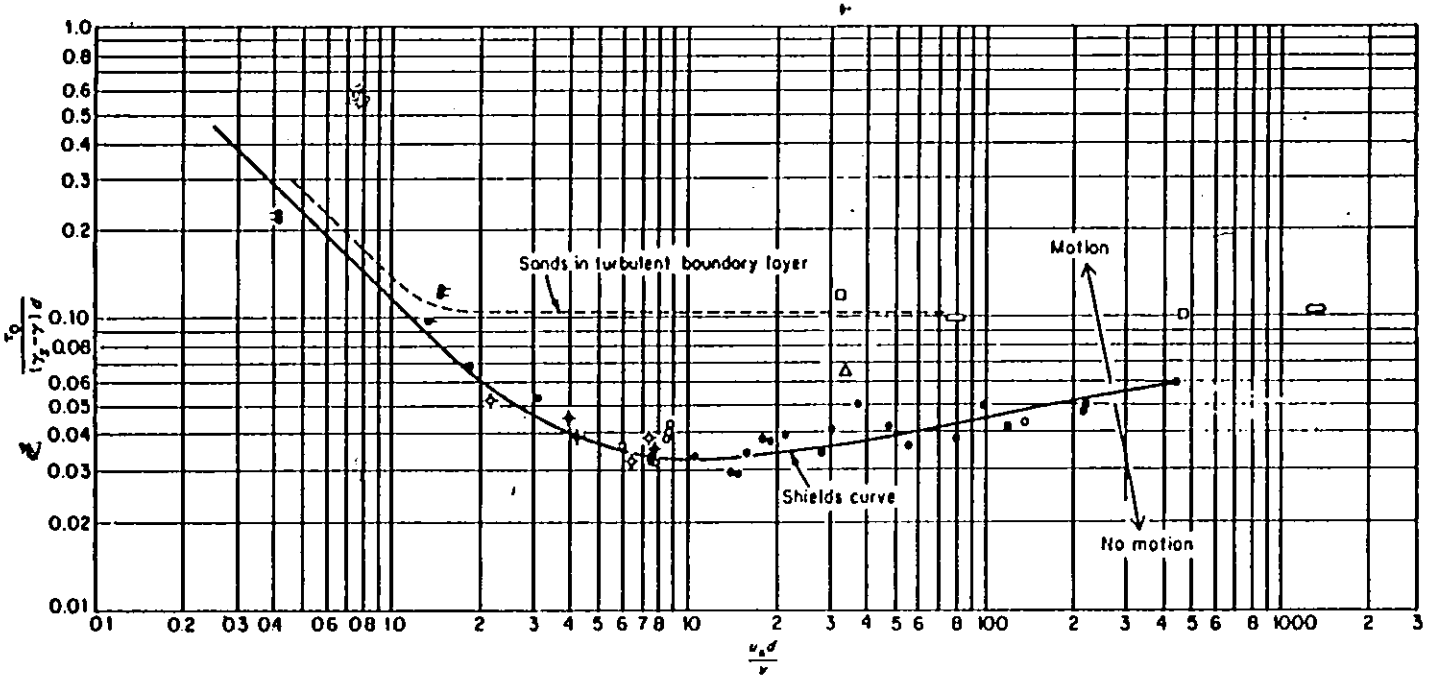

Fully developed turbulent velocity profile	Sym	Description		γ_s, g/cm³
	o	Amber	(Shields)	1.06
	•	Lignite		1.27
	•	Granite		2.7
	•	Barite		4.25
	•	Sand (Casey)		2.65
	✧	Sand (Kramer)		2.65
	✦	Sand (USWES)		2.65
	•	Sand (Gilbert)		2.65

Turbulent boundary layer		
•-	Sand (Vanoni)	2.65
-•	Glass beads (Vanoni)	2.49
□	Sand (White)	2.61
⬭	Sand in air (White)	2.10
△	Steel shot (White)	7.9

Fig.4: Shields Digram; Dimensionless Critical Shear Stress vs. Shear Reynlods Number (after Vanoni, 1964).

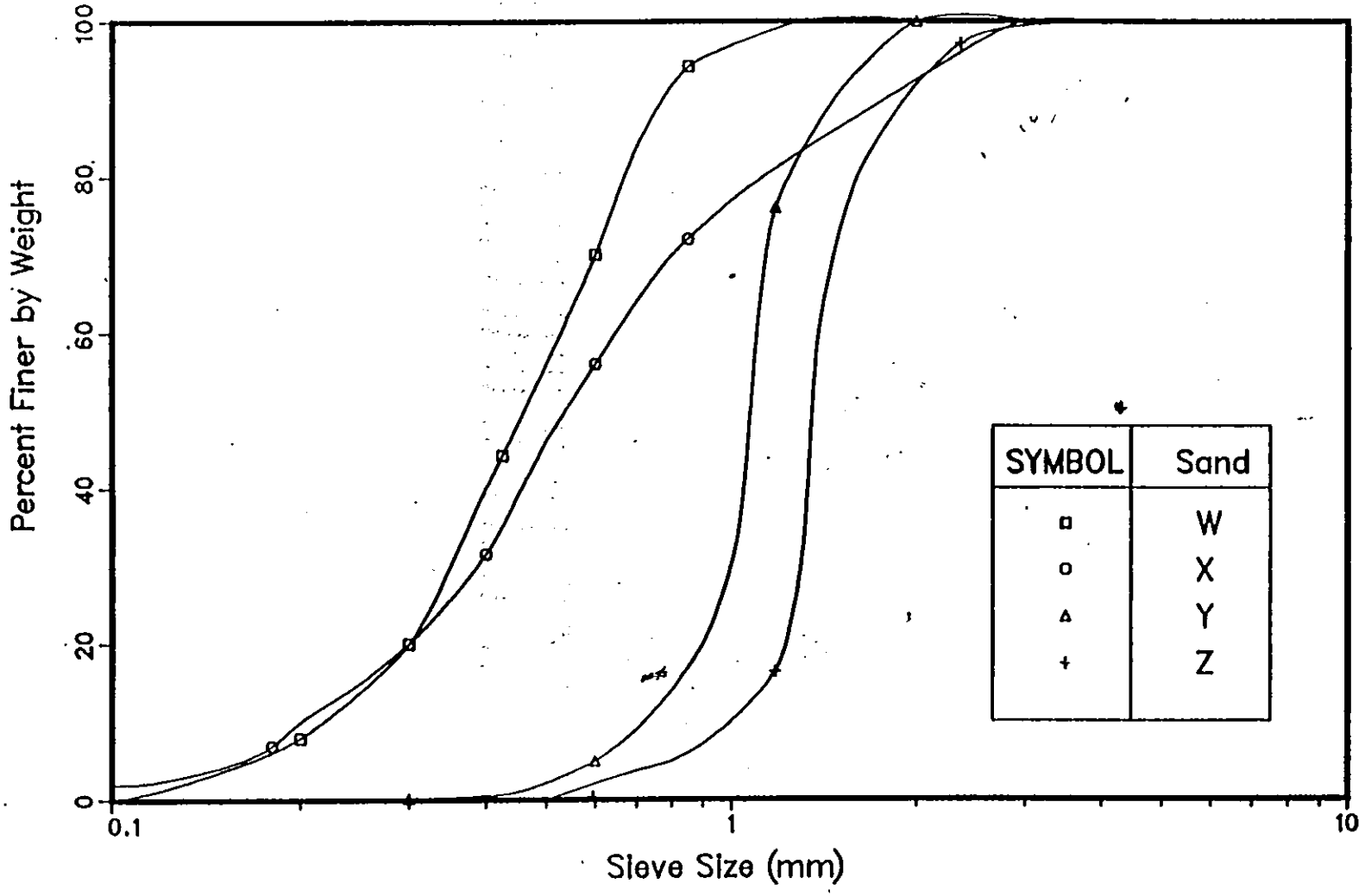

Fig.5: Grain Size Distributions for the Four Types of Sand Examined.

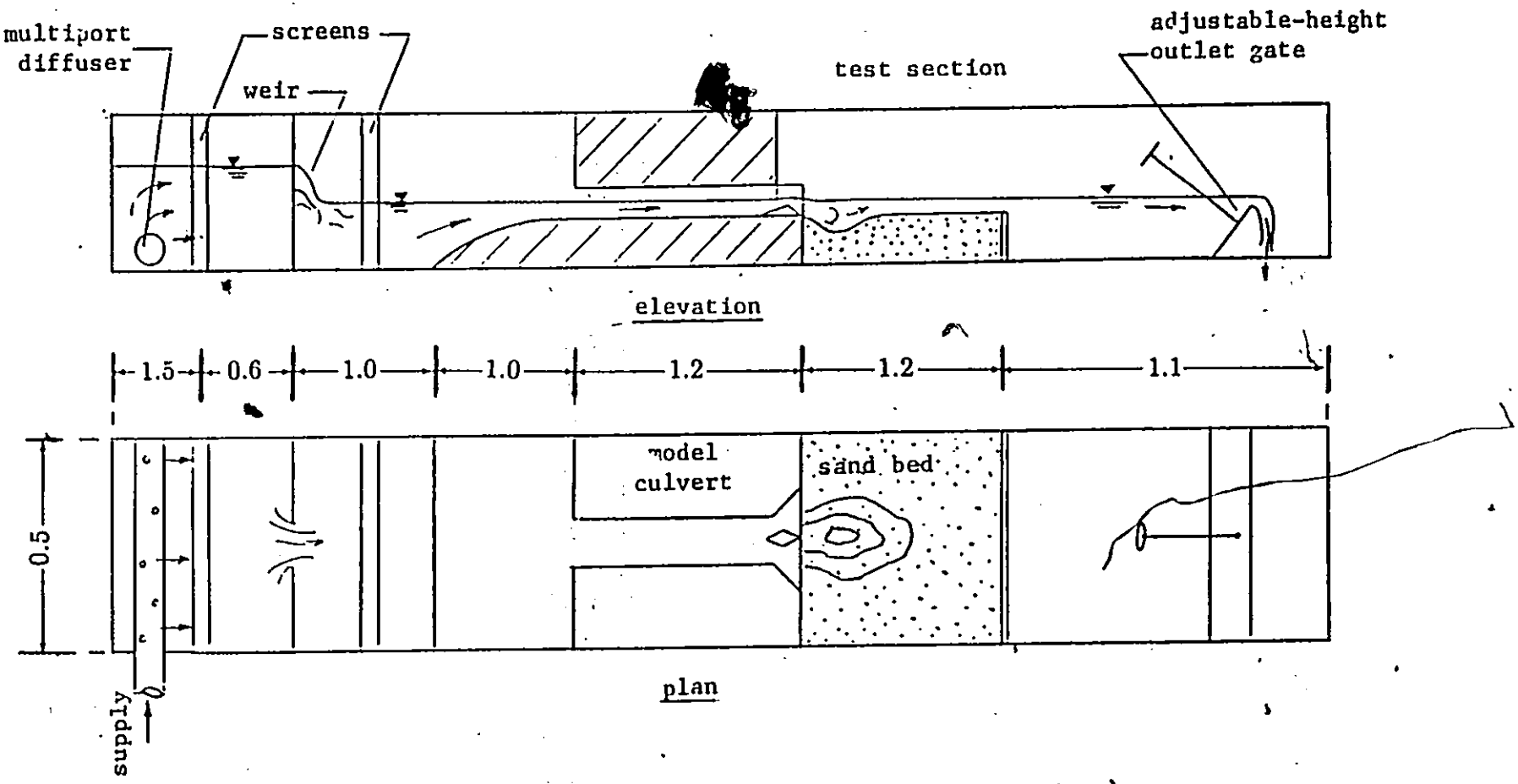

Fig.6: Experimental Apparatus (not to scale, all dimensions are in meters).

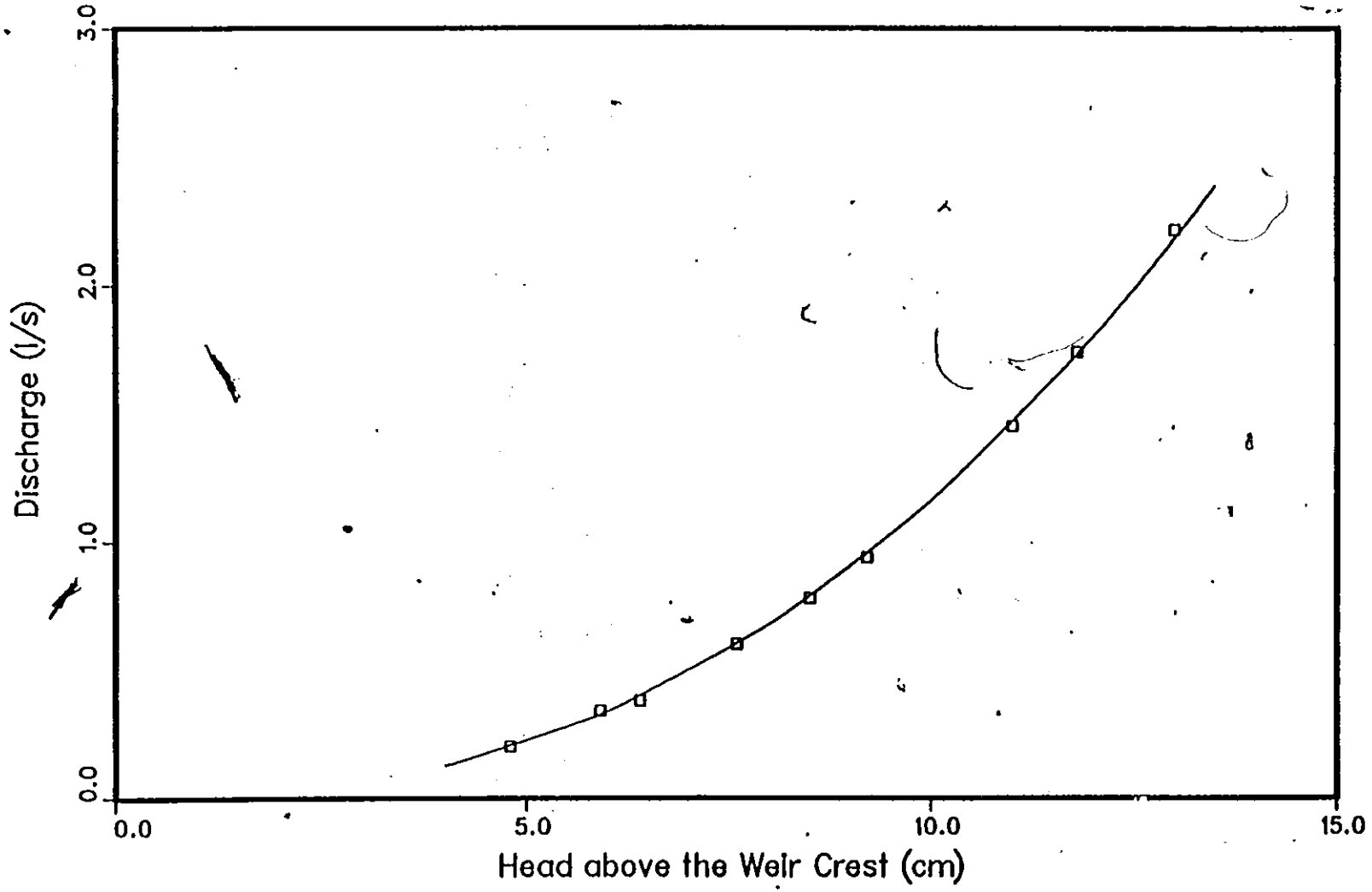

Fig.7: Calibration of the Triangular Weir.

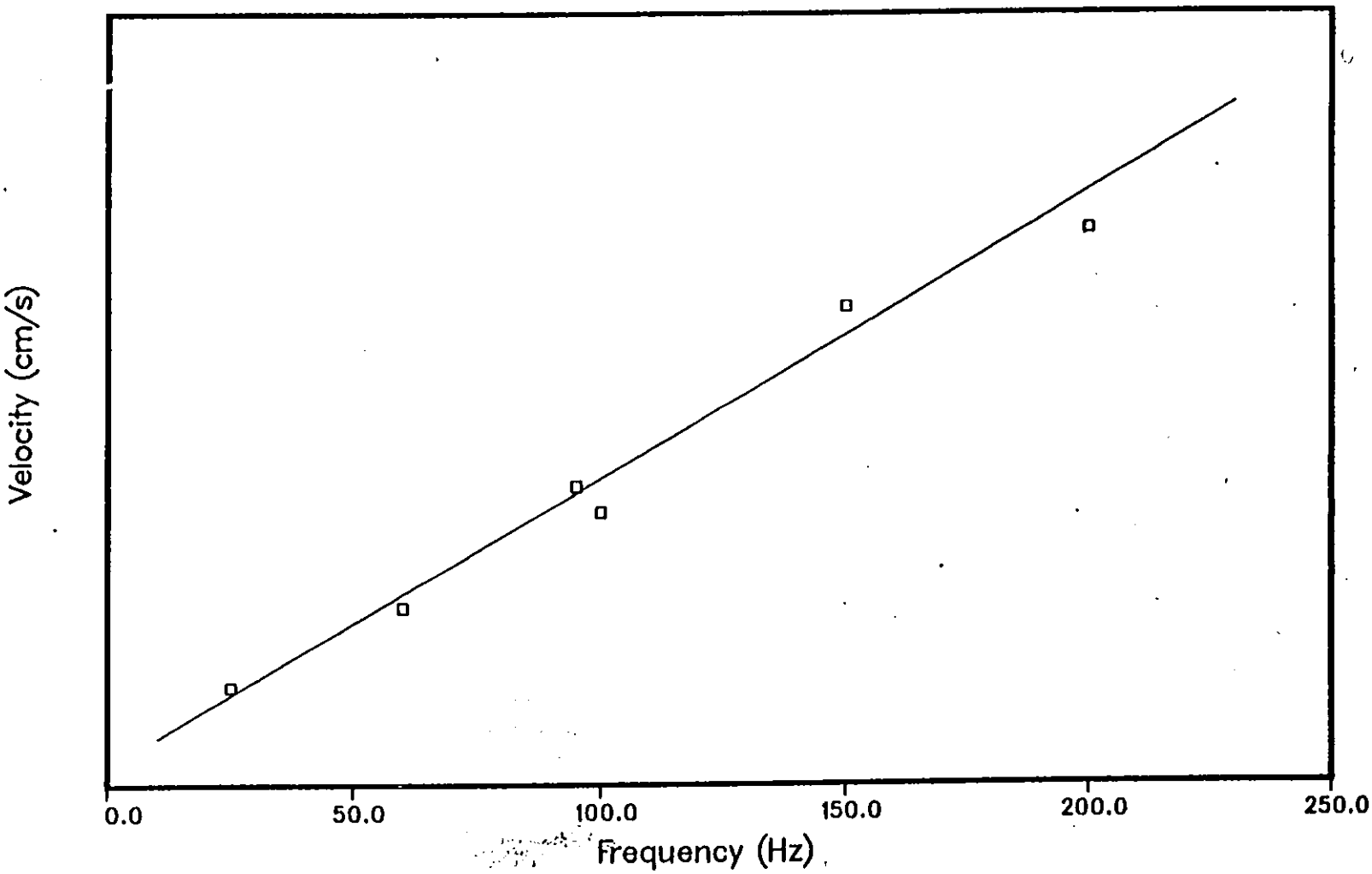

Fig.8: Validation of the Supplied Equation Correlating Velocities and the Current Meter Frequency Readings.

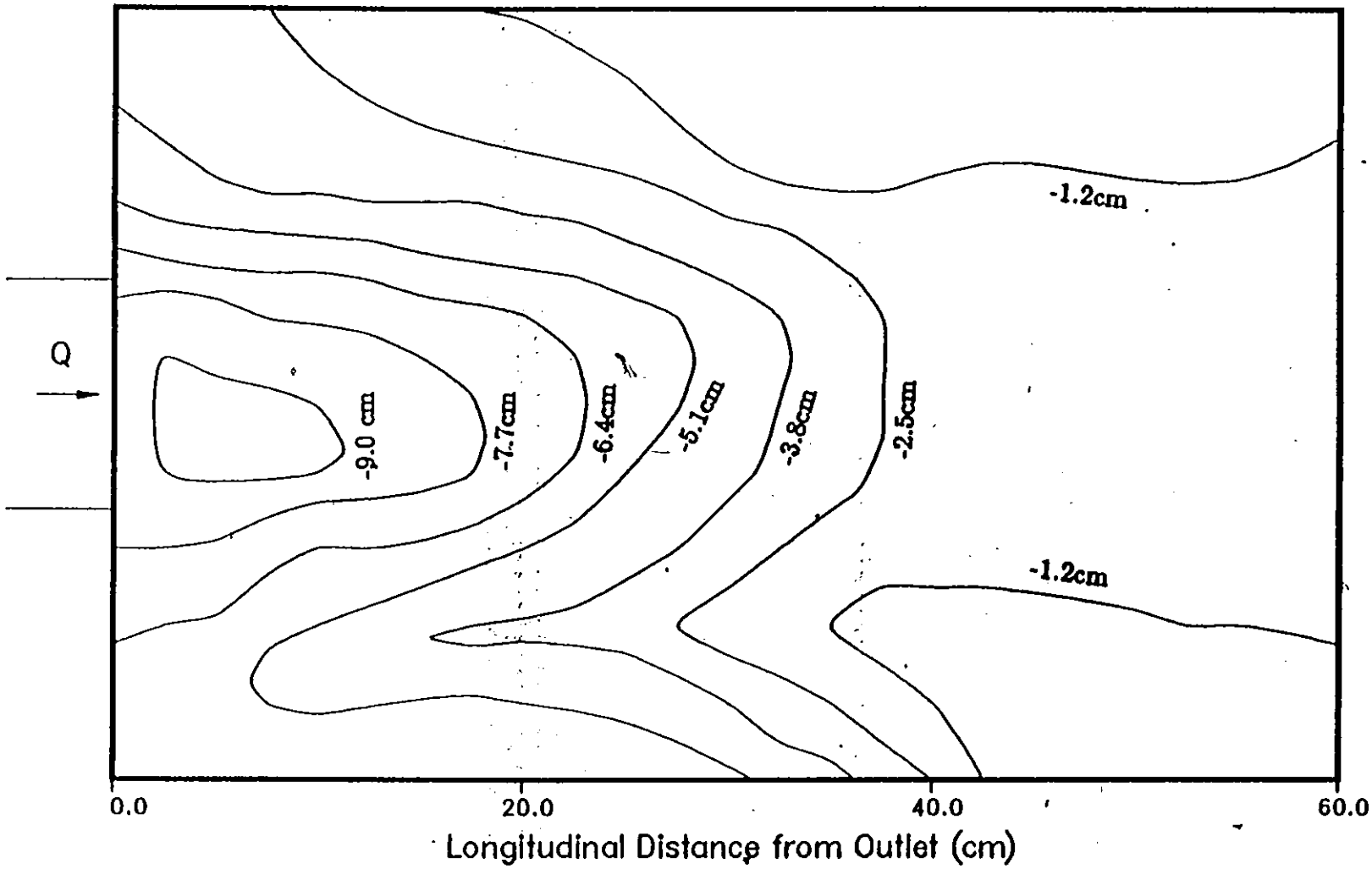

Fig.9: Contours Showing Scour Hole Pattern for Run BX26.

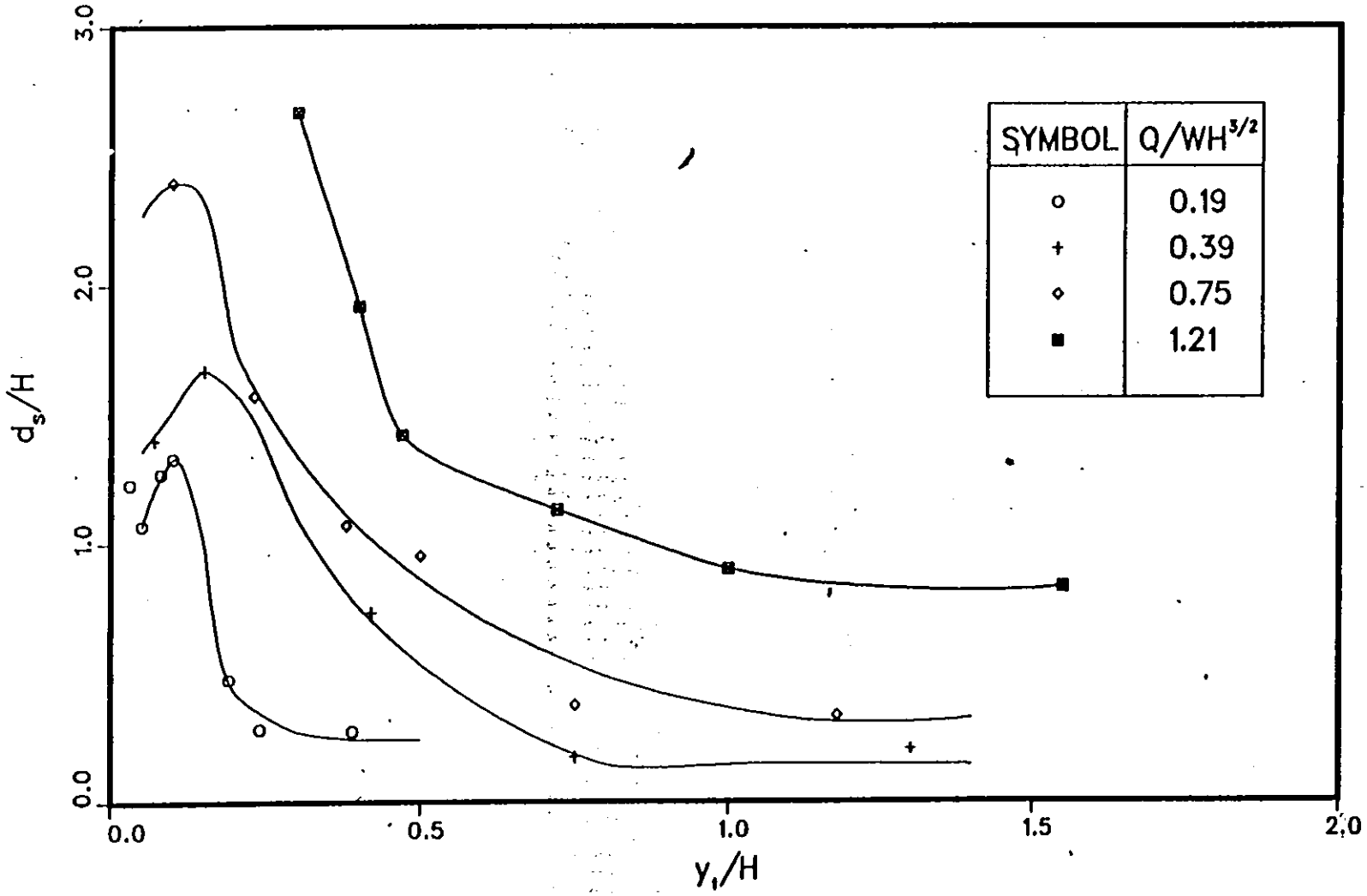

Fig.10: Functional Relationships Between Scour Depth and Principal Flow Characteristics for a Given Culvert Size.

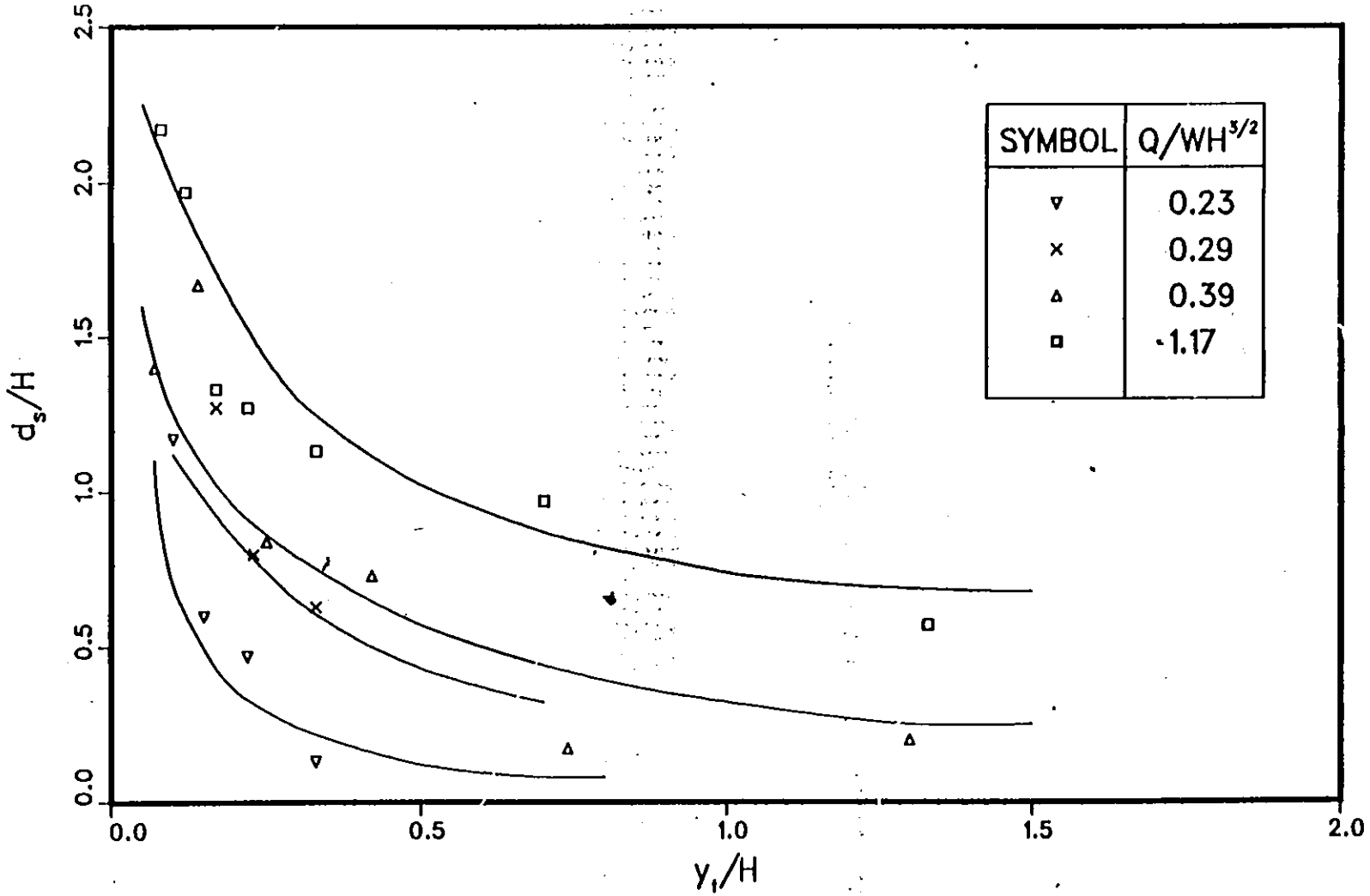

Fig.11: Functional Relationships Between Scour Depth and Principal Flow Characteristics for a Given Discharge (Q = 1.25l/s) and Different Culvert Sizes.

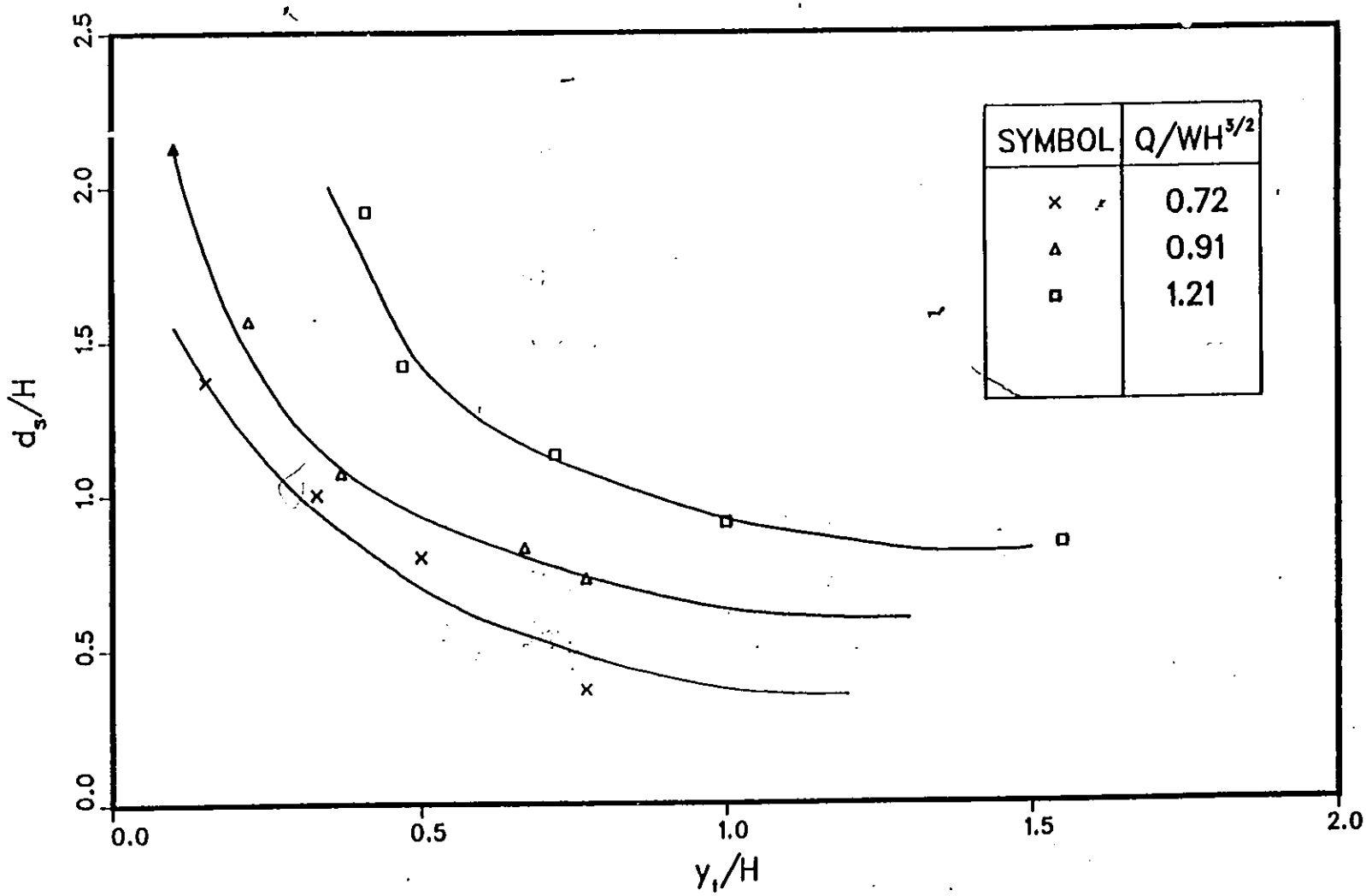

Fig.12: Functional Relationships Between Scour Depth and Principal Flow Characteristics for a Given Discharge (Q = 3.87l/s) and Different Culvert Sizes.

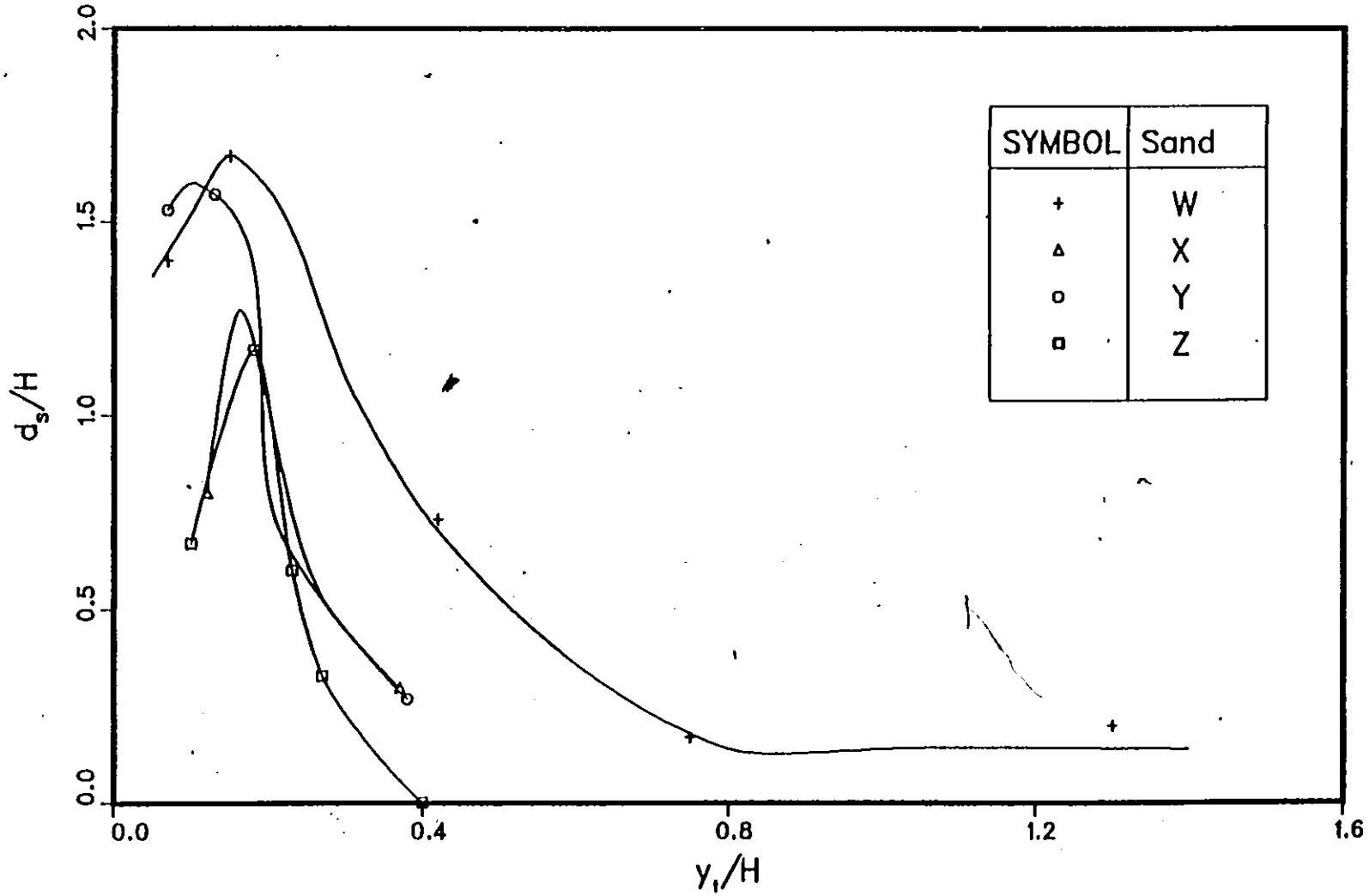

Fig.13: Functional Relationships Between Scour and Tailwater Depths for Different Types of Sand.

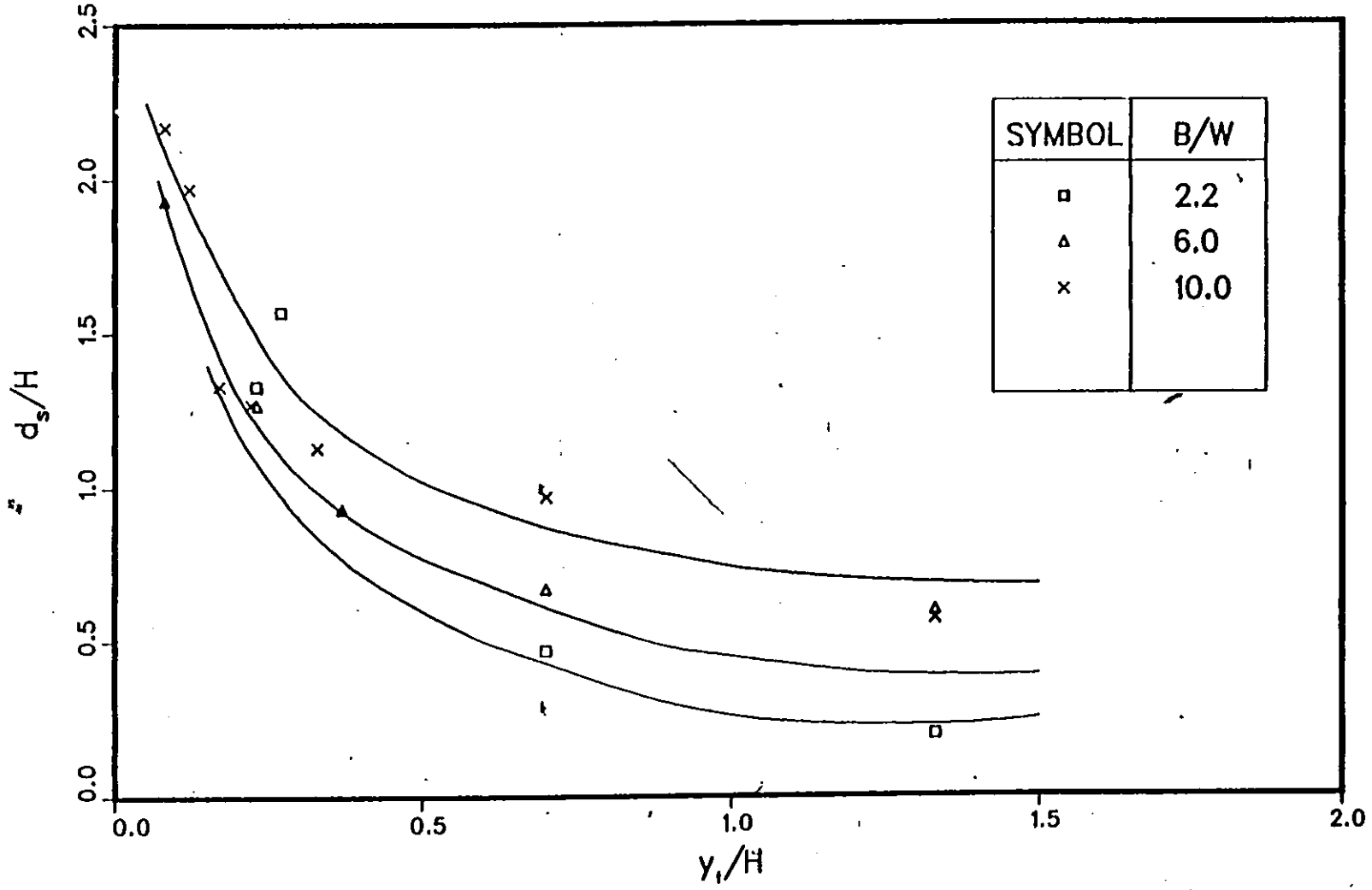

Fig.14: Functional Relationships Between Scour and Tailwater Depth for Different Downstream Channel Widths.

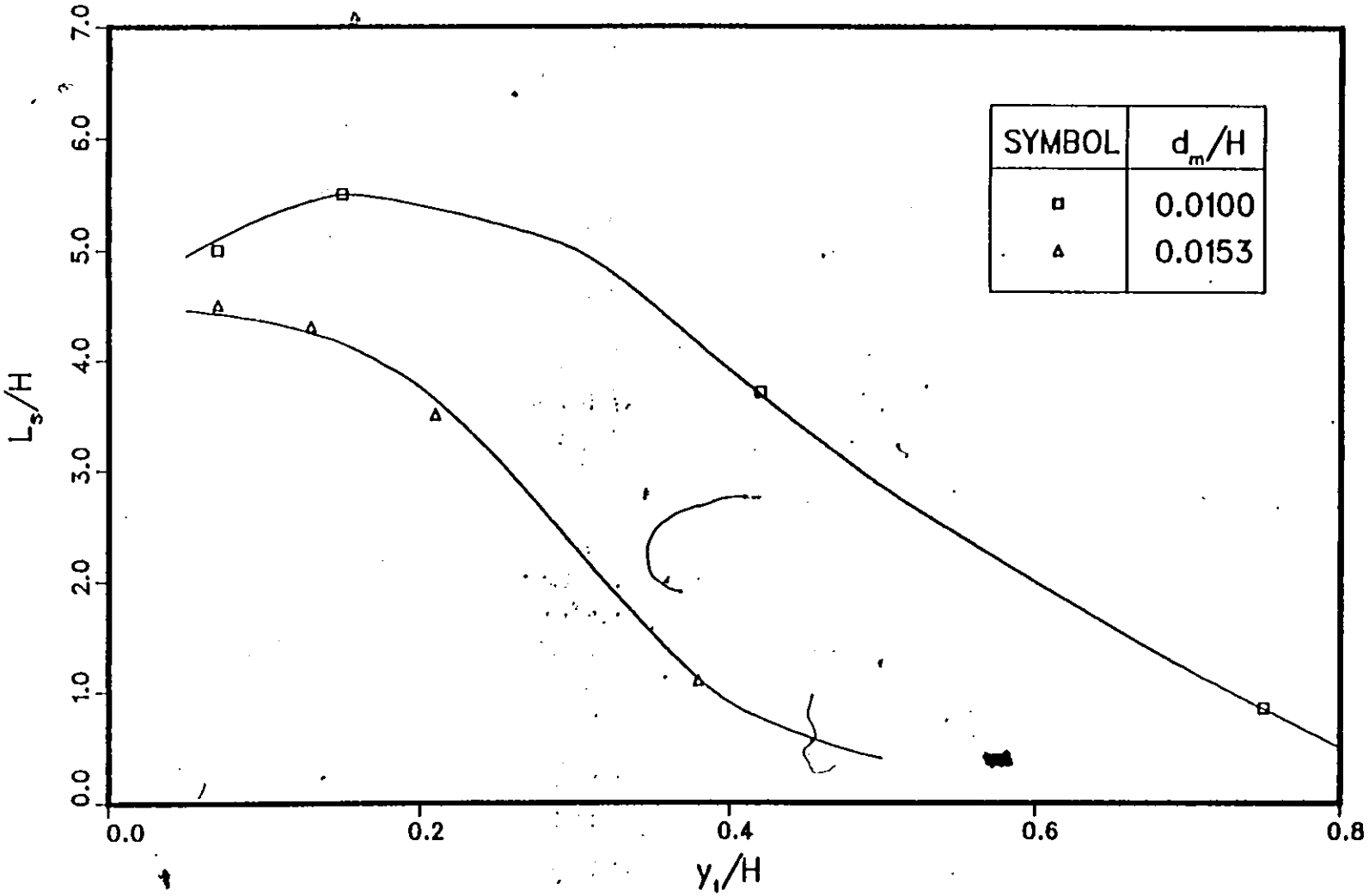

Fig.15: Functional Relationships Between Scour Length, Tailwater Depth and Bed Material Effective Grain Size.

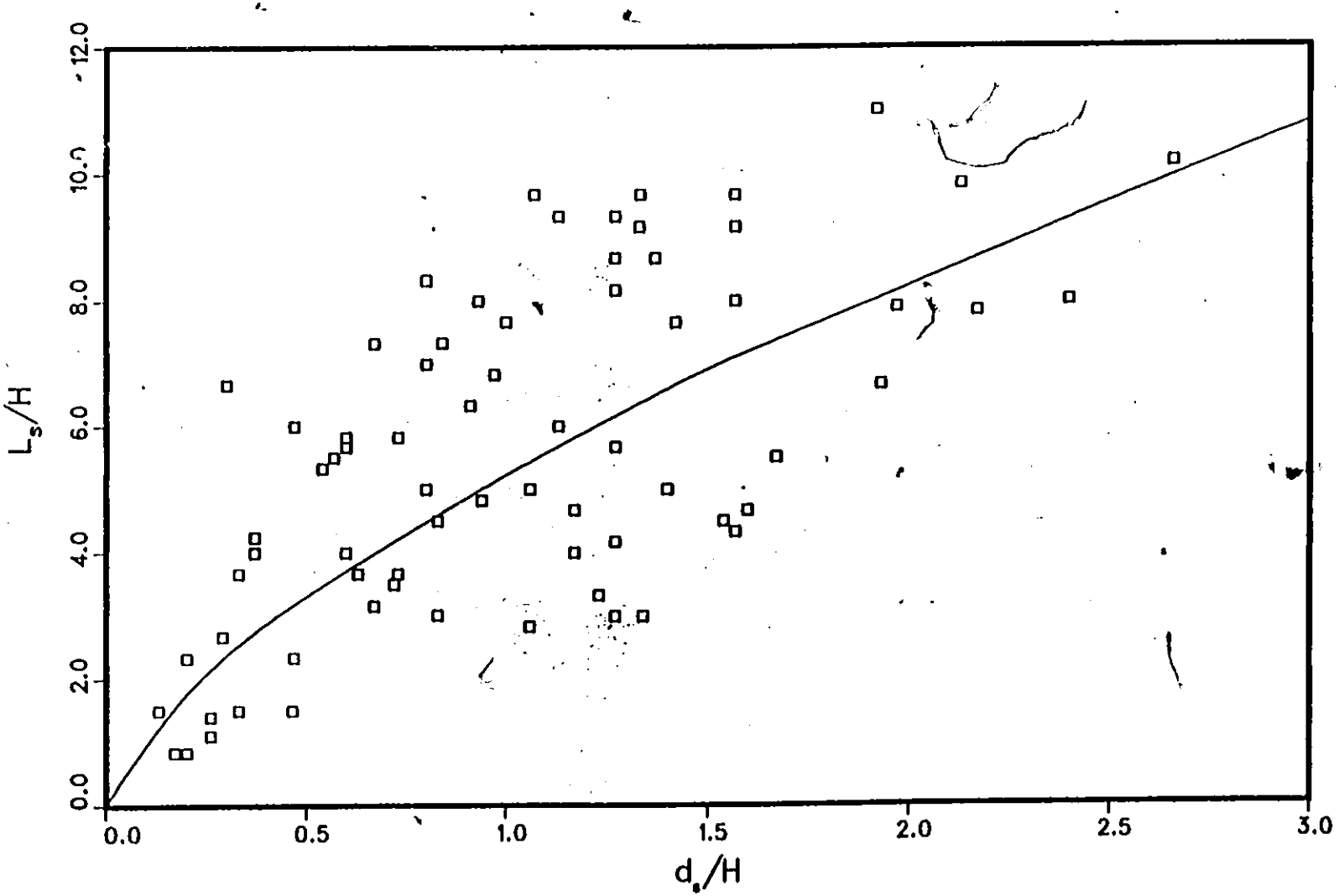

Fig.16: Functional Relationship Between Scour Length and the Maximum Depth of Scour

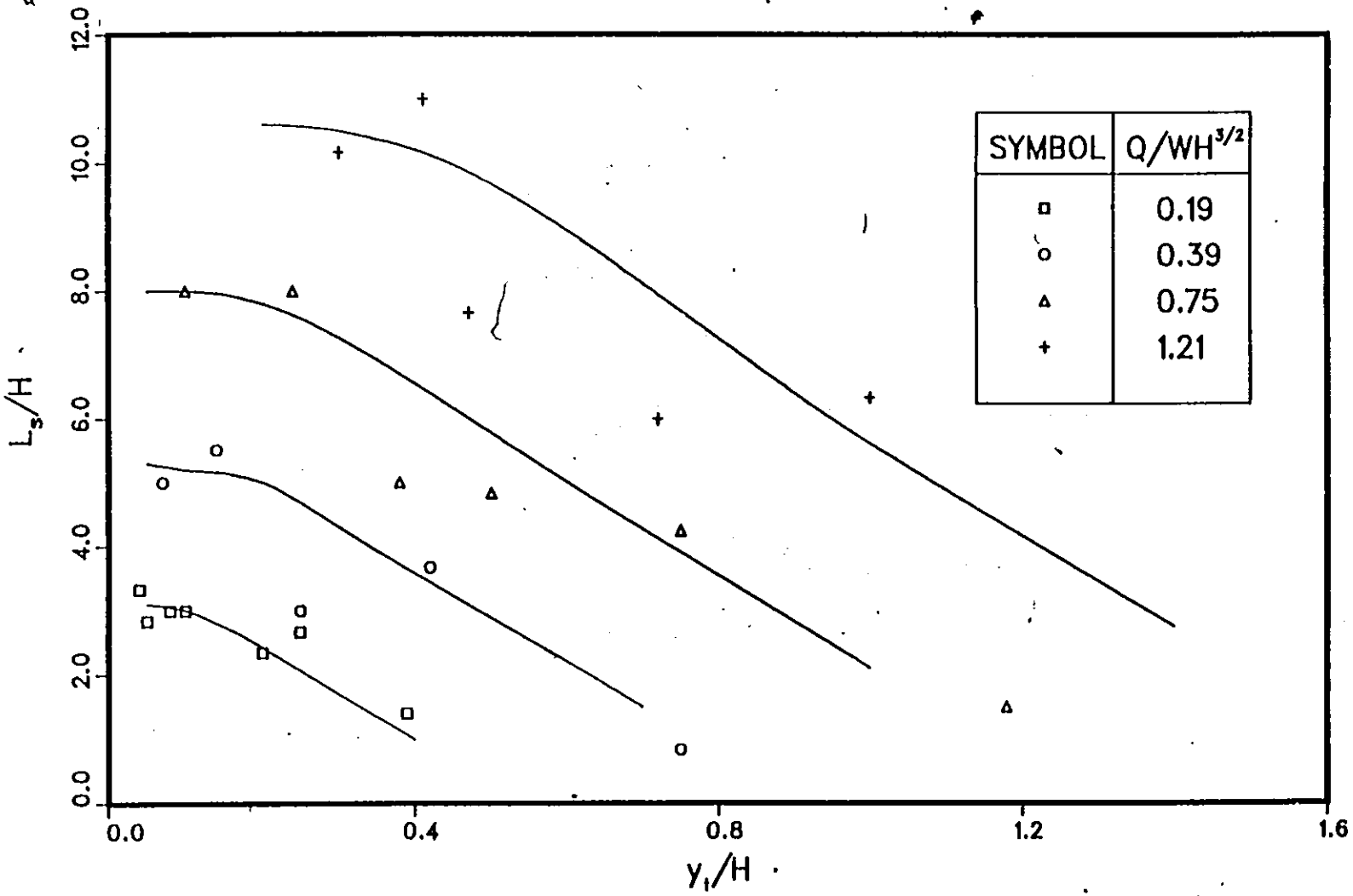

Fig.17: Functional Relationships Between Scour Length and Flow Principal Characteristics.

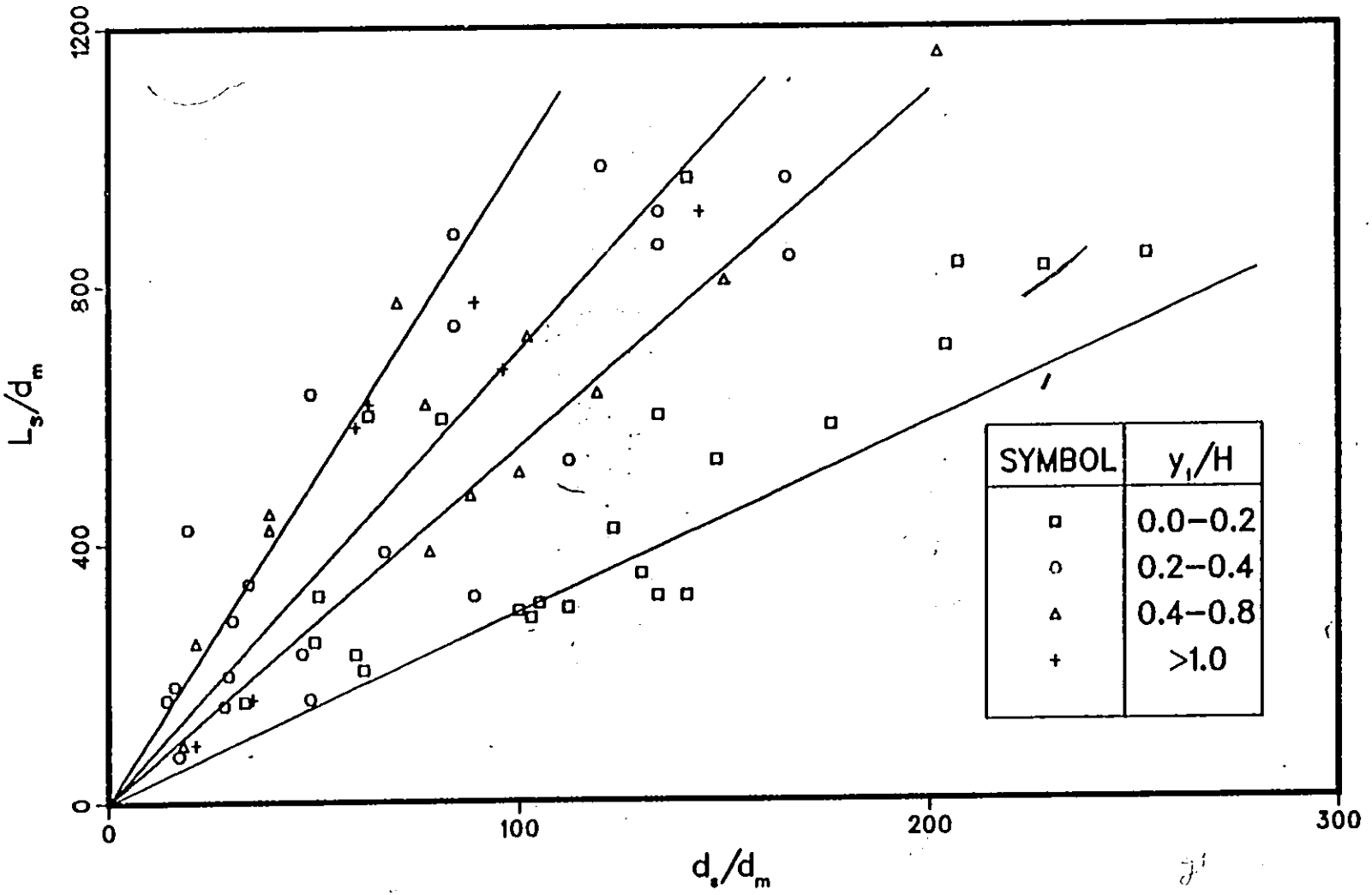

Fig.18: Functional Relationships Between Scour Length and Maximum Depth of Scour for Different Tailwater Depths.

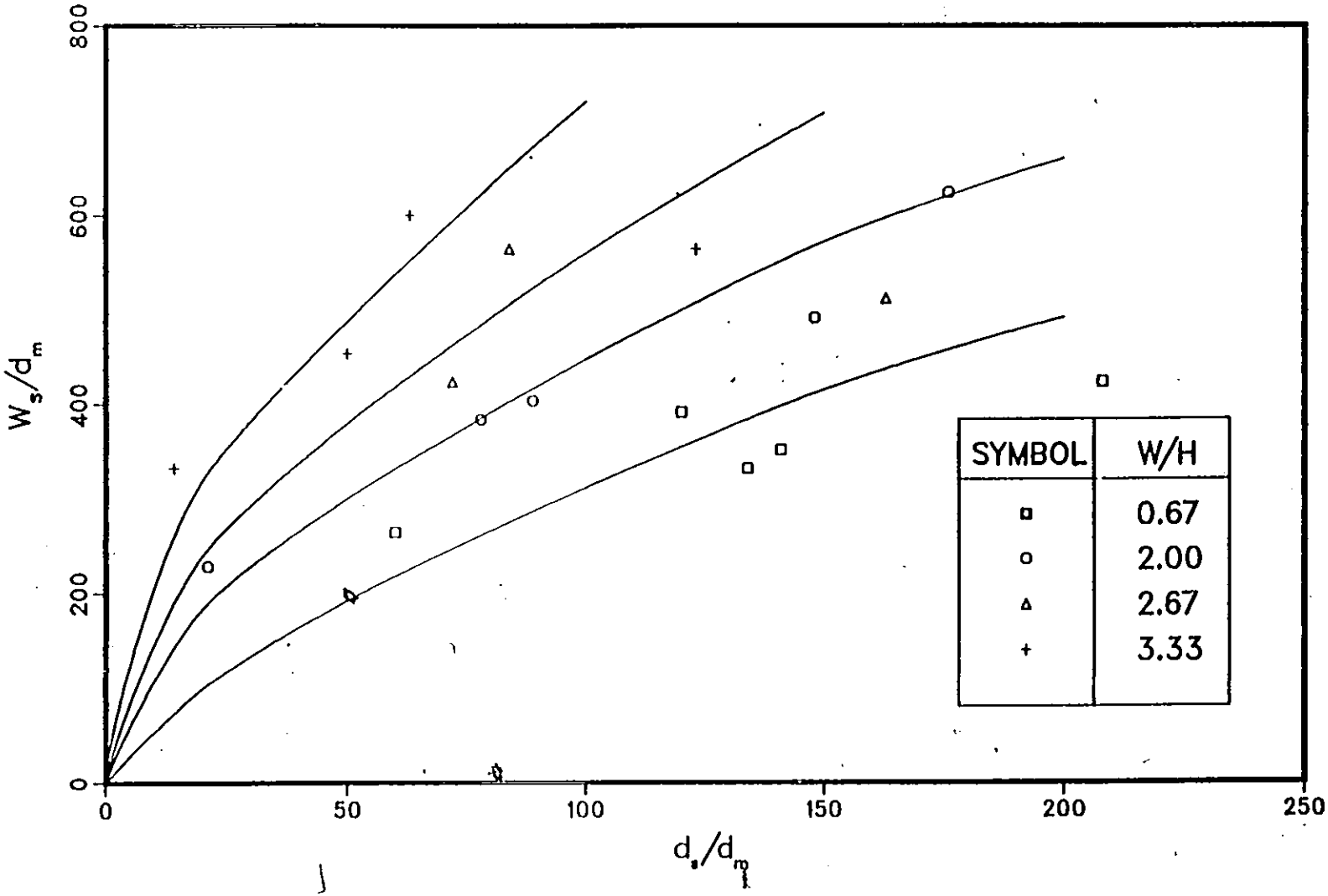

Fig.19: Functional Relationships Between Scour Width, Maximum Depth of Scour and Culvert Width.

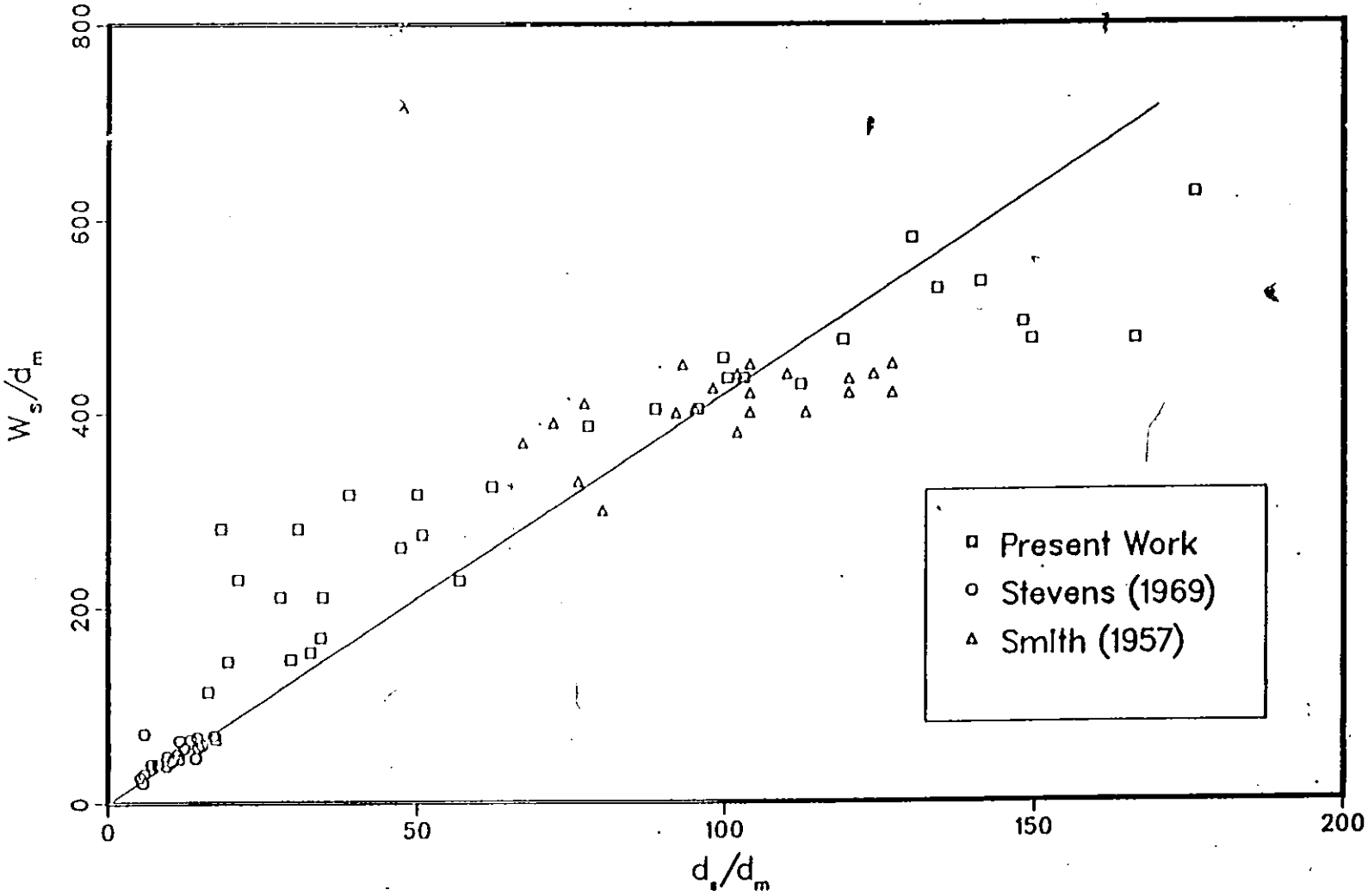

Fig.20: Functional Relationship Between Scour Width and the Maximum Depth of Scour

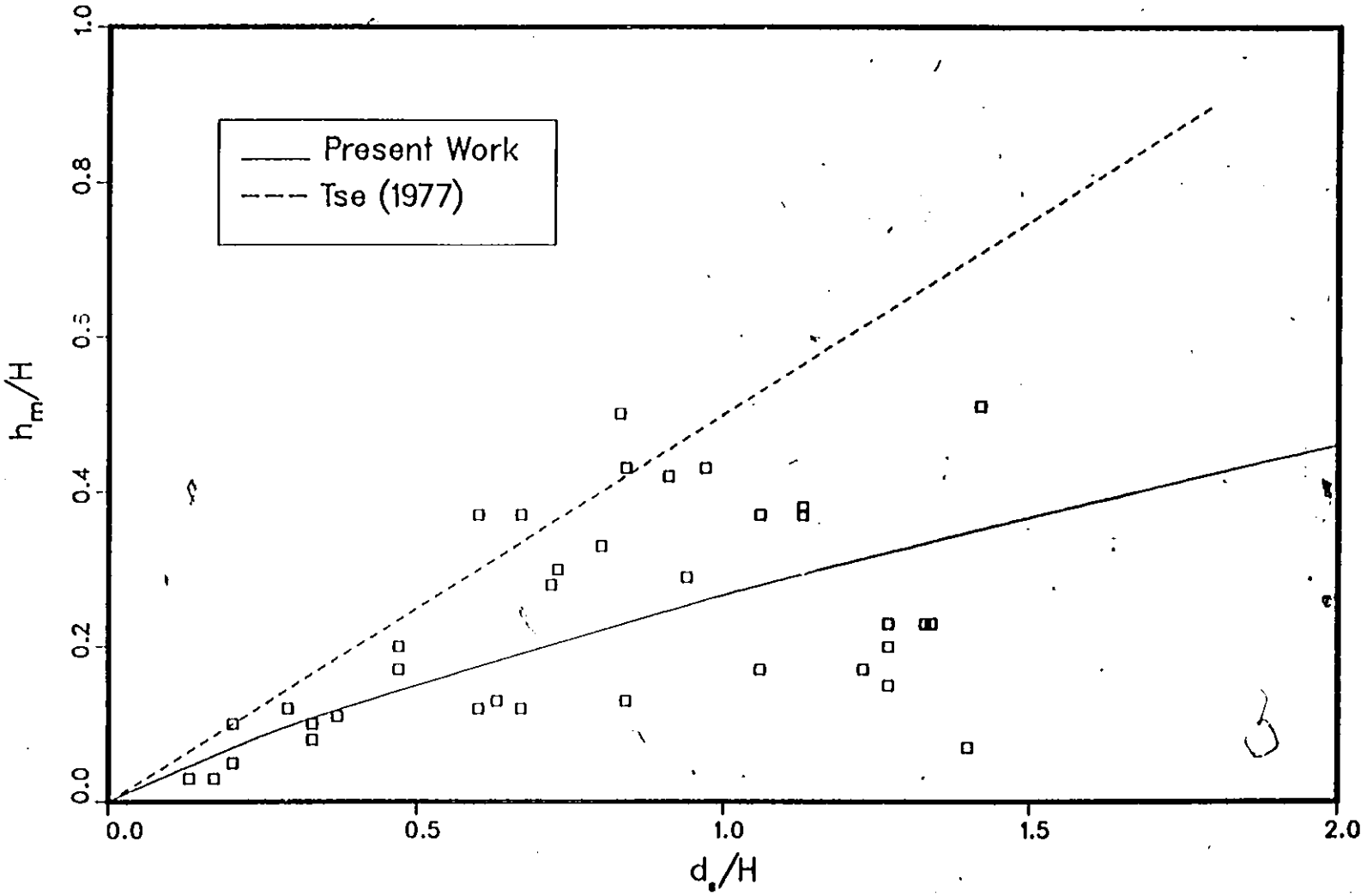

Fig.21: Functional Relationship Between the Height of Sediment Mound and the Maximum Depth of Scour

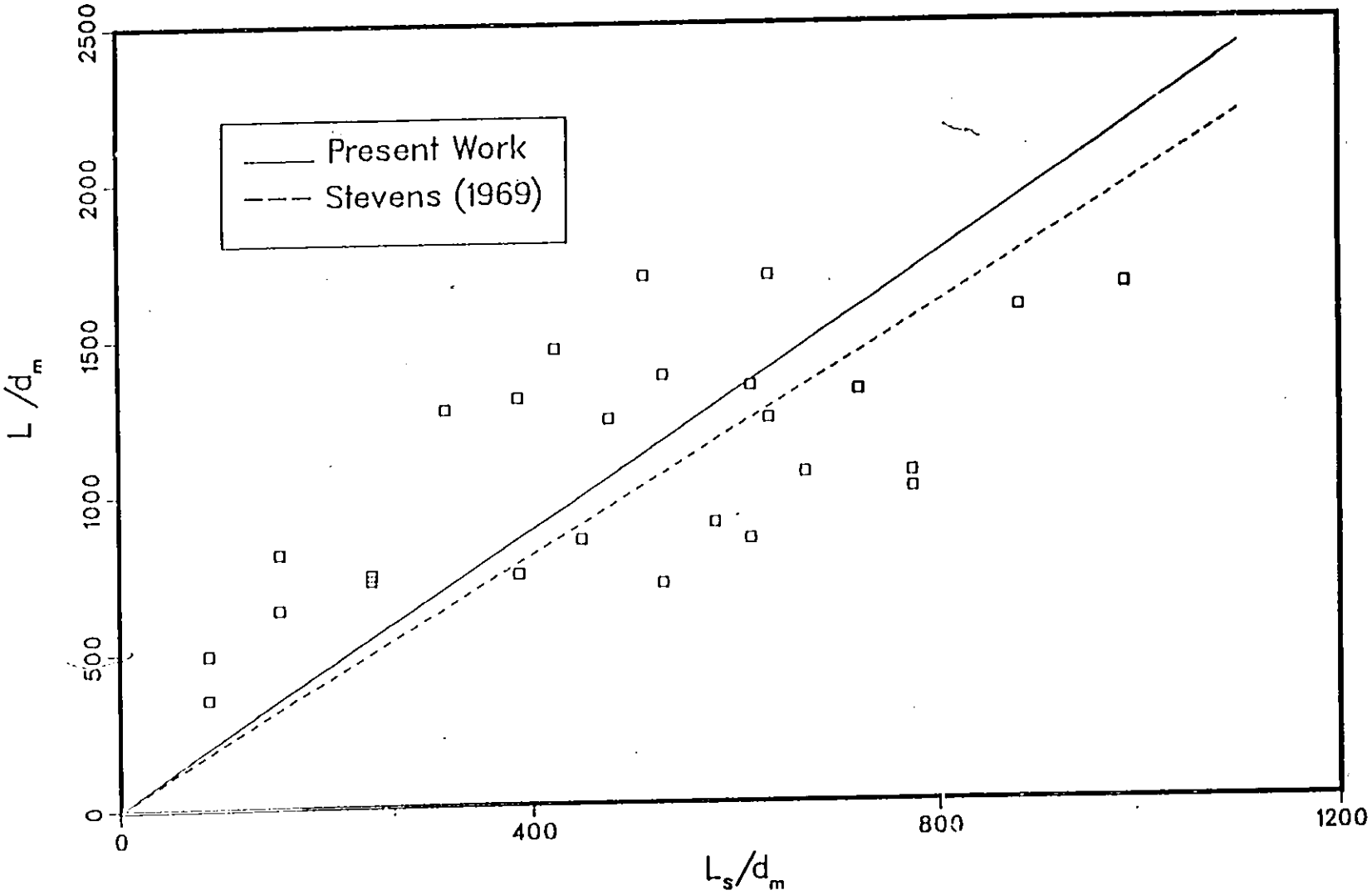

Fig.22: Functional Relationship Between the Distance to the End of Sediment Deposition and the Scour Hole Length.

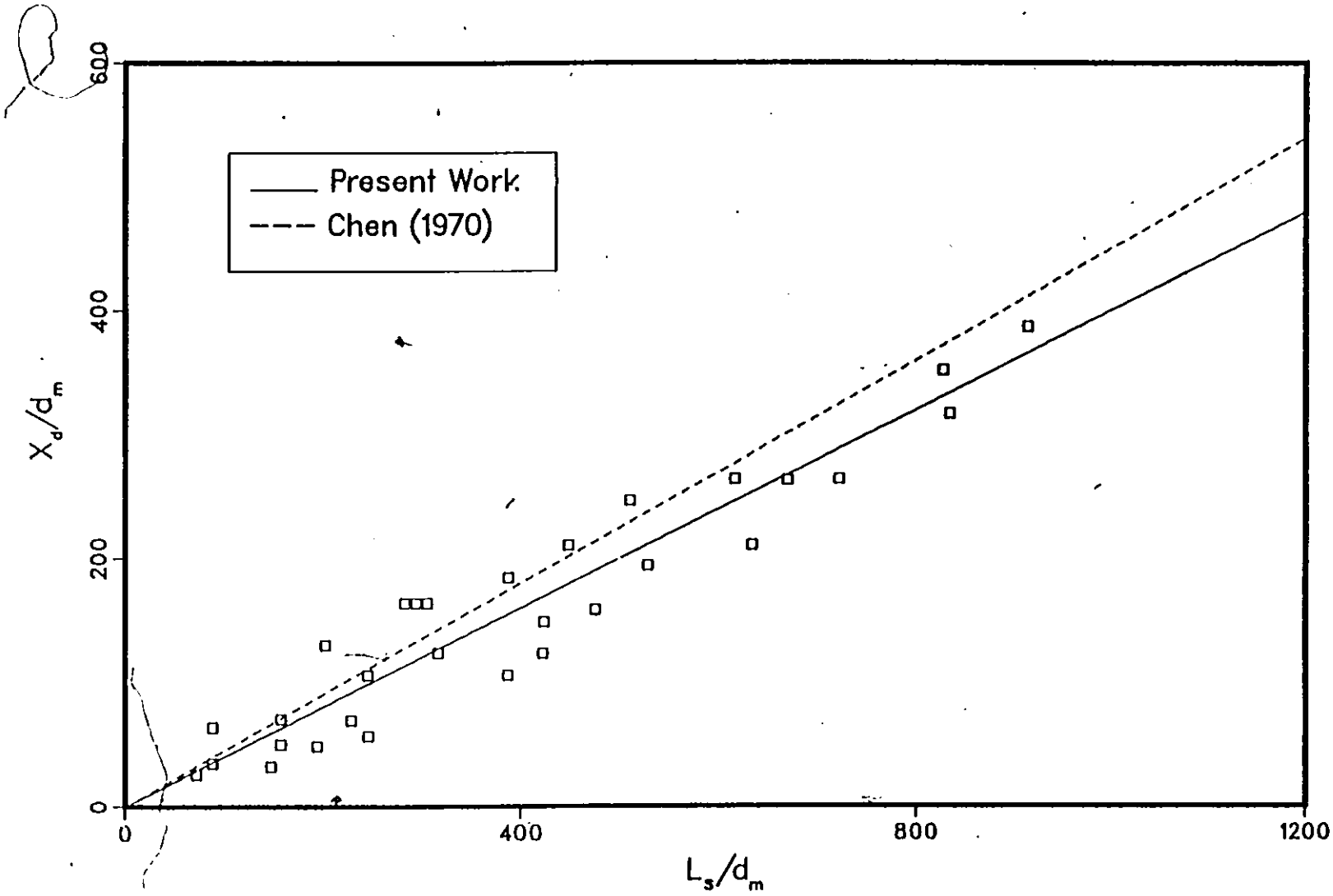

Fig.23: Functional Relationship Between the Distance to the Point of Deepest Scour and the Scour Hole Length.

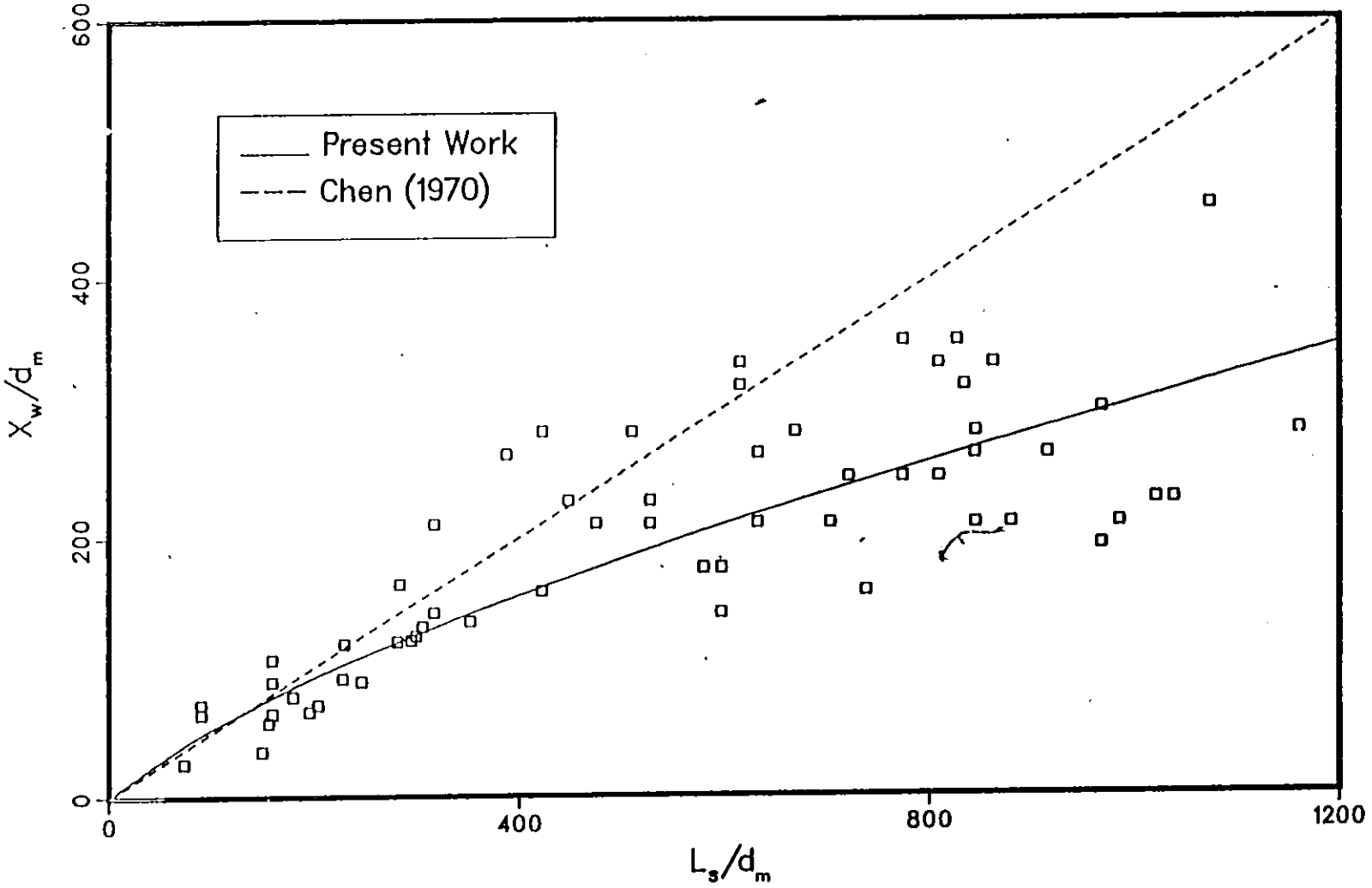

Fig.24: Functional Relationship Between the Distance to the Point of Widest Scour and the Scour Hole Length.

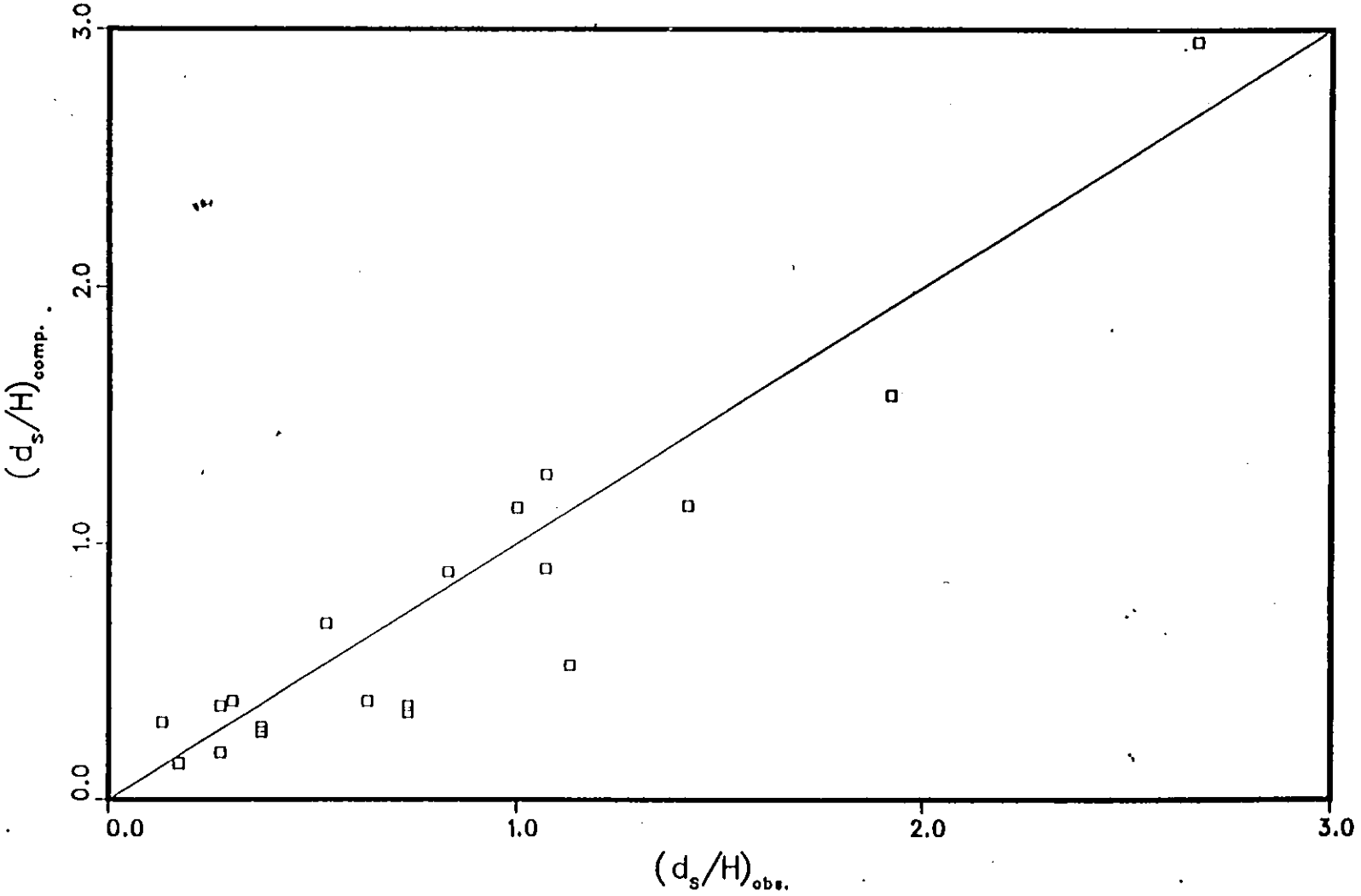

Fig.25: Comparison of Measured Scour Depths with the Proposed Equation.

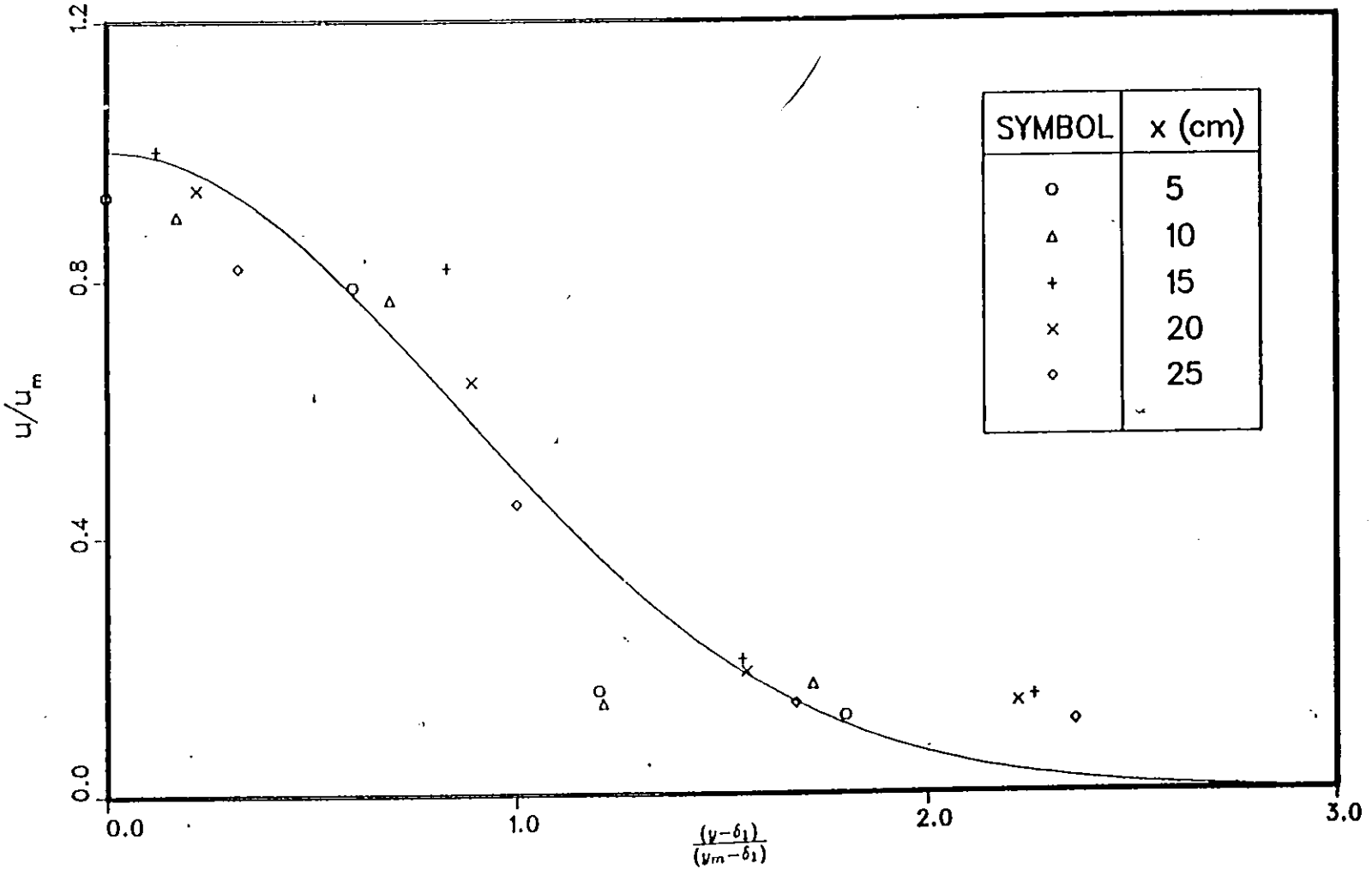

Fig.26: Similarity Between Vertical Velocity Profiles in the Fully Developed Flow Region.

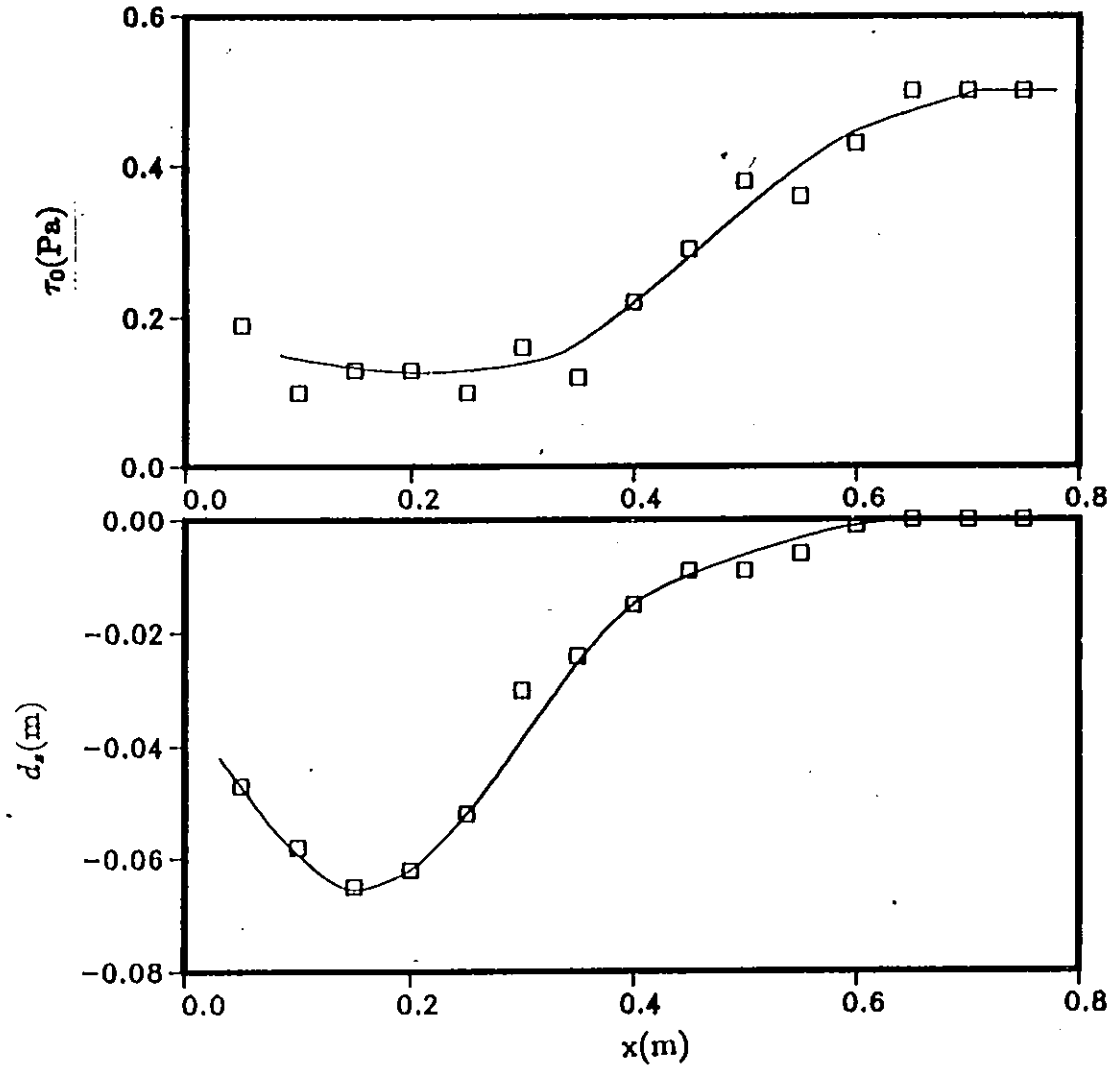

Fig.27: Boundary Shear Stress Distribution Accompanied with the Corresponding Scour Profile.

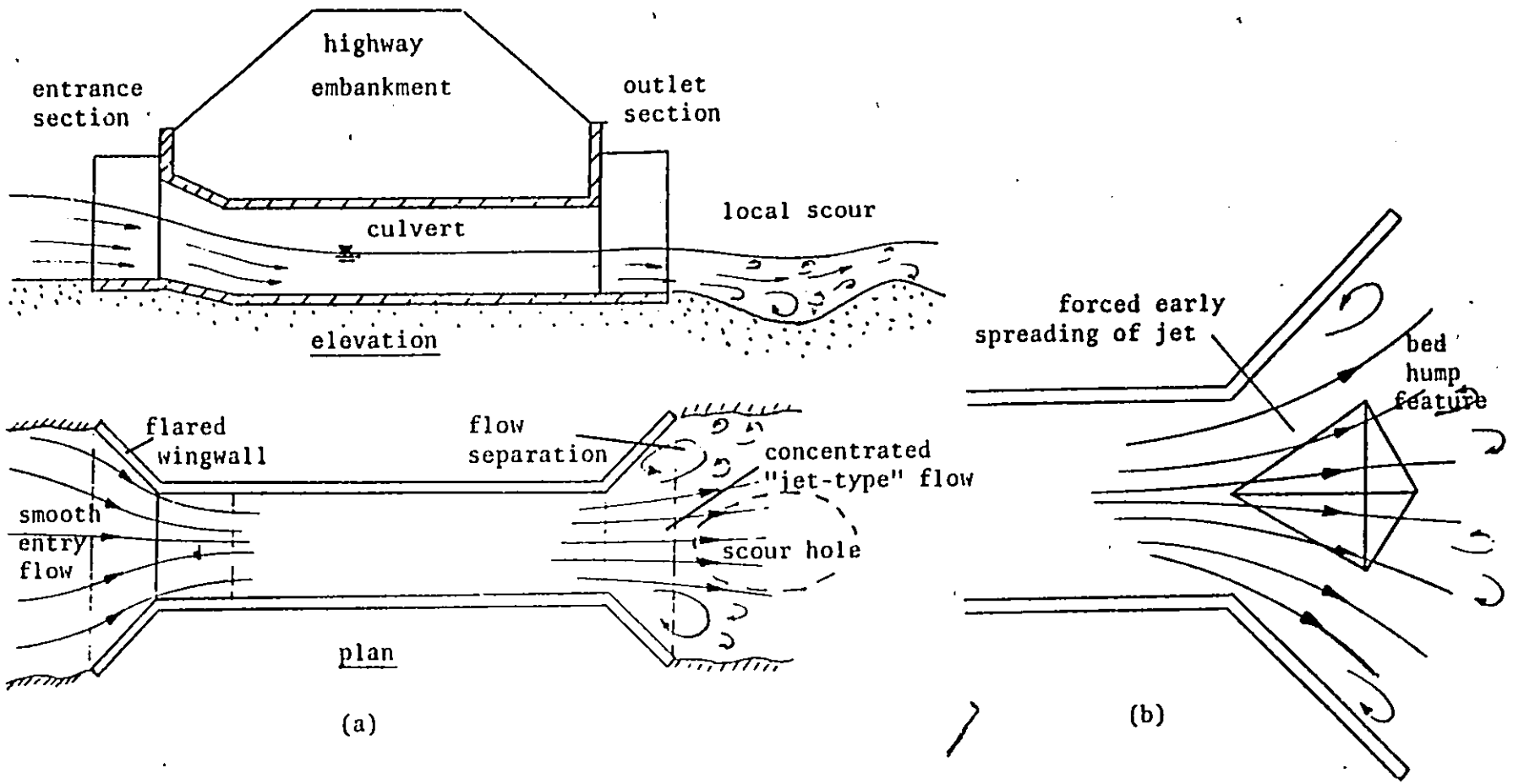

Fig.28(a): "Inlet" versus "Outlet" Flow Characteristics of a Culvert (b): Outlet Detail with Bed Hump Feature in Place.

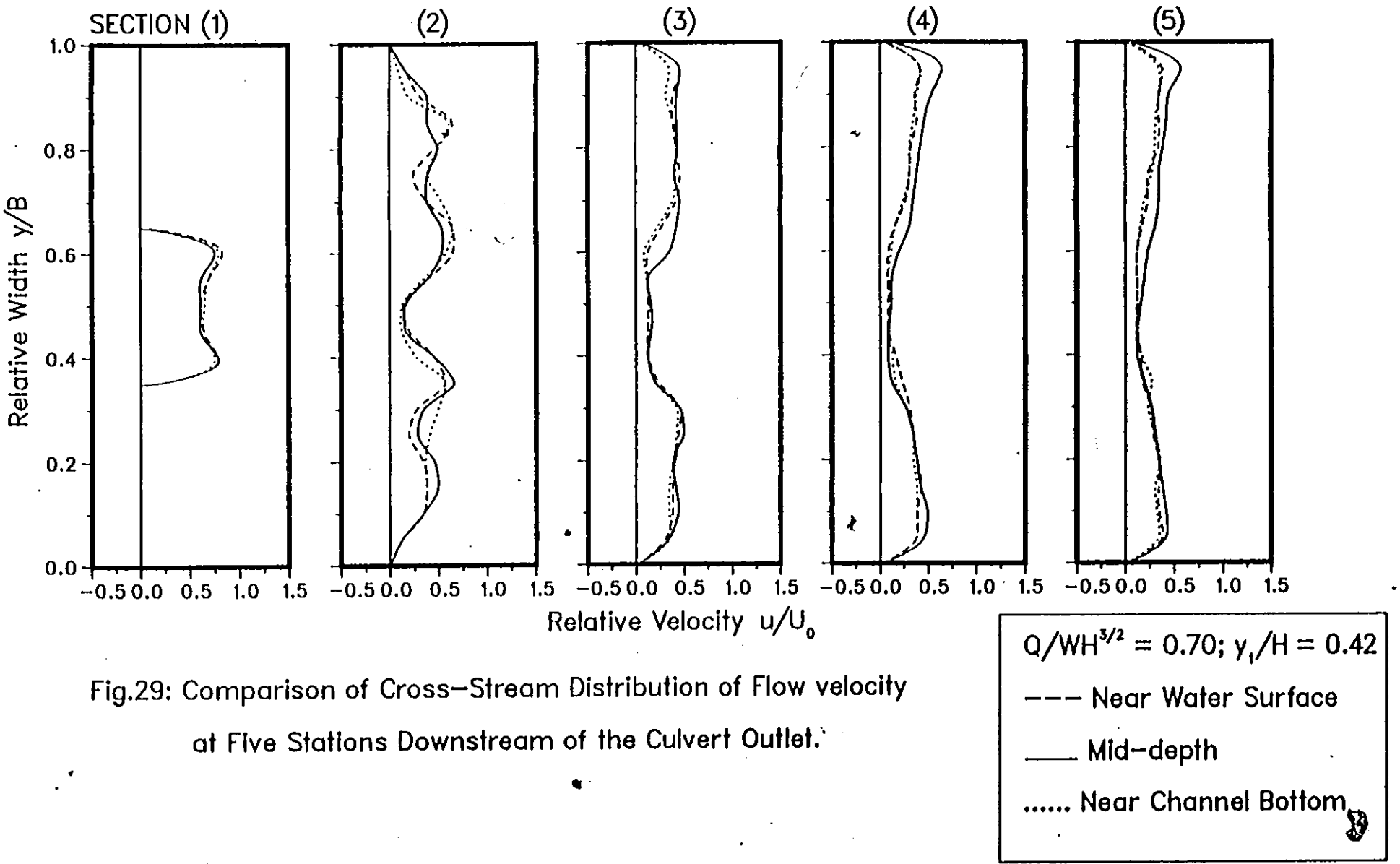

Fig.29: Comparison of Cross-Stream Distribution of Flow velocity at Five Stations Downstream of the Culvert Outlet.

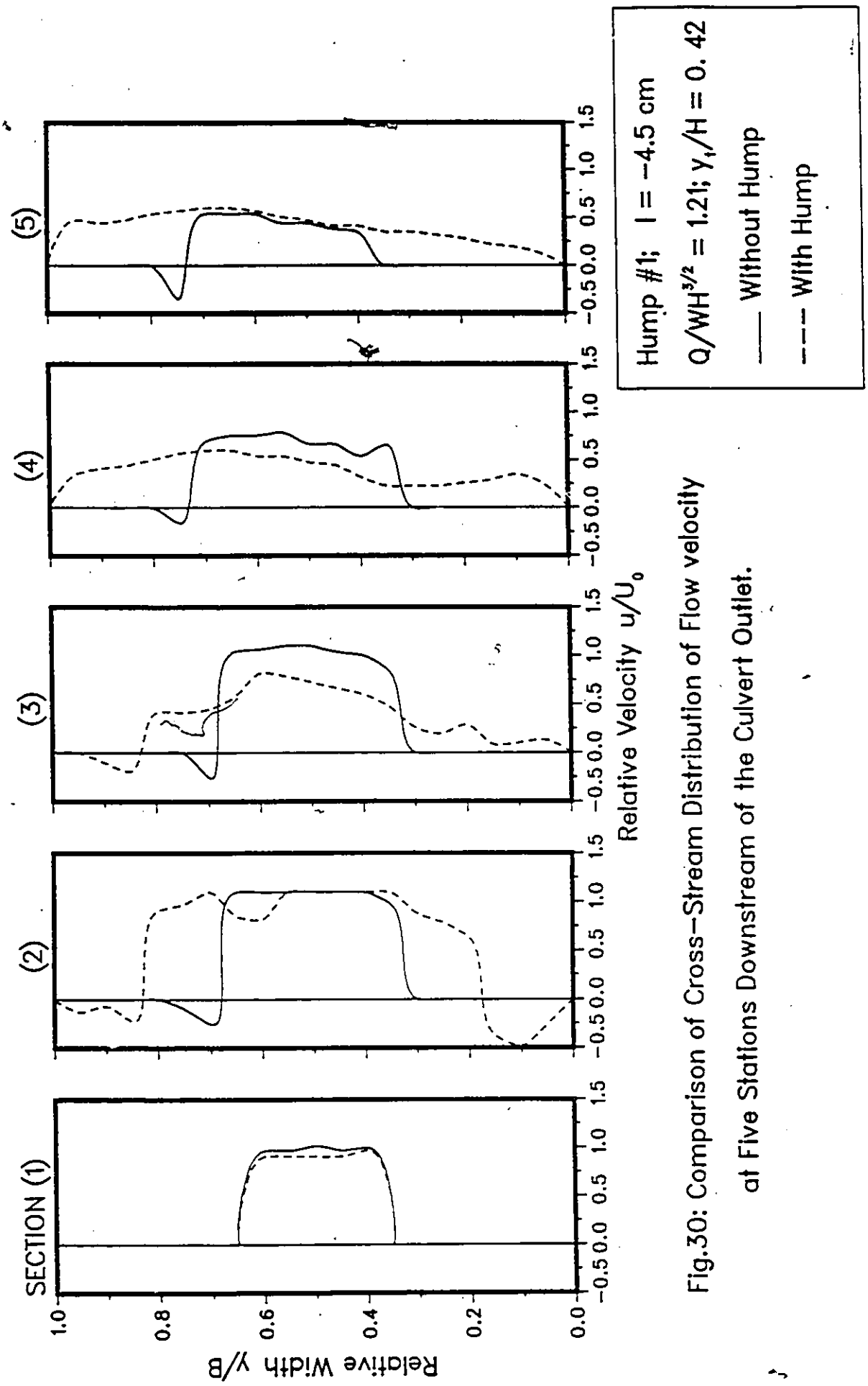

Fig.30: Comparison of Cross-Stream Distribution of Flow velocity at Five Stations Downstream of the Culvert Outlet.

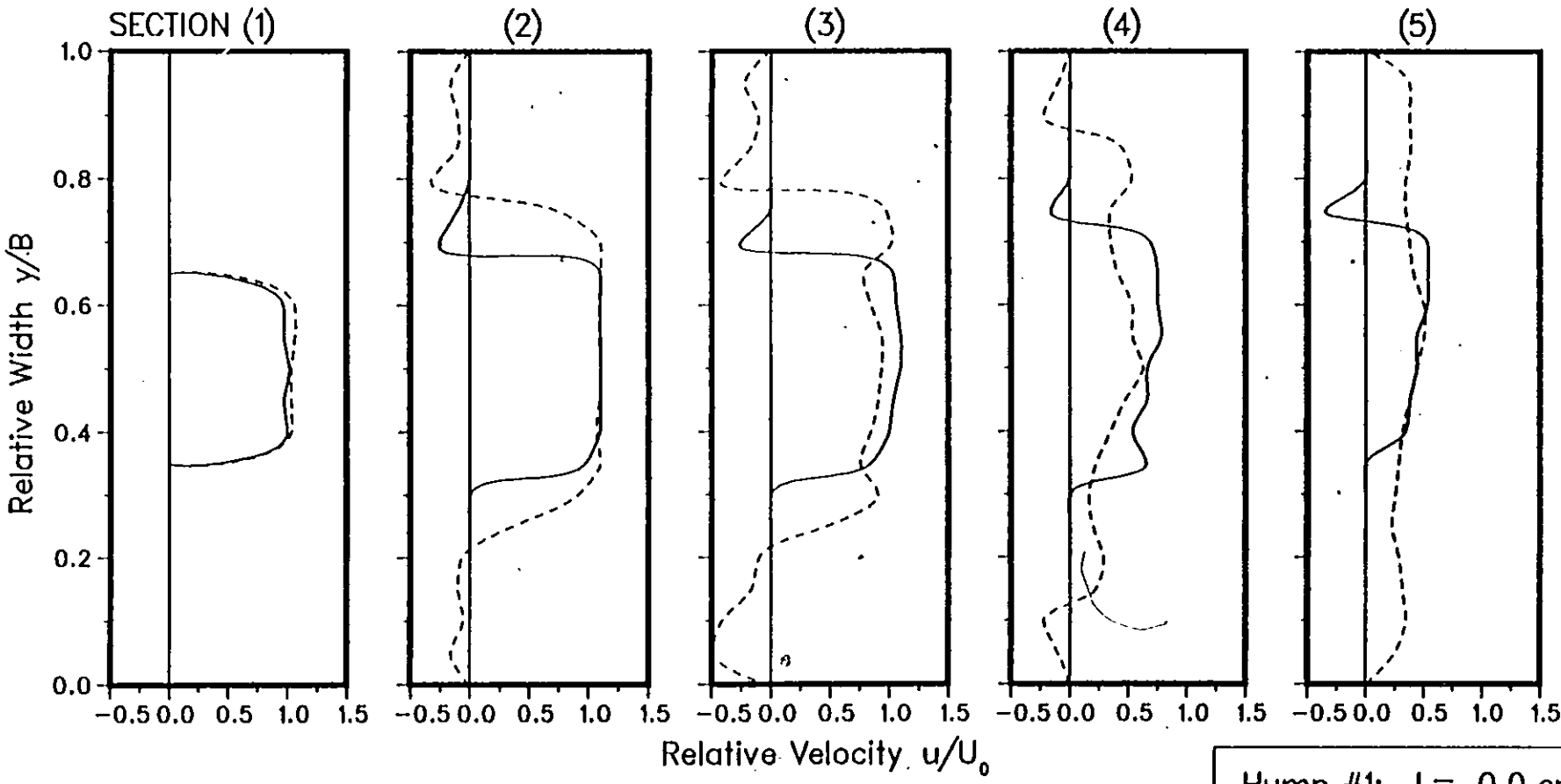

Fig.31: Comparison of Cross–Stream Distribution of Flow velocity at Five Stations Downstream of the Culvert Outlet.

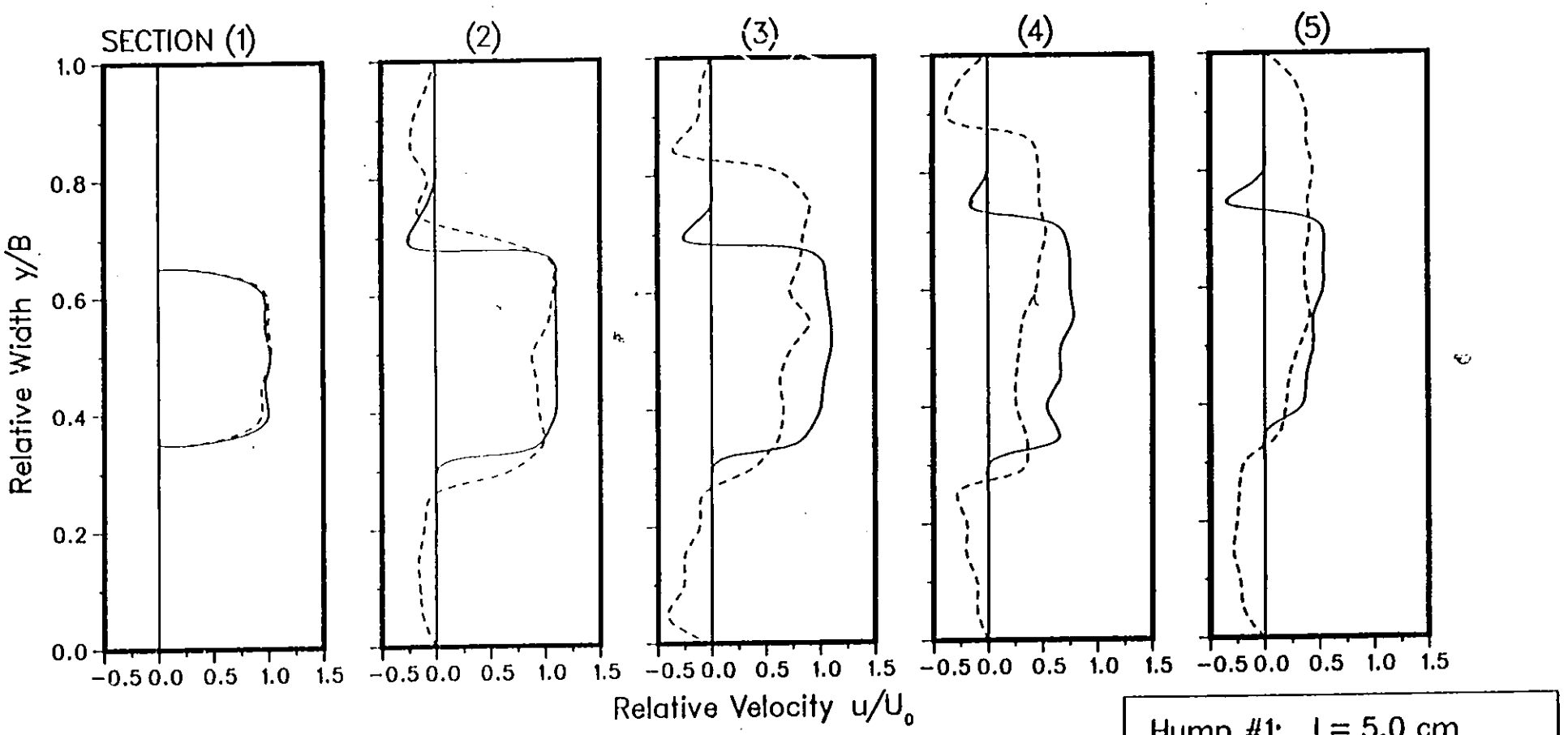

Fig.32: Comparison of Cross-Stream Distribution of Flow velocity at Five Stations Downstream of the Culvert Outlet.

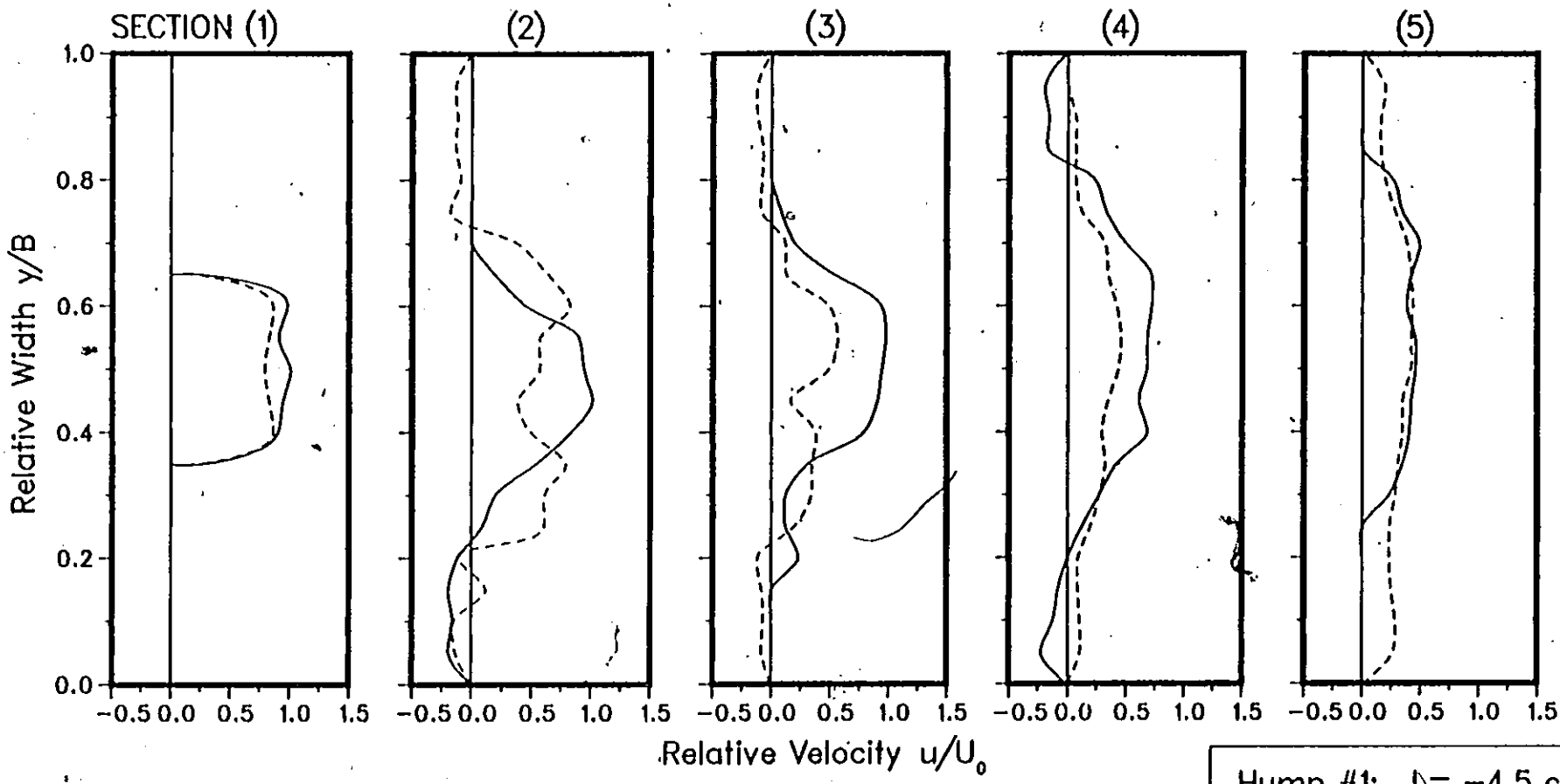

Fig.33: Comparison of Cross-Stream Distribution of Flow velocity at Five Stations Downstream of the Culvert Outlet.

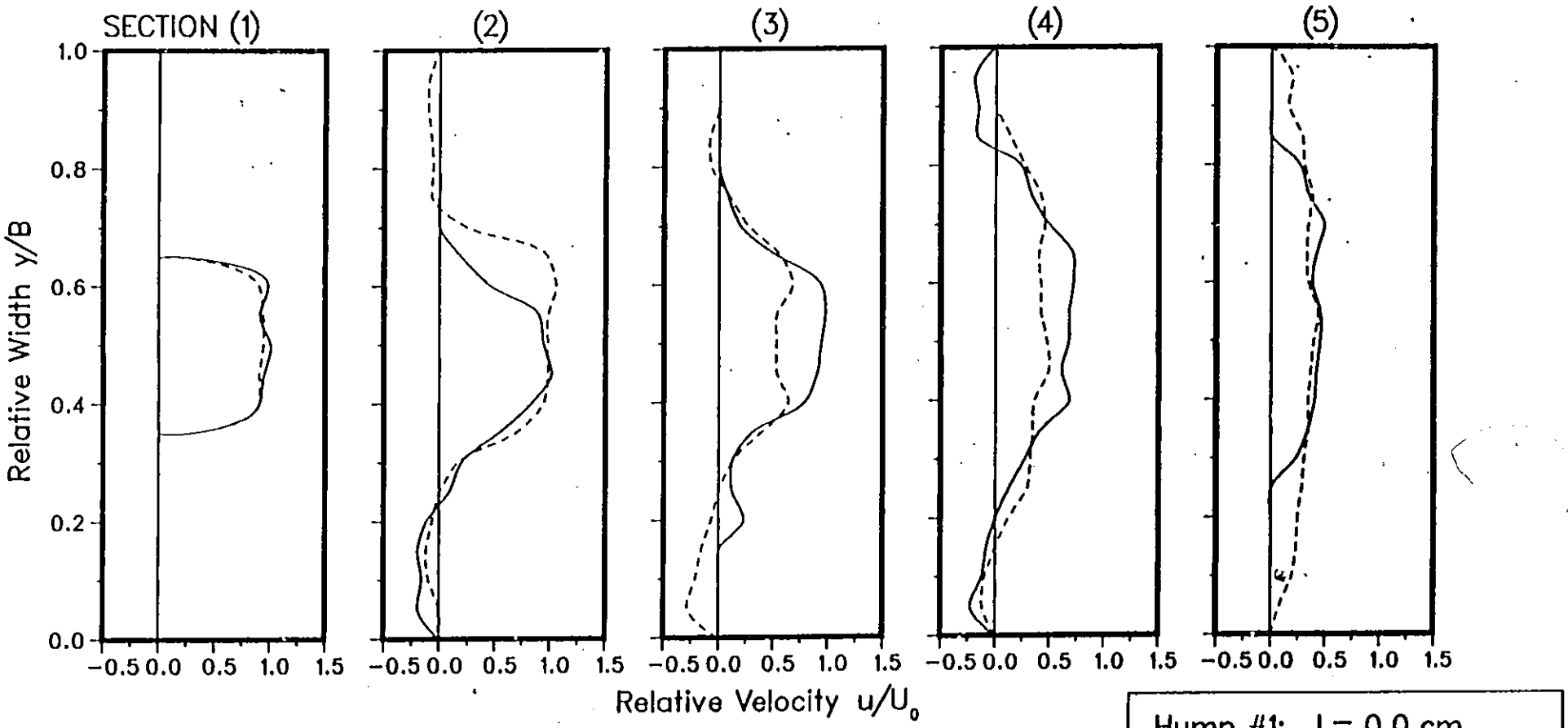

Fig.34: Comparison of Cross-Stream Distribution of Flow velocity at Five Stations Downstream of the Culvert Outlet.

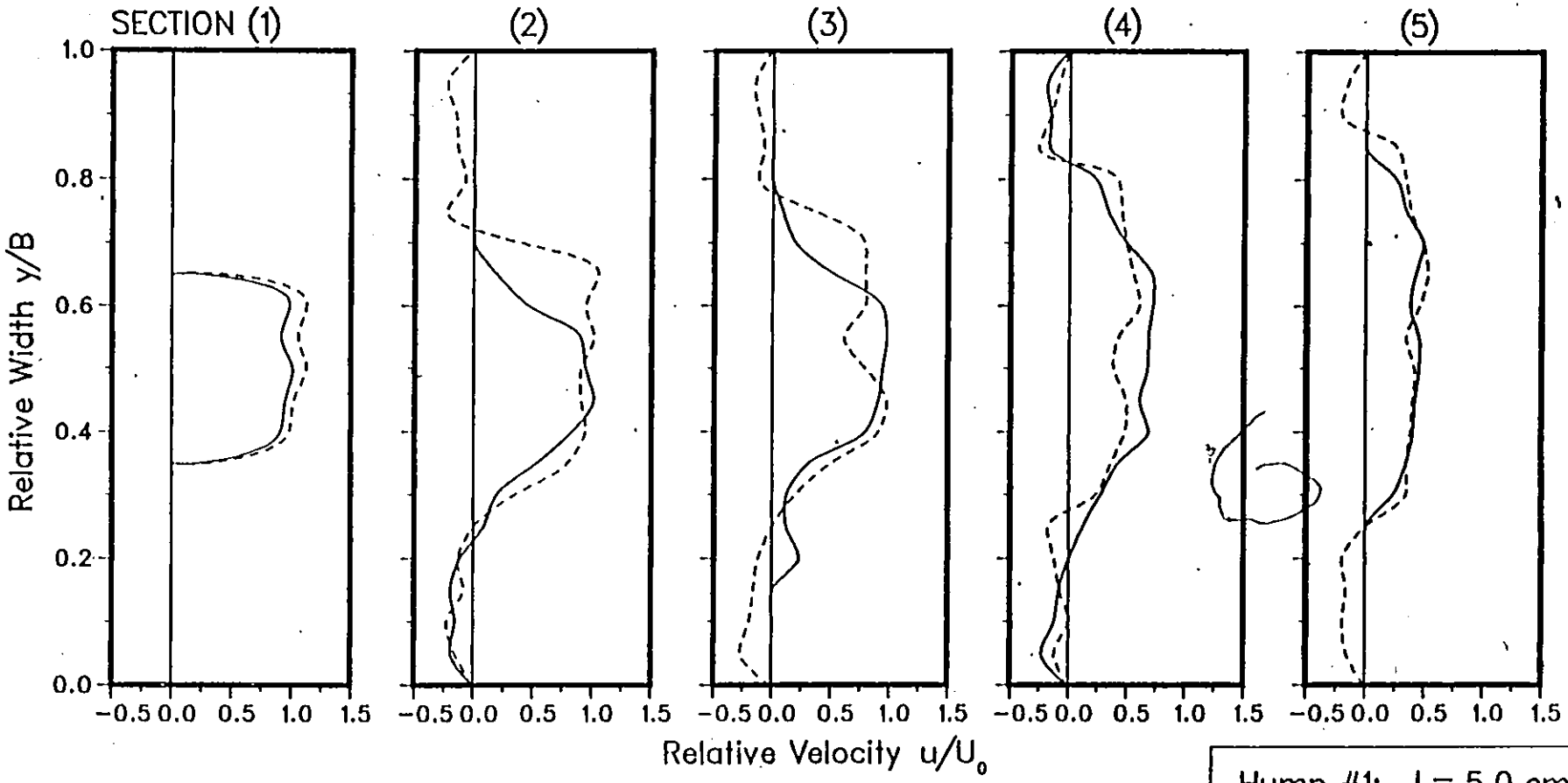

Fig.35: Comparison of Cross-Stream Distribution of Flow velocity at Five Stations Downstream of the Culvert Outlet.

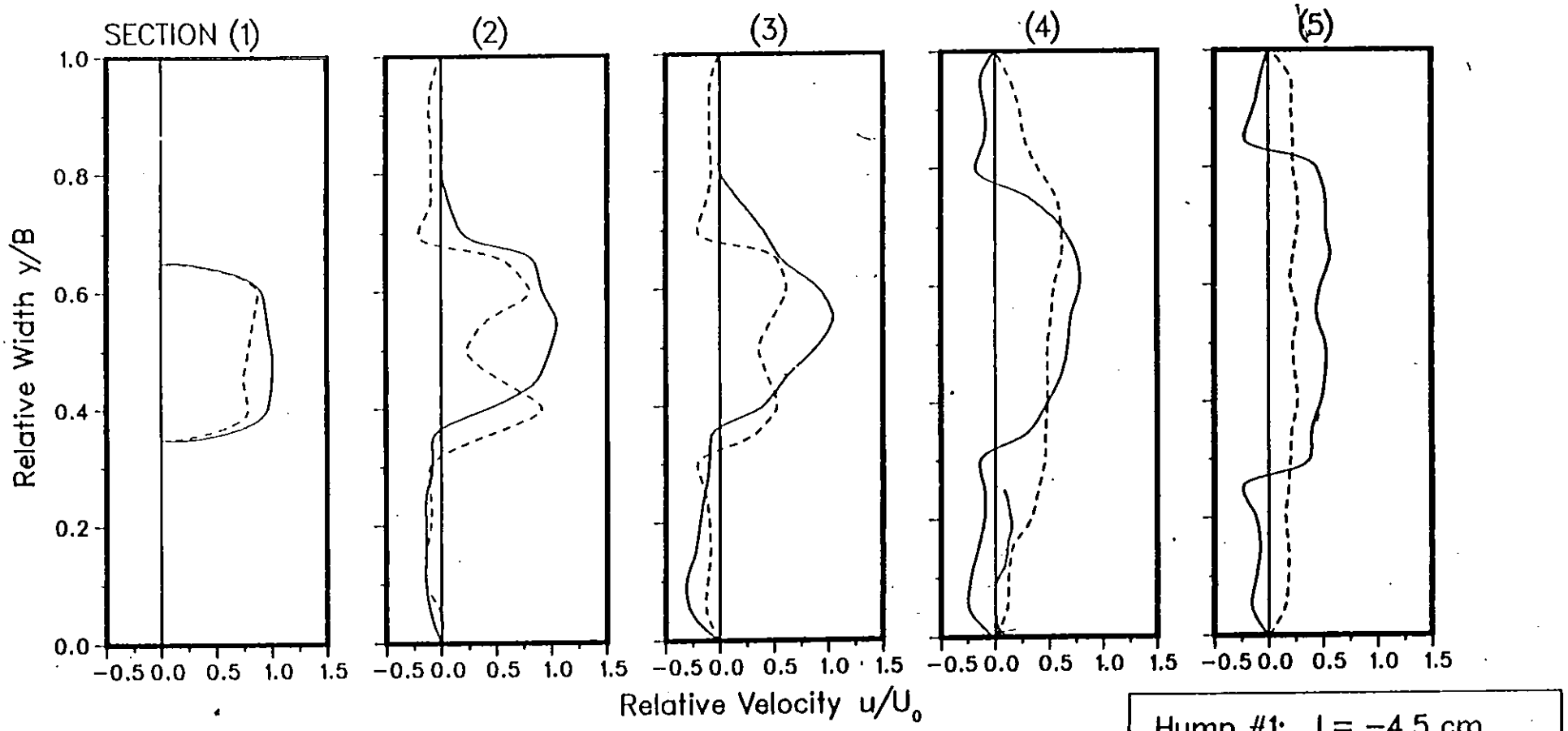

Fig.36: Comparison of Cross-Stream Distribution of Flow velocity at Five Stations Downstream of the Culvert Outlet.

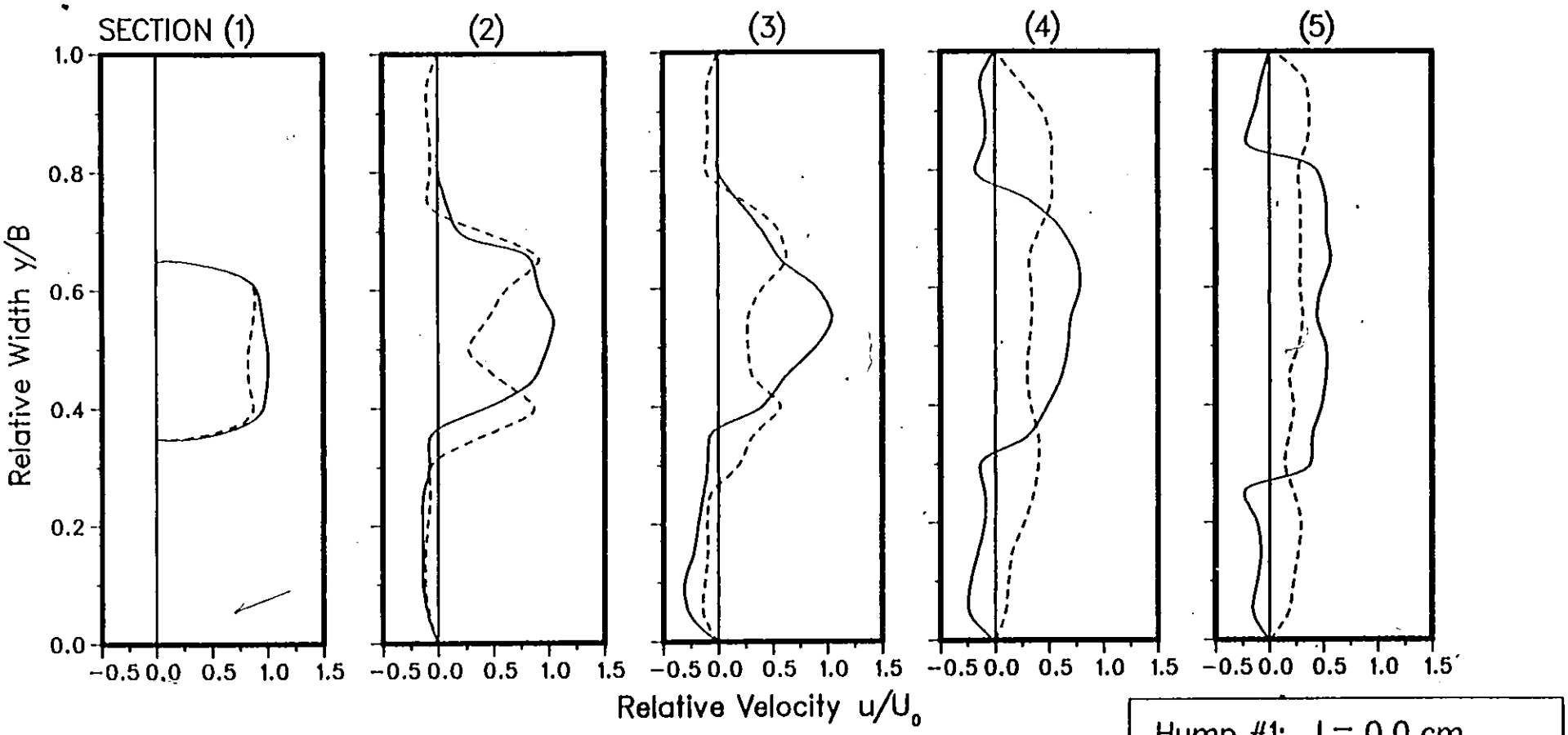

Fig.37: Comparison of Cross-Stream Distribution of Flow velocity at Five Stations Downstream of the Culvert Outlet.

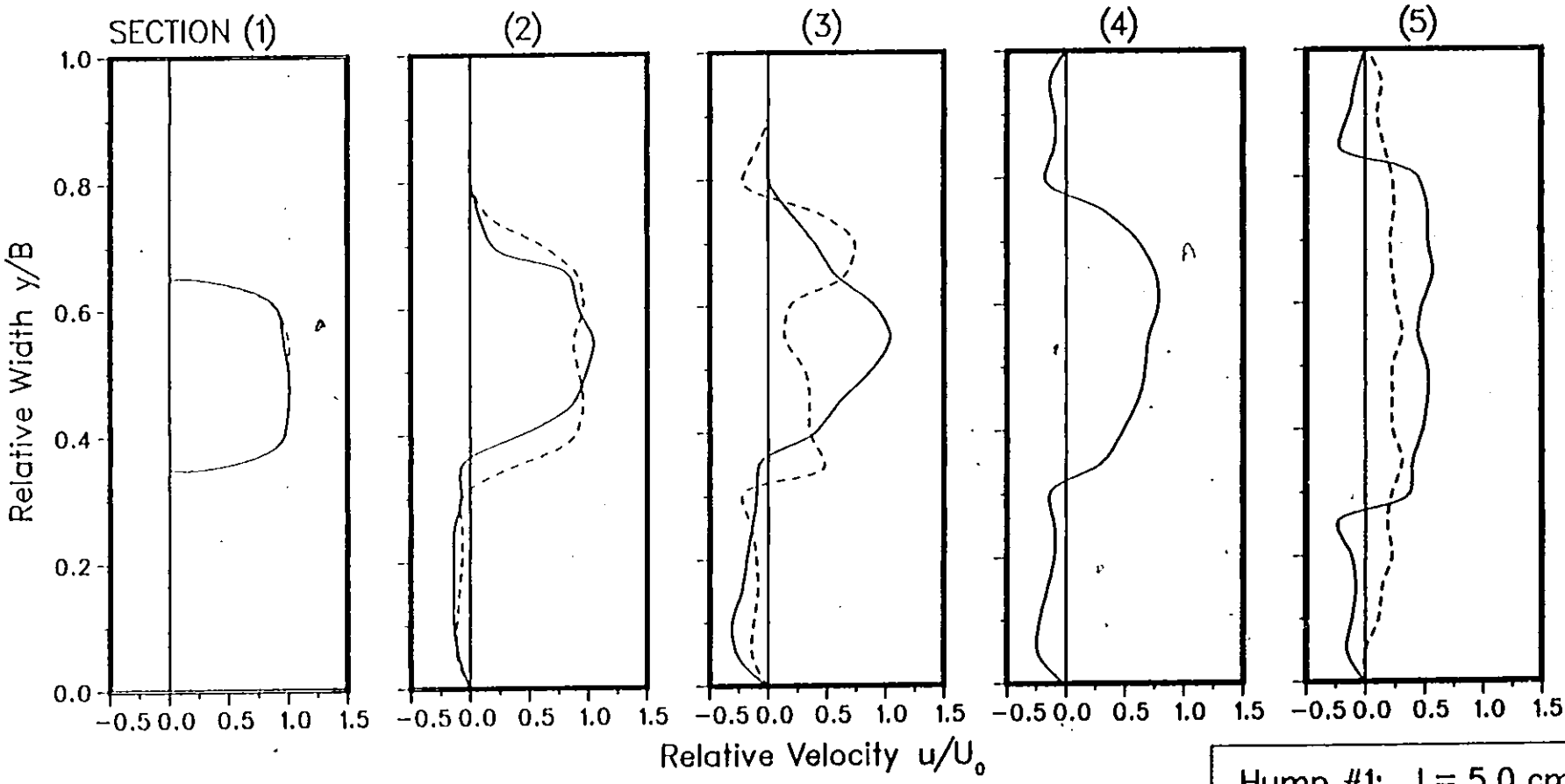

Fig.38: Comparison of Cross–Stream Distribution of Flow velocity at Five Stations Downstream of the Culvert Outlet.

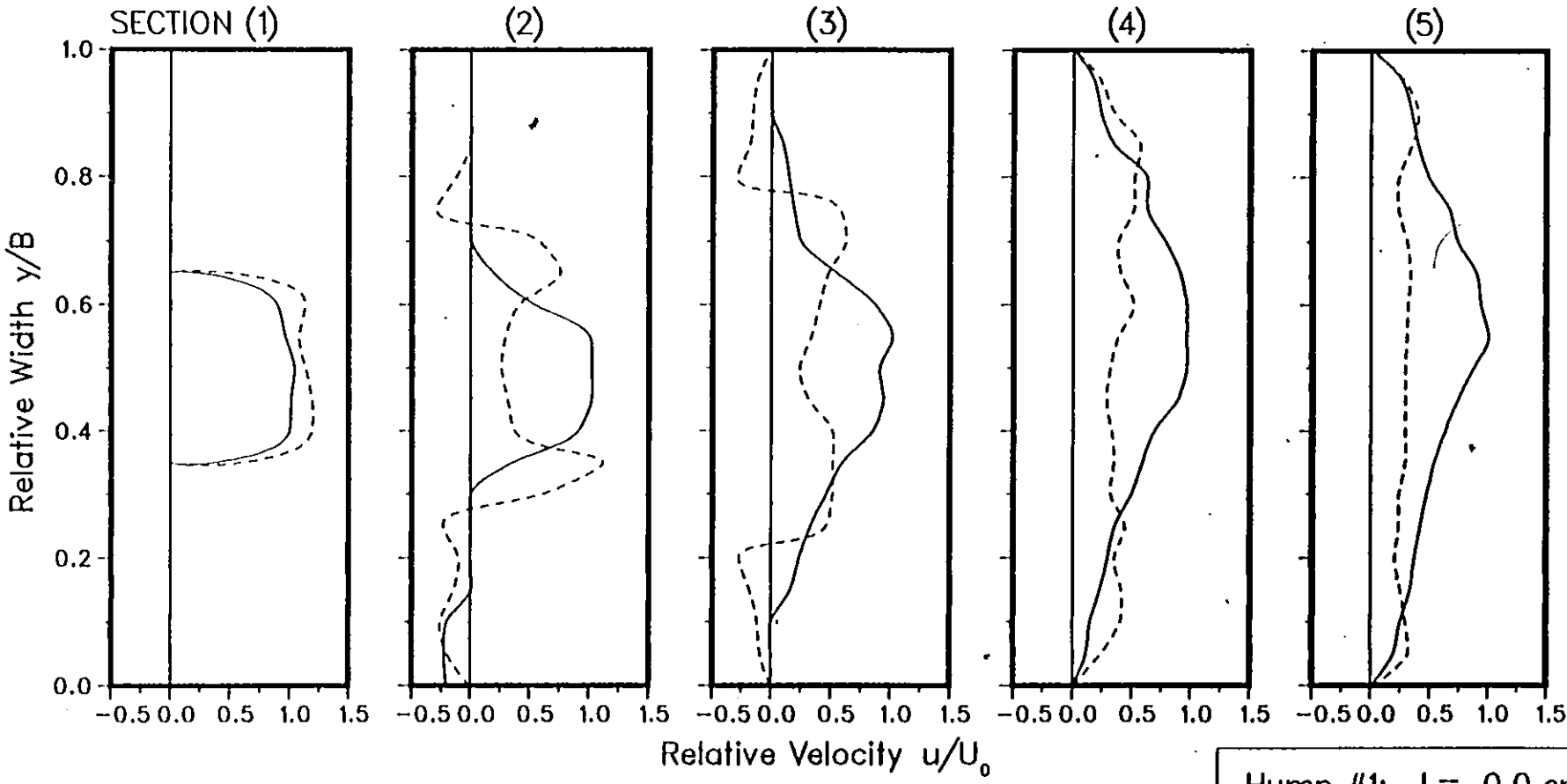

Fig.39: Comparison of Cross--Stream Distribution of Flow velocity at Five Stations Downstream of the Culvert Outlet.

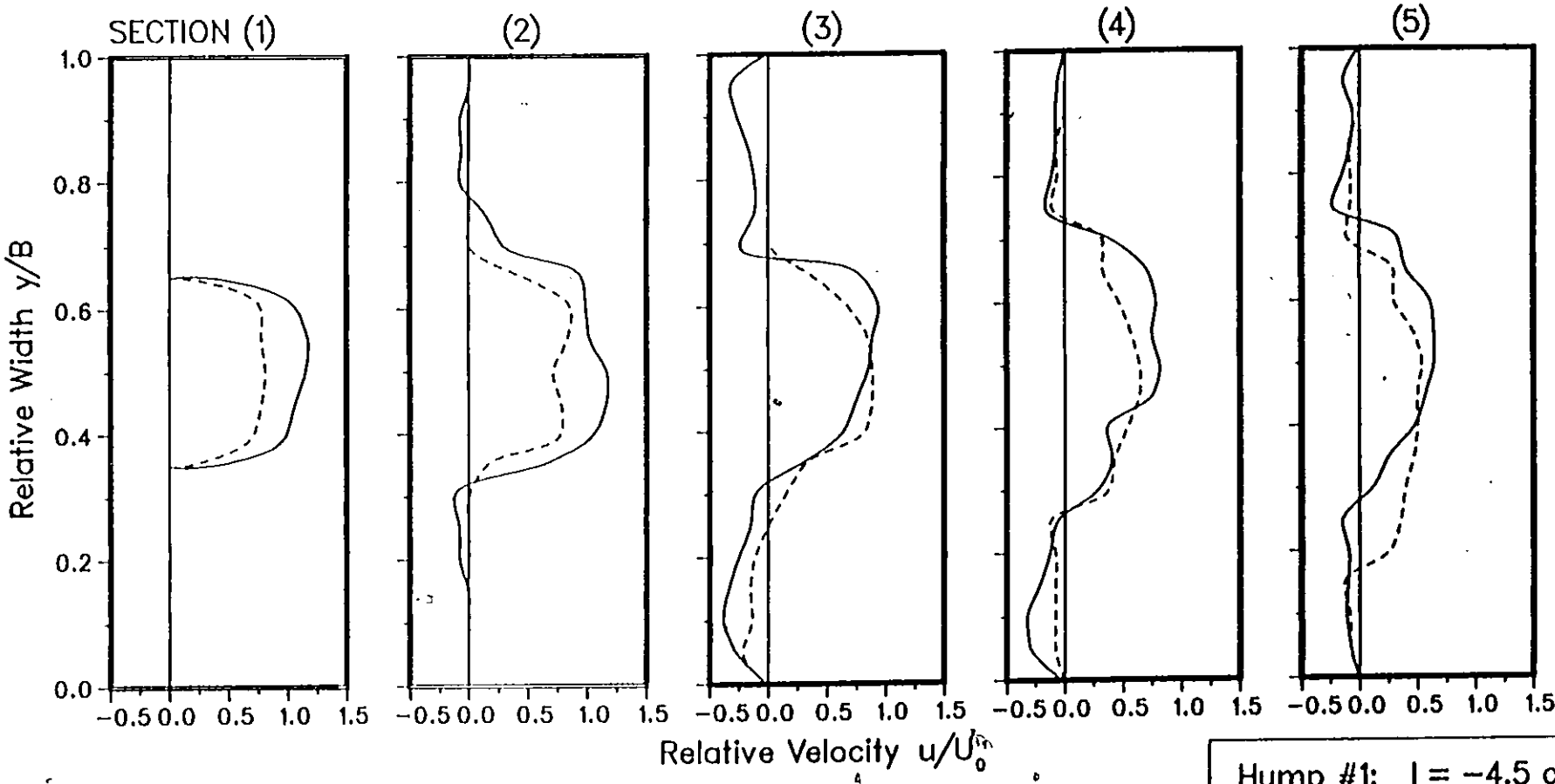

Fig.40: Comparison of Cross-Stream Distribution of Flow velocity at Five Stations Downstream of the Culvert Outlet.

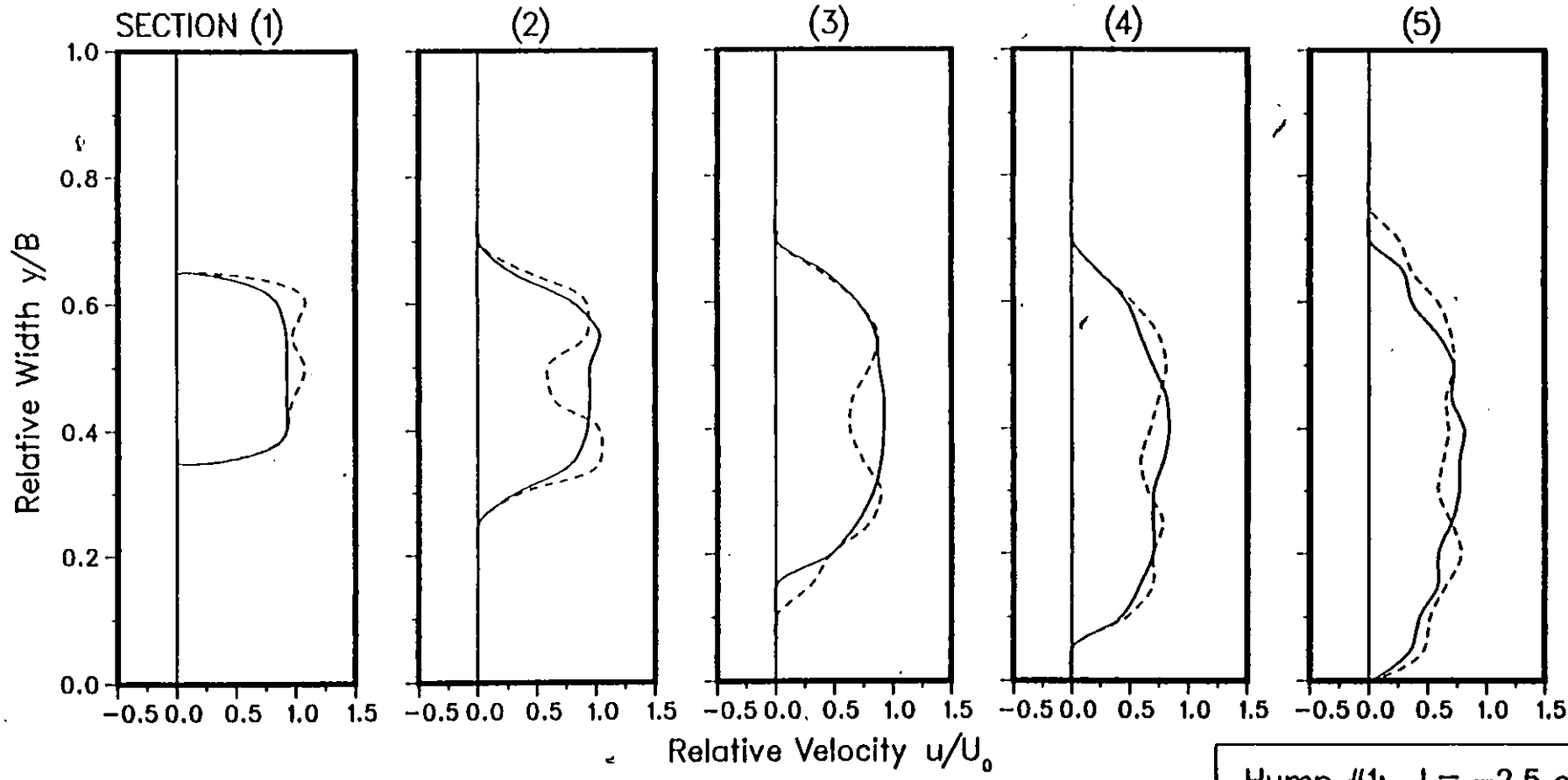

Fig.41: Comparison of Cross-Stream Distribution of Flow velocity at Five Stations Downstream of the Culvert Outlet.

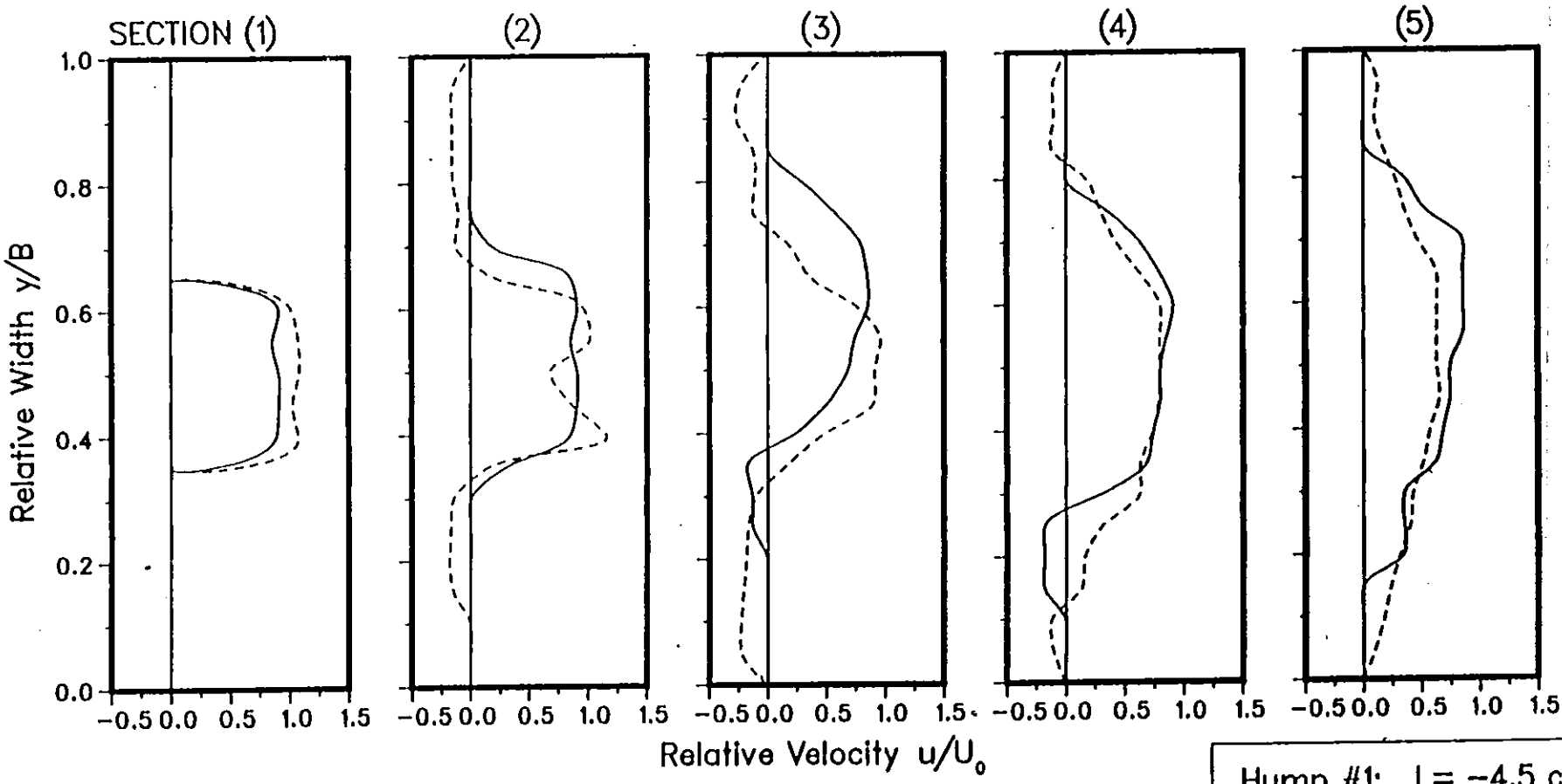

Fig.42: Comparison of Cross–Stream Distribution of Flow velocity at Five Stations Downstream of the Culvert Outlet.

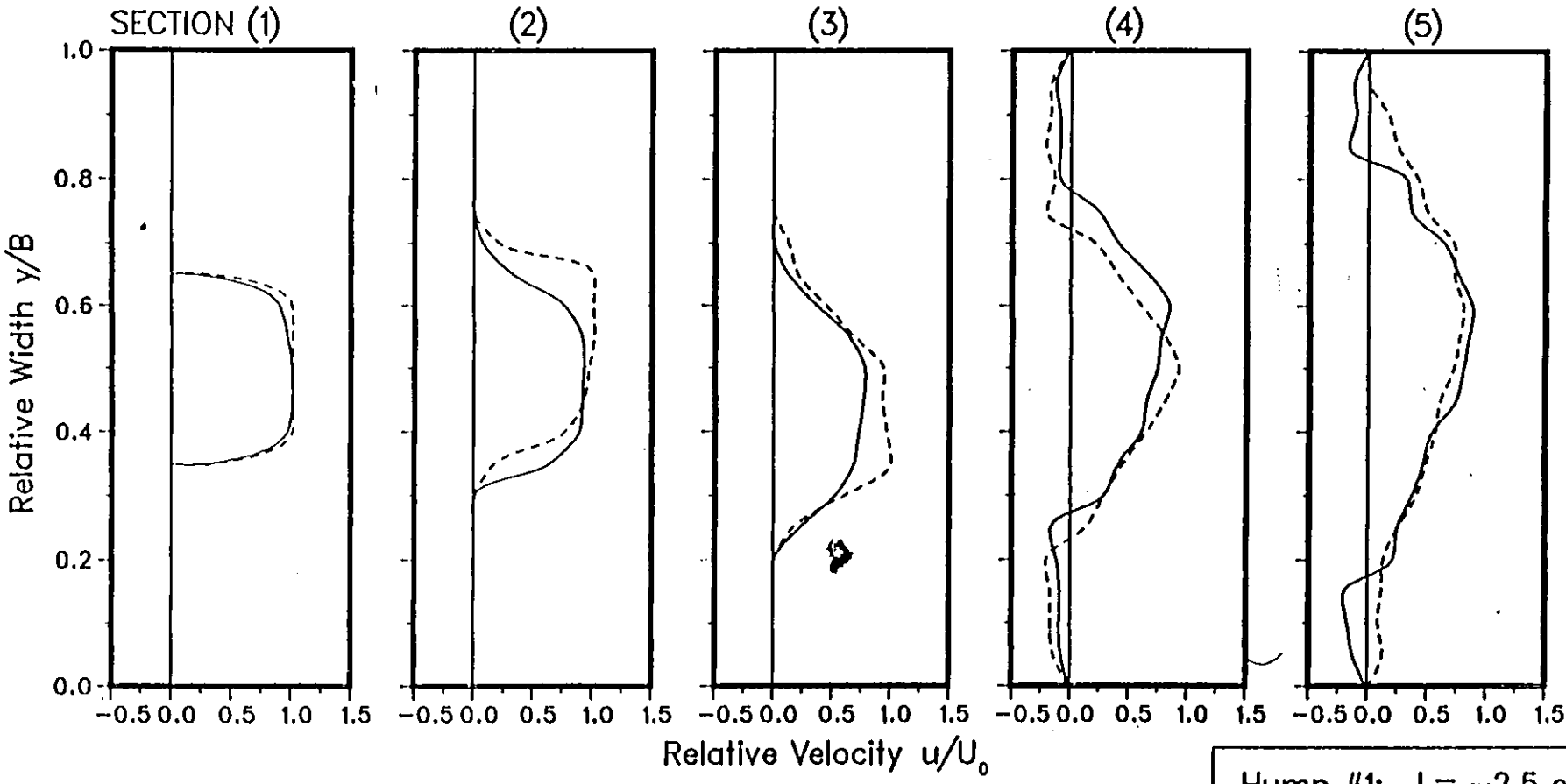

Fig.43: Comparison of Cross–Stream Distribution of Flow velocity at Five Stations Downstream of the Culvert Outlet.

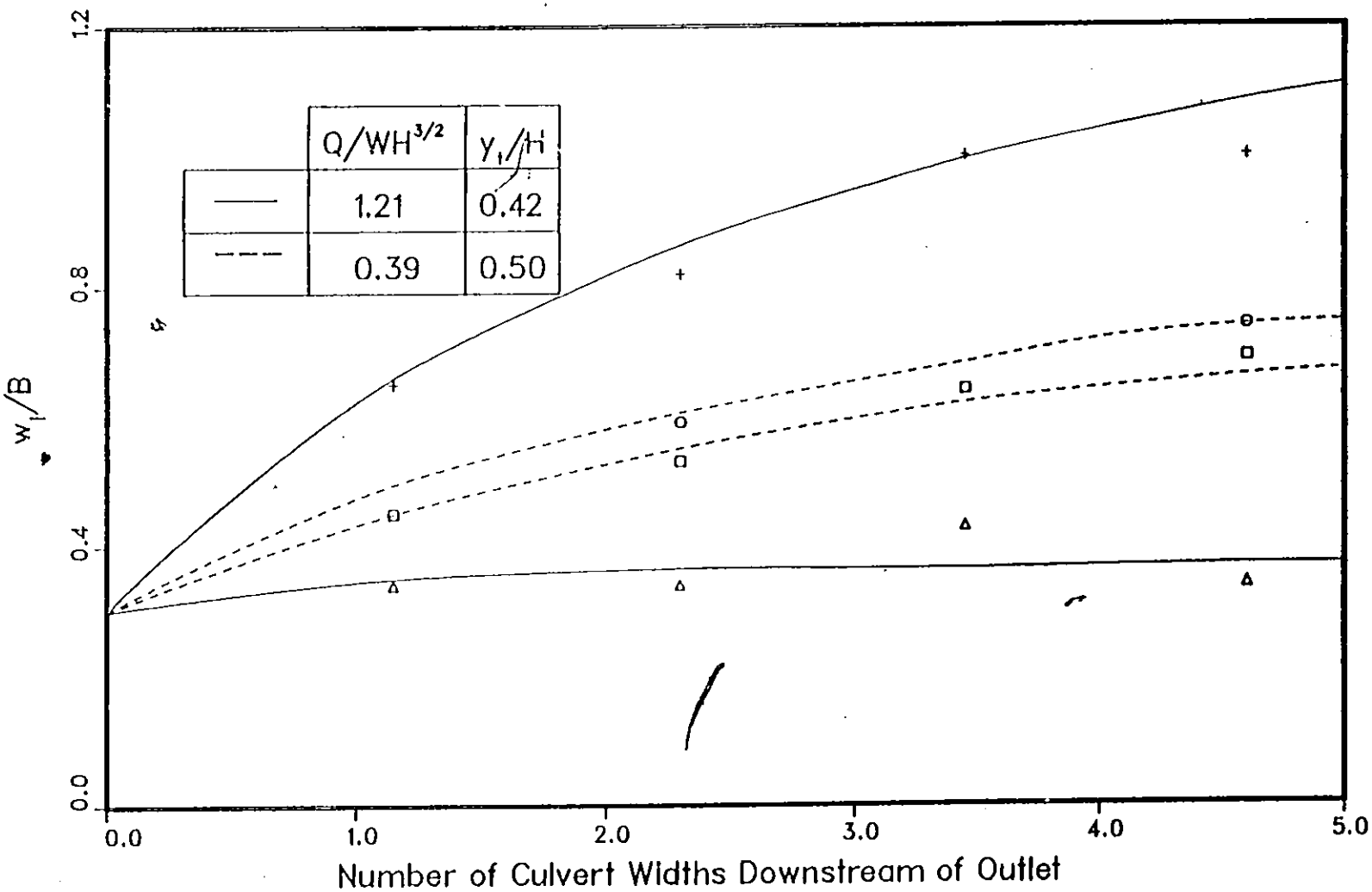

Fig.44: Jet Expansion Rate With and Without the Pyramidal Hump Feature ("Mobile Bed" Condition).

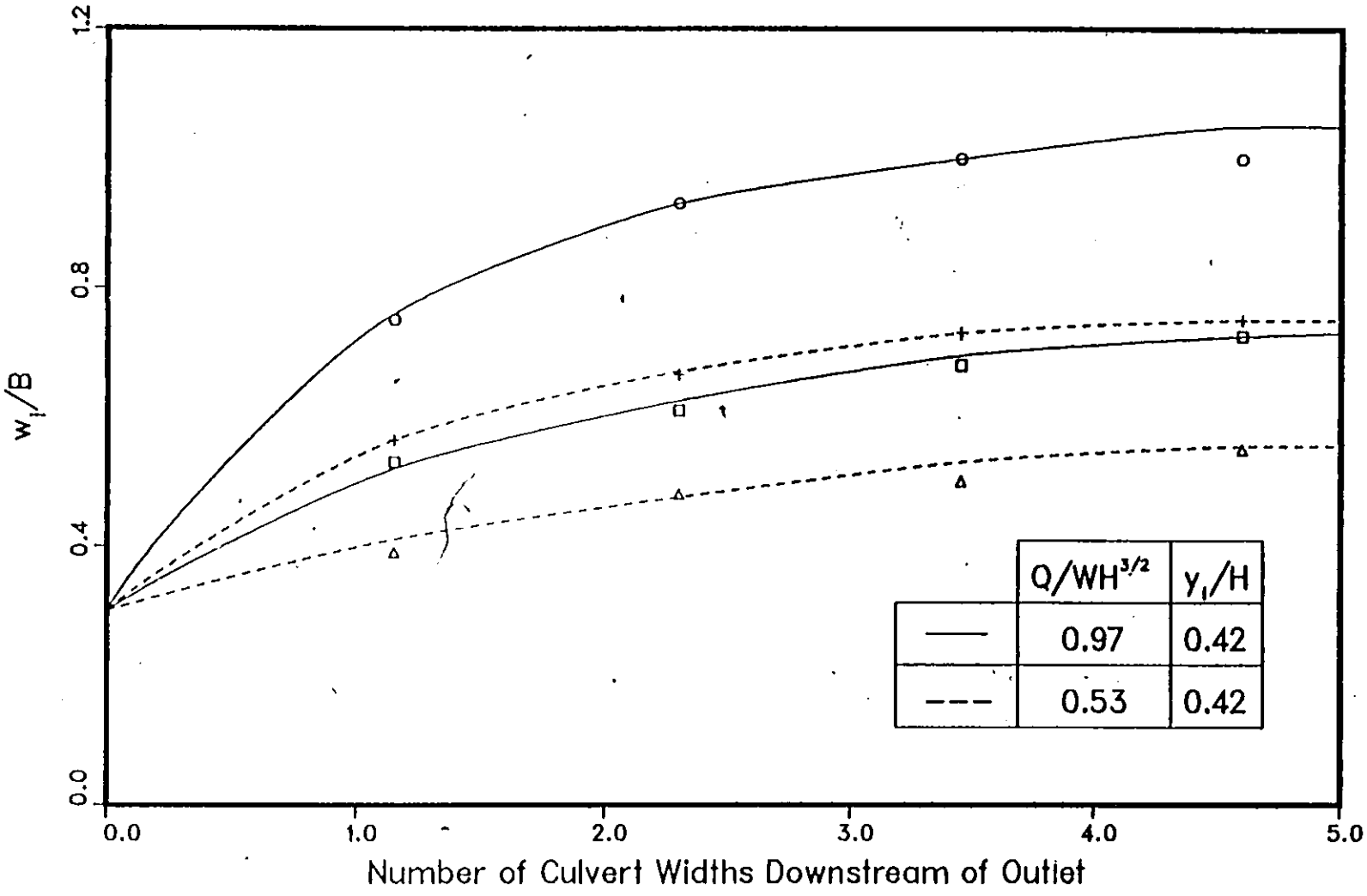

Fig.45: Jet Expansion Rate with and without the Pyramidal Hump Feature ("Fixed Bed" Condition).

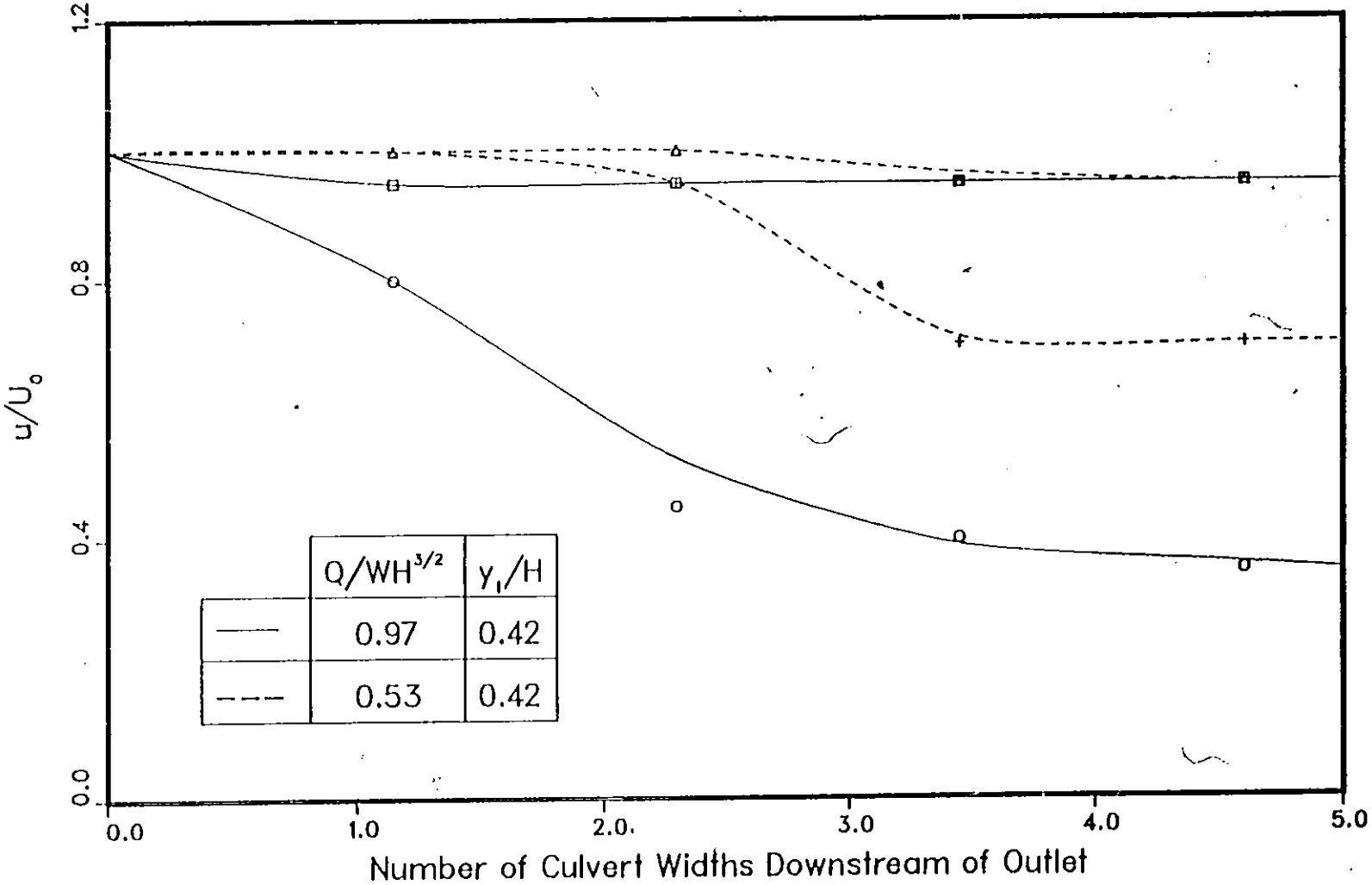

Fig.46: Rate of Velocity Reduction with and without the Pyramidal Hump Feature ("Fixed Bed" Condition).

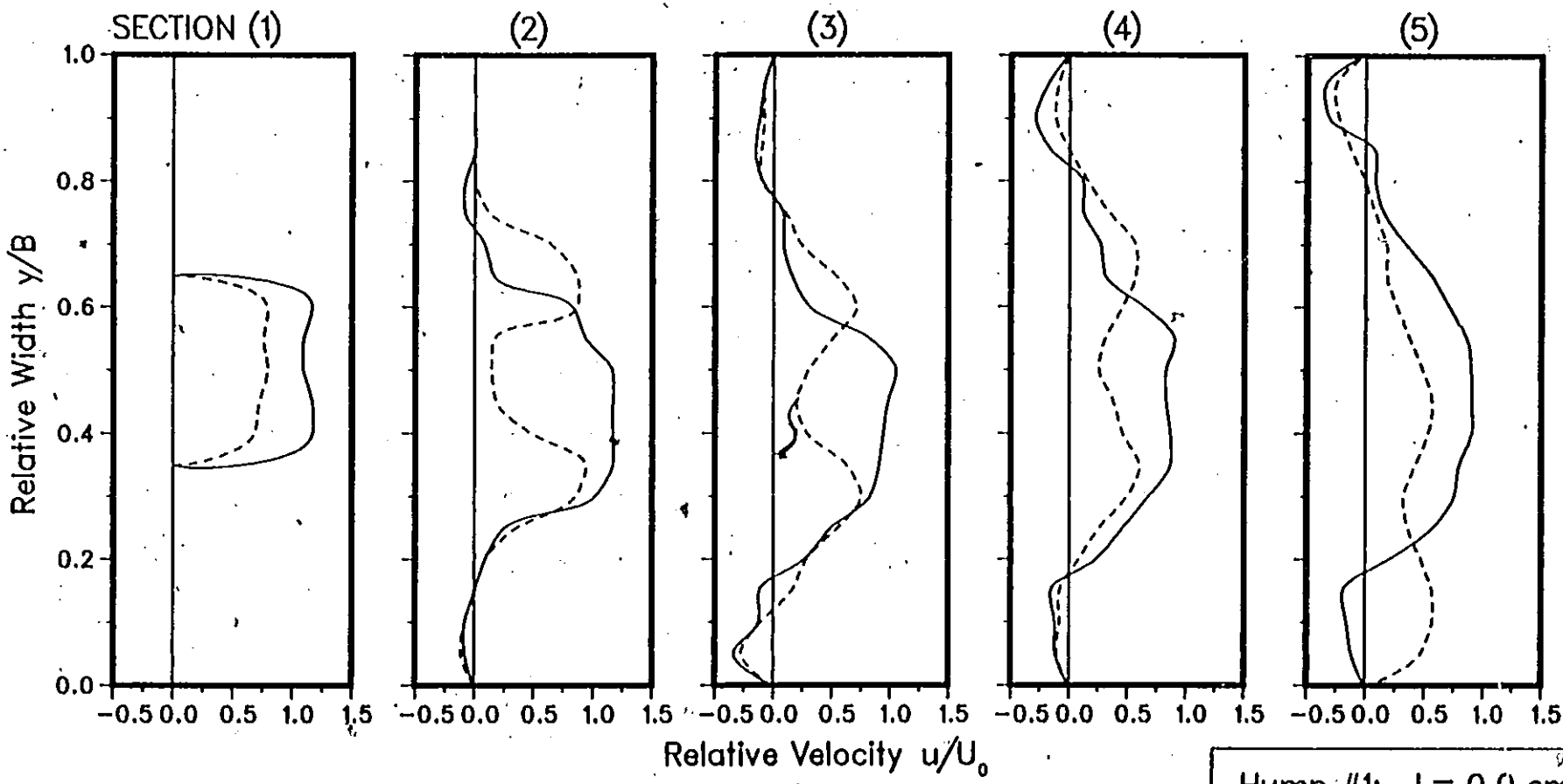

Fig.47: Comparison of Cross-Stream Distribution of Flow velocity at Five Stations Downstream of the Culvert Outlet.

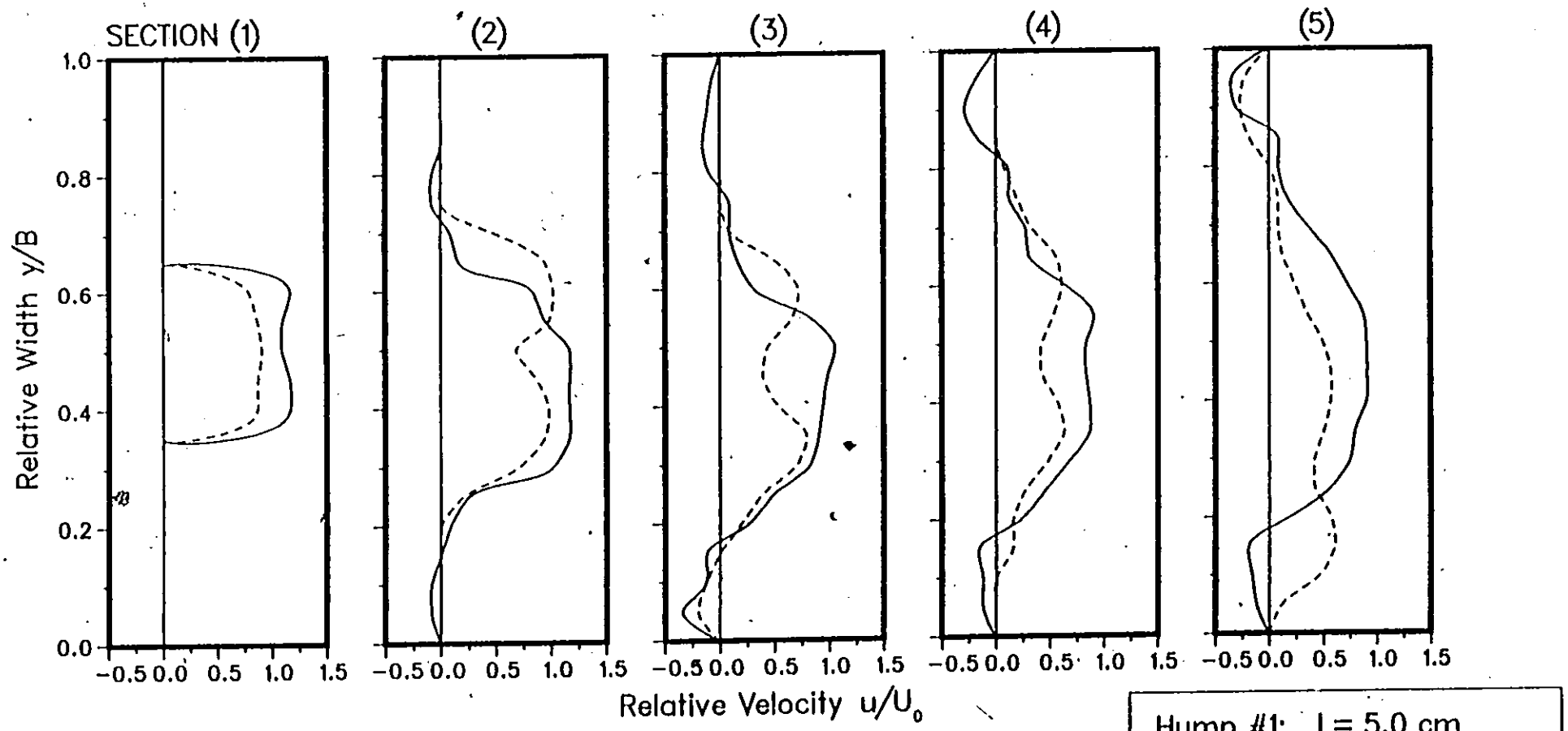

Fig.48: Comparison of Cross-Stream Distribution of Flow velocity at Five Stations Downstream of the Culvert Outlet.

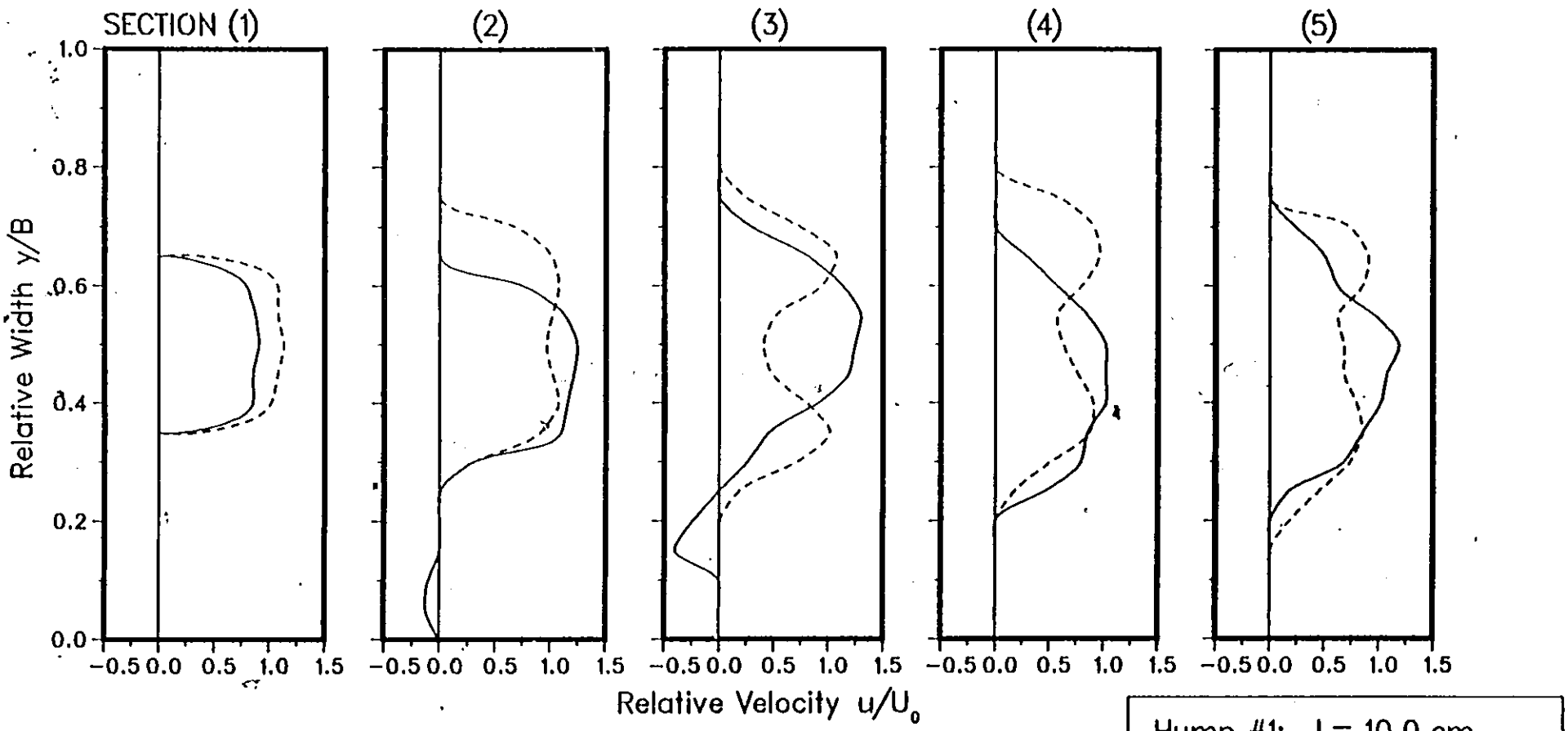

Fig.49: Comparison of Cross-Stream Distribution of Flow velocity at Five Stations Downstream of the Culvert Outlet.

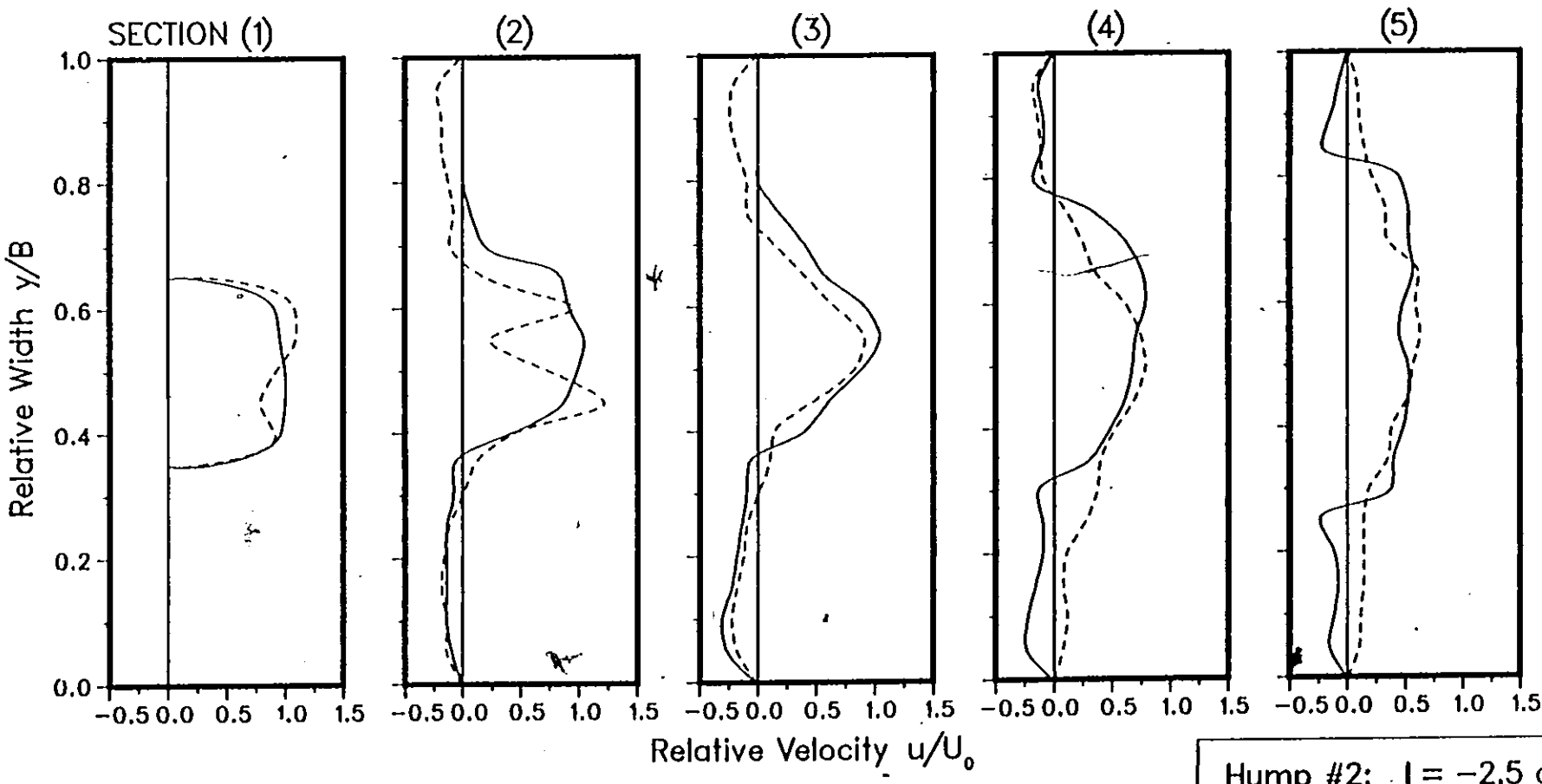

Fig.50: Comparison of Cross-Stream Distribution of Flow velocity at Five Stations Downstream of the Culvert Outlet.

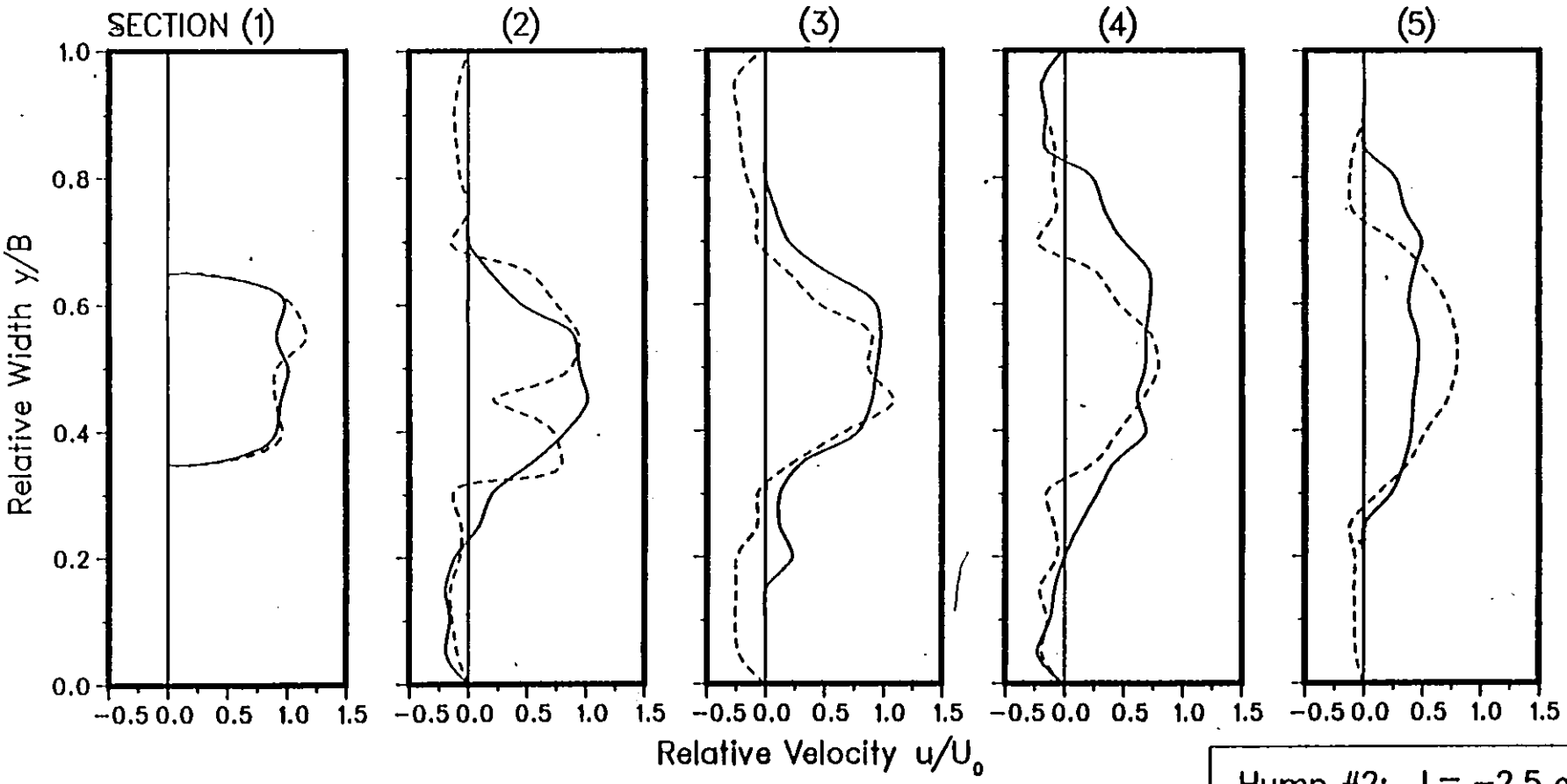

Fig.51: Comparison of Cross–Stream Distribution of Flow velocity at Five Stations Downstream of the Culvert Outlet.

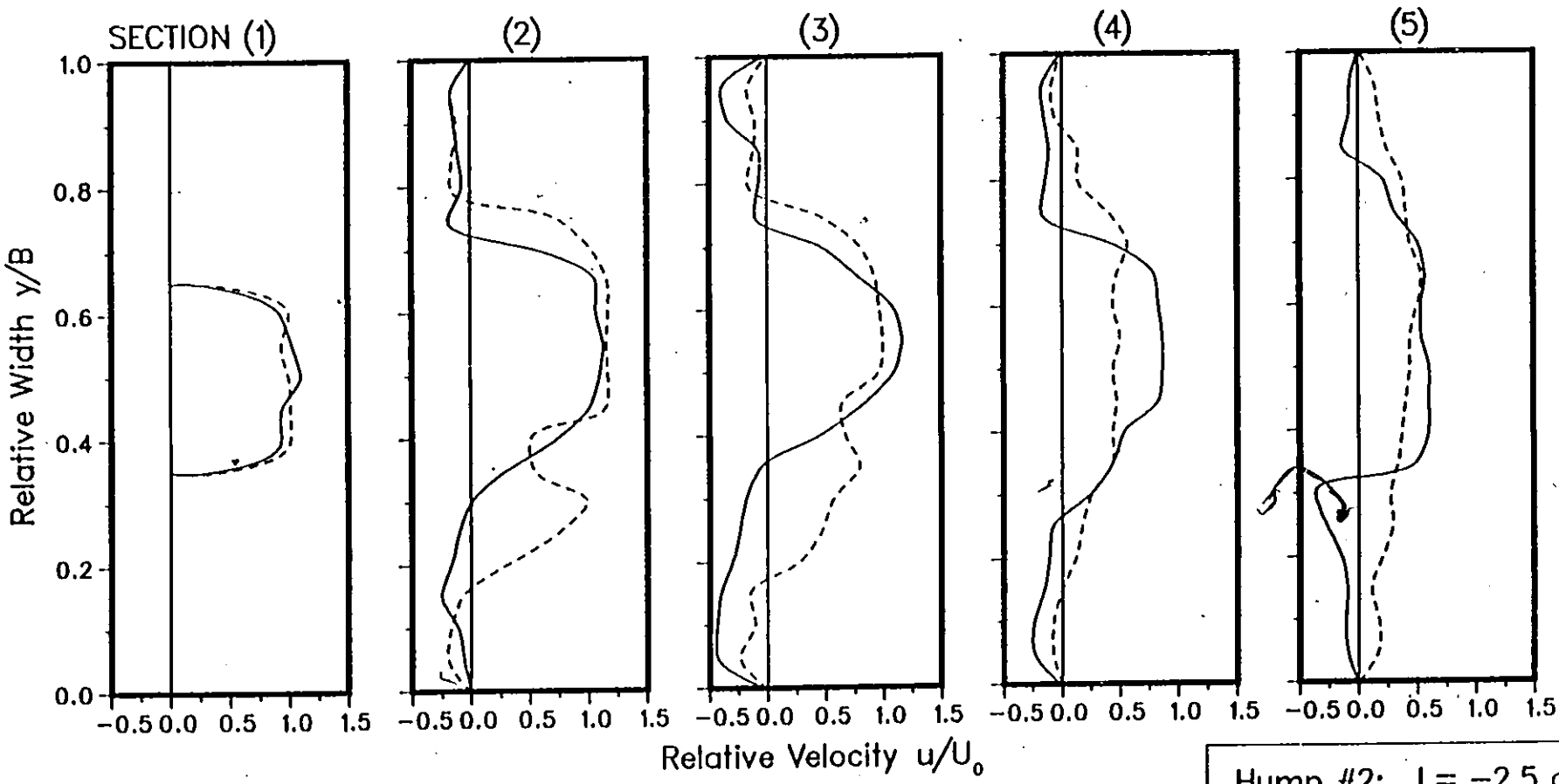

Fig.52: Comparison of Cross-Stream Distribution of Flow velocity at Five Stations Downstream of the Culvert Outlet.

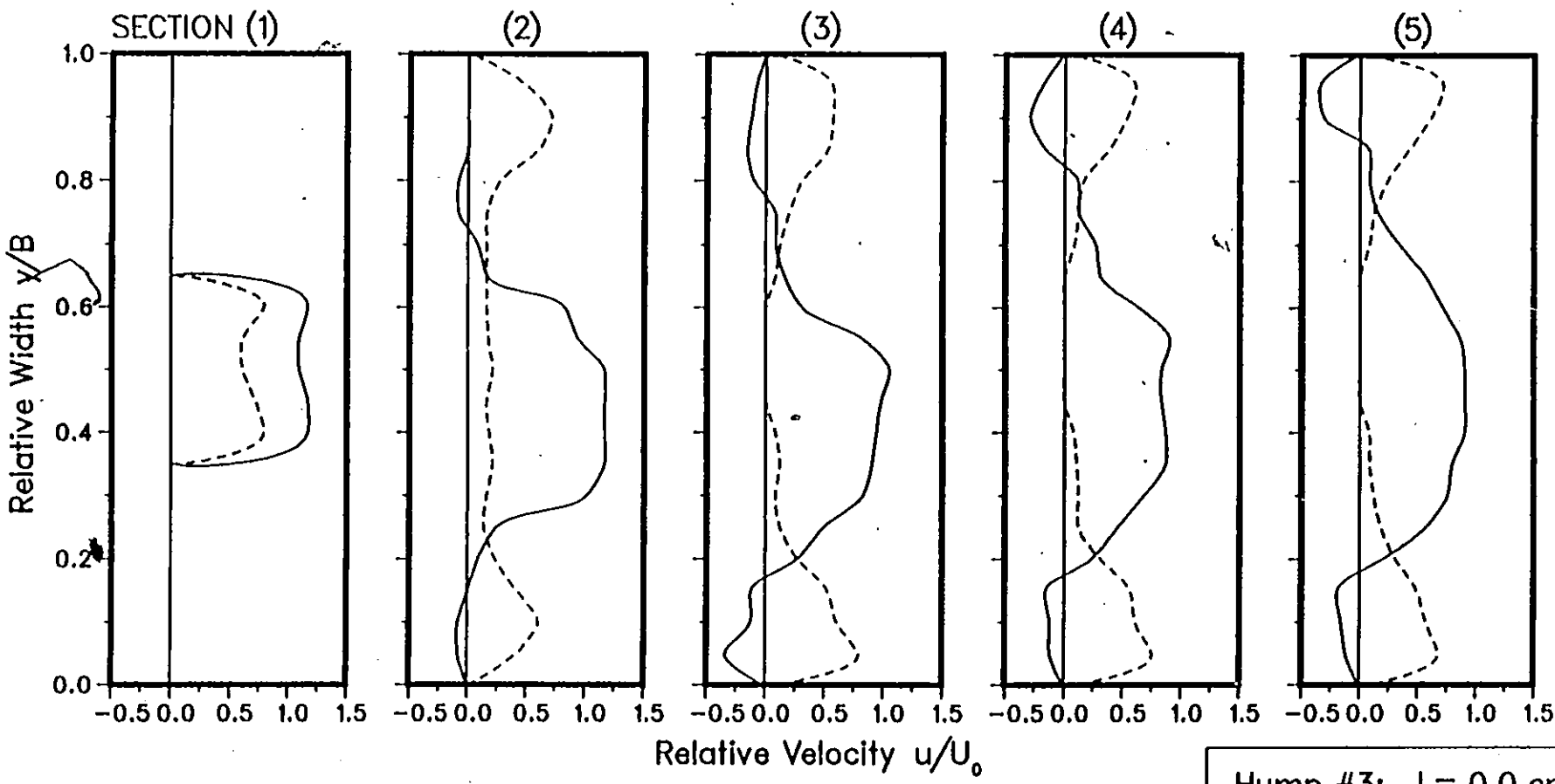

Fig.53: Comparison of Cross-Stream Distribution of Flow velocity at Five Stations Downstream of the Culvert Outlet.

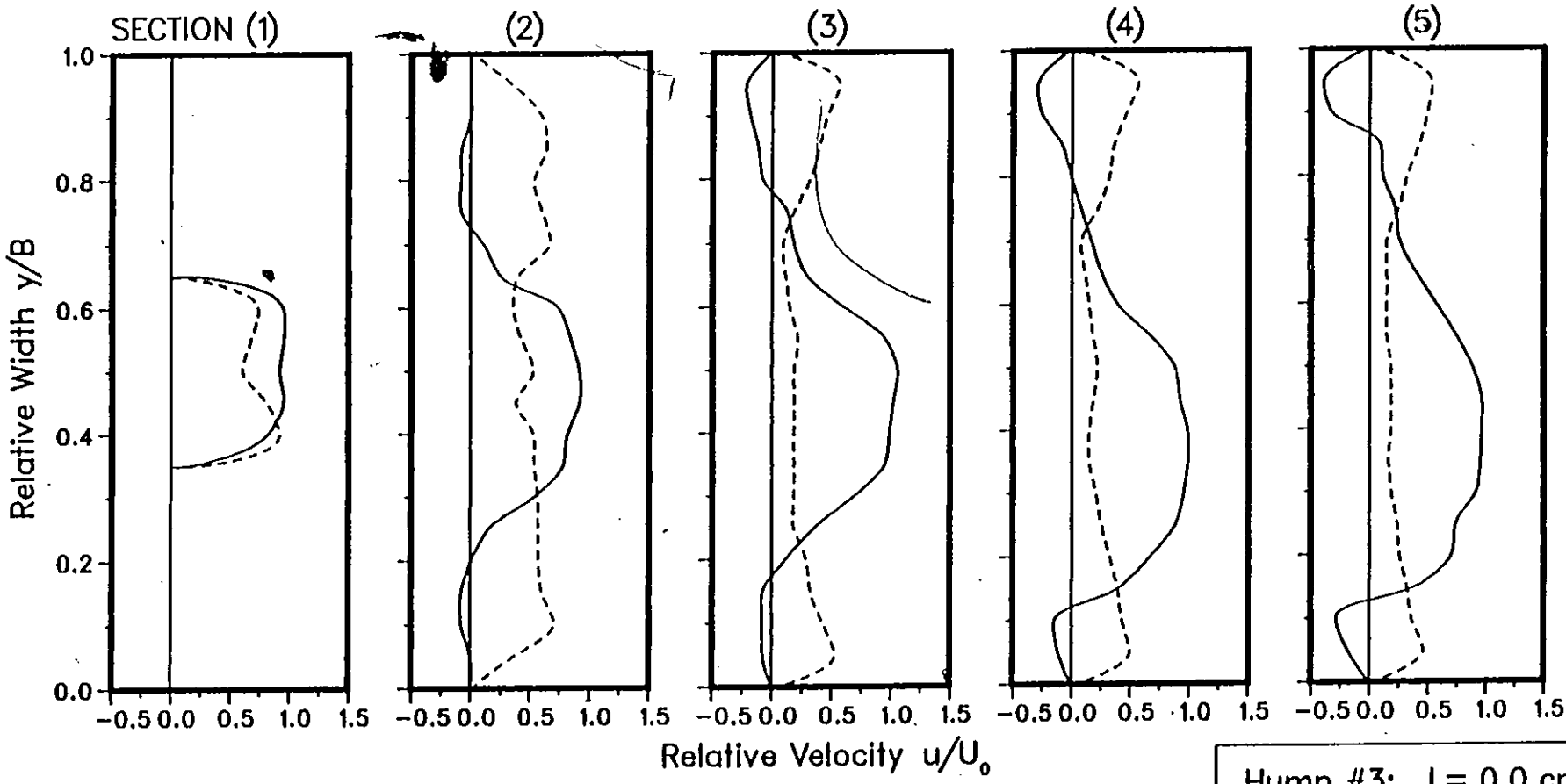

Fig.54: Comparison of Cross-Stream Distribution of Flow velocity at Five Stations Downstream of the Culvert Outlet.

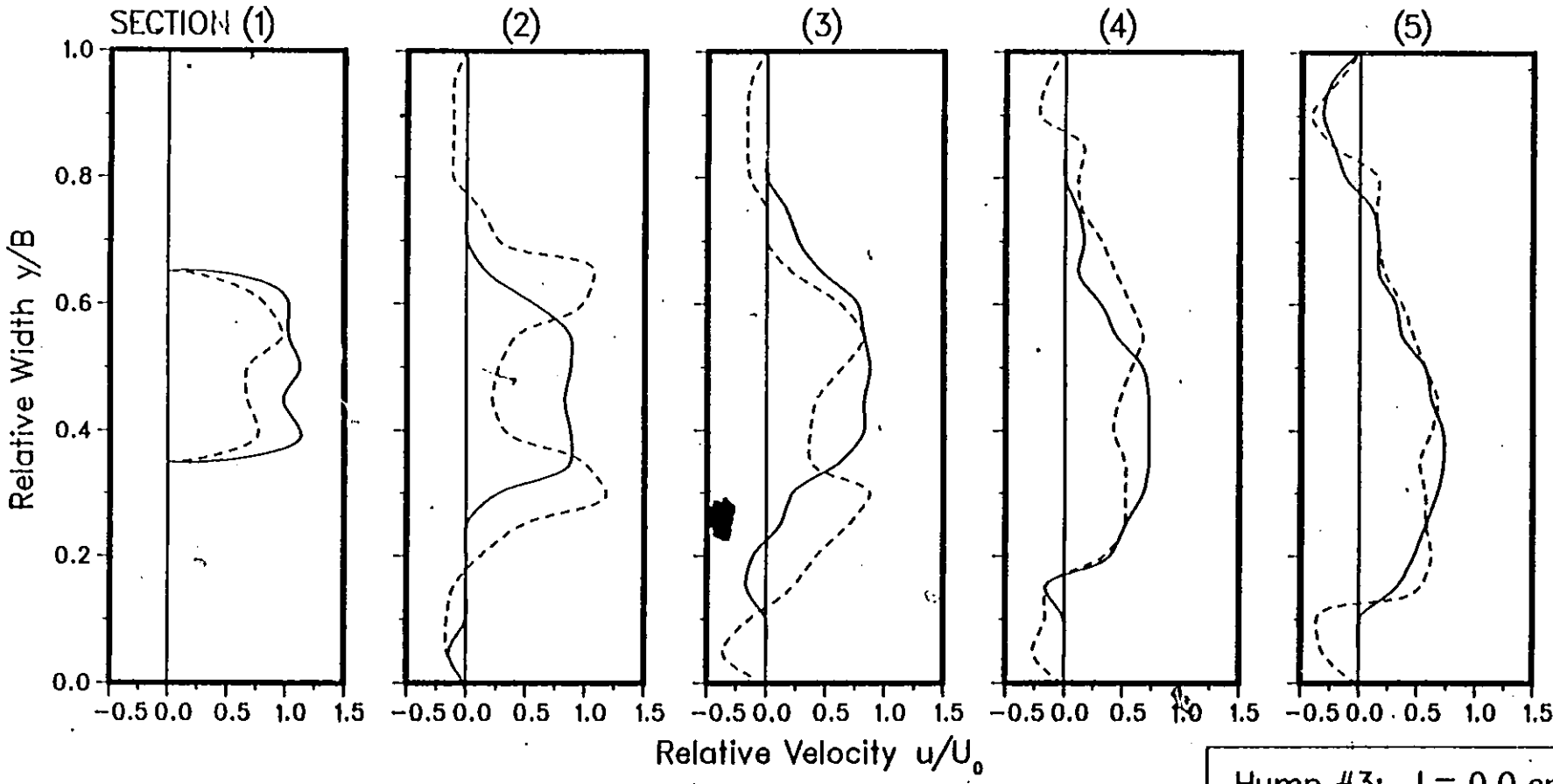

Fig.55: Comparison of Cross-Stream Distribution of Flow velocity at Five Stations Downstream of the Culvert Outlet.

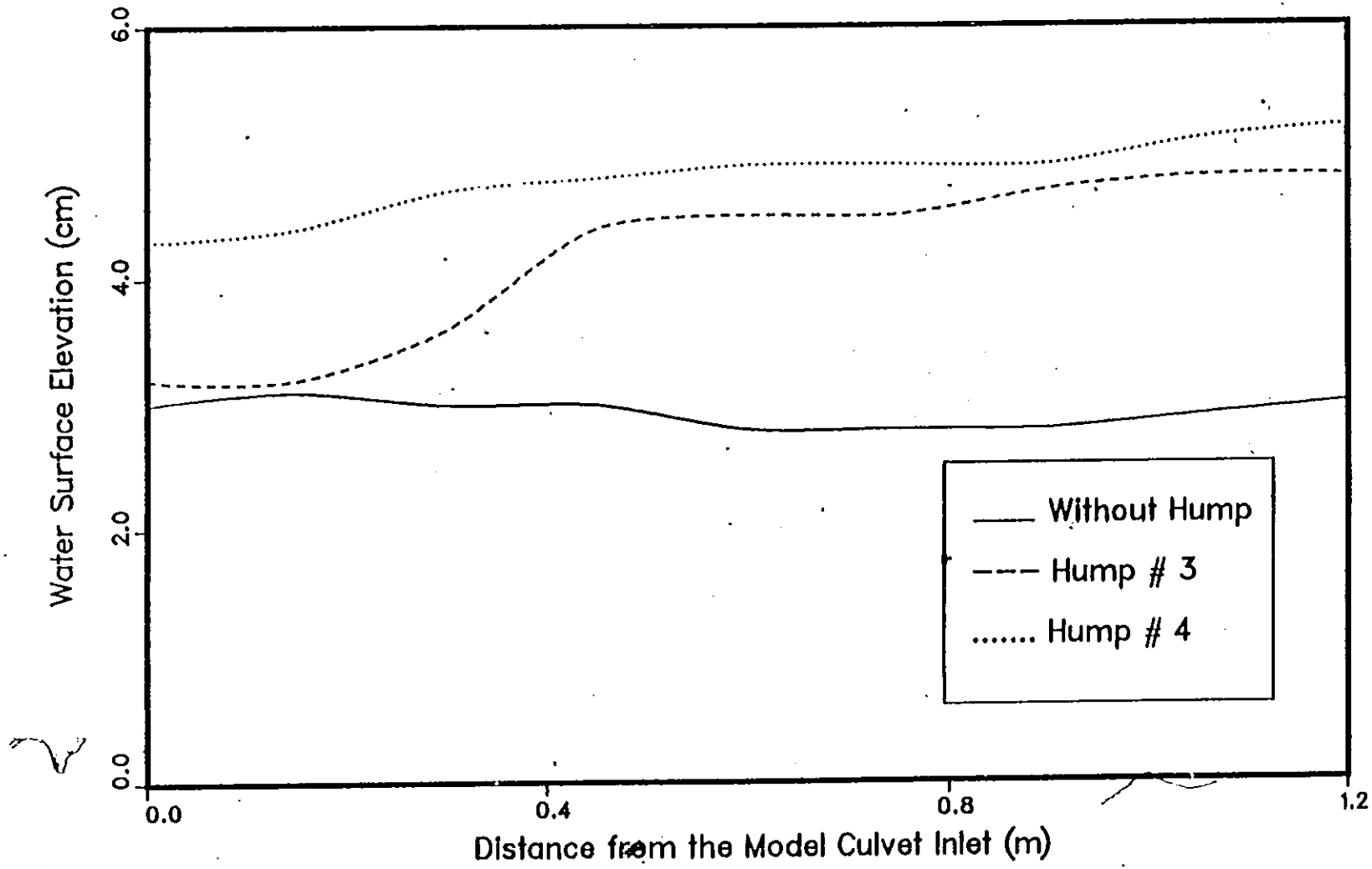

Fig.56: Water Surface Profiles Inside the Model Culvert Showing a Backwater Effect Generated Using Humps # 3 and 4.

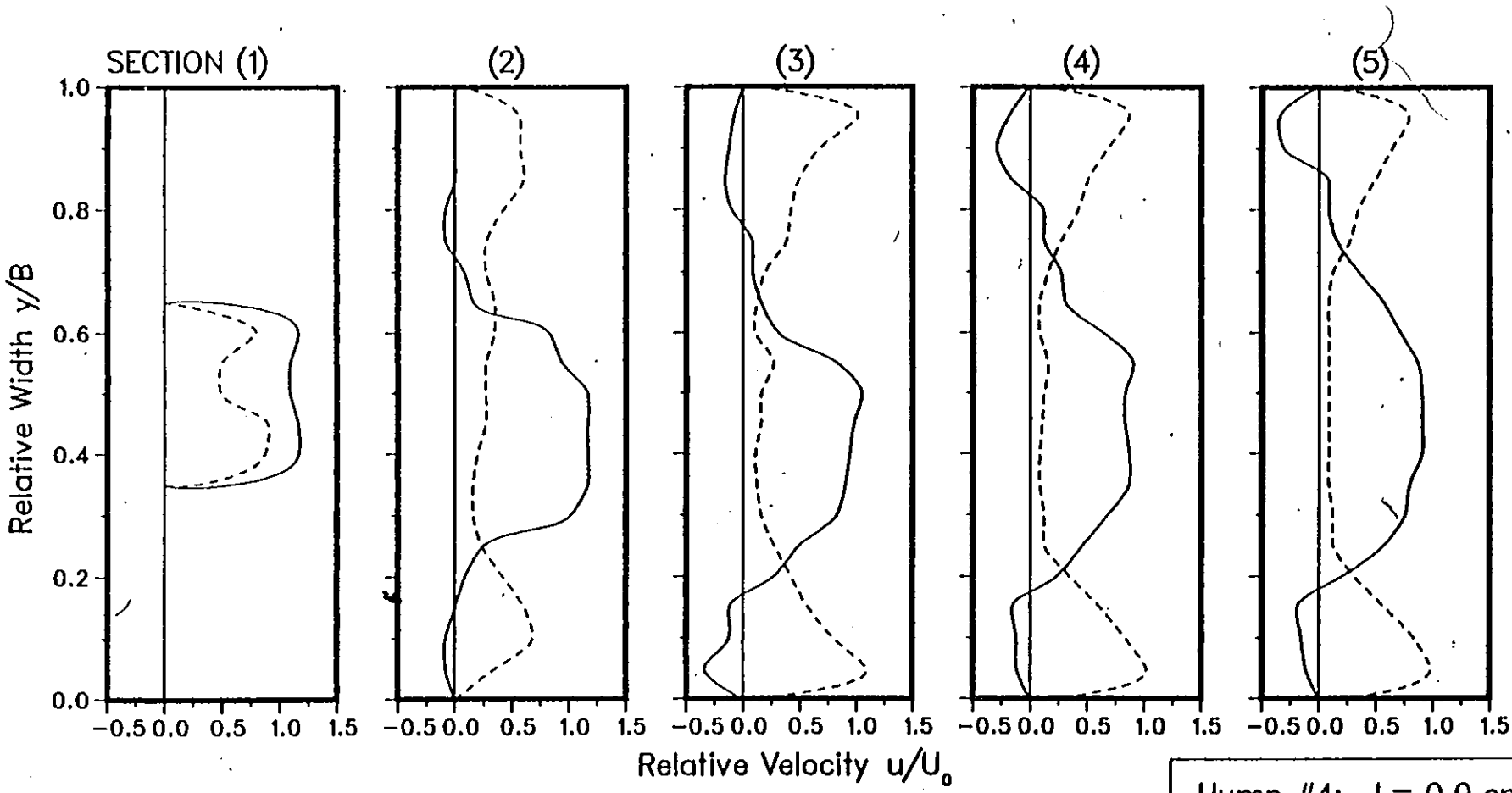

Fig.57: Comparison of Cross-Stream Distribution of Flow velocity at Five Stations Downstream of the Culvert Outlet.

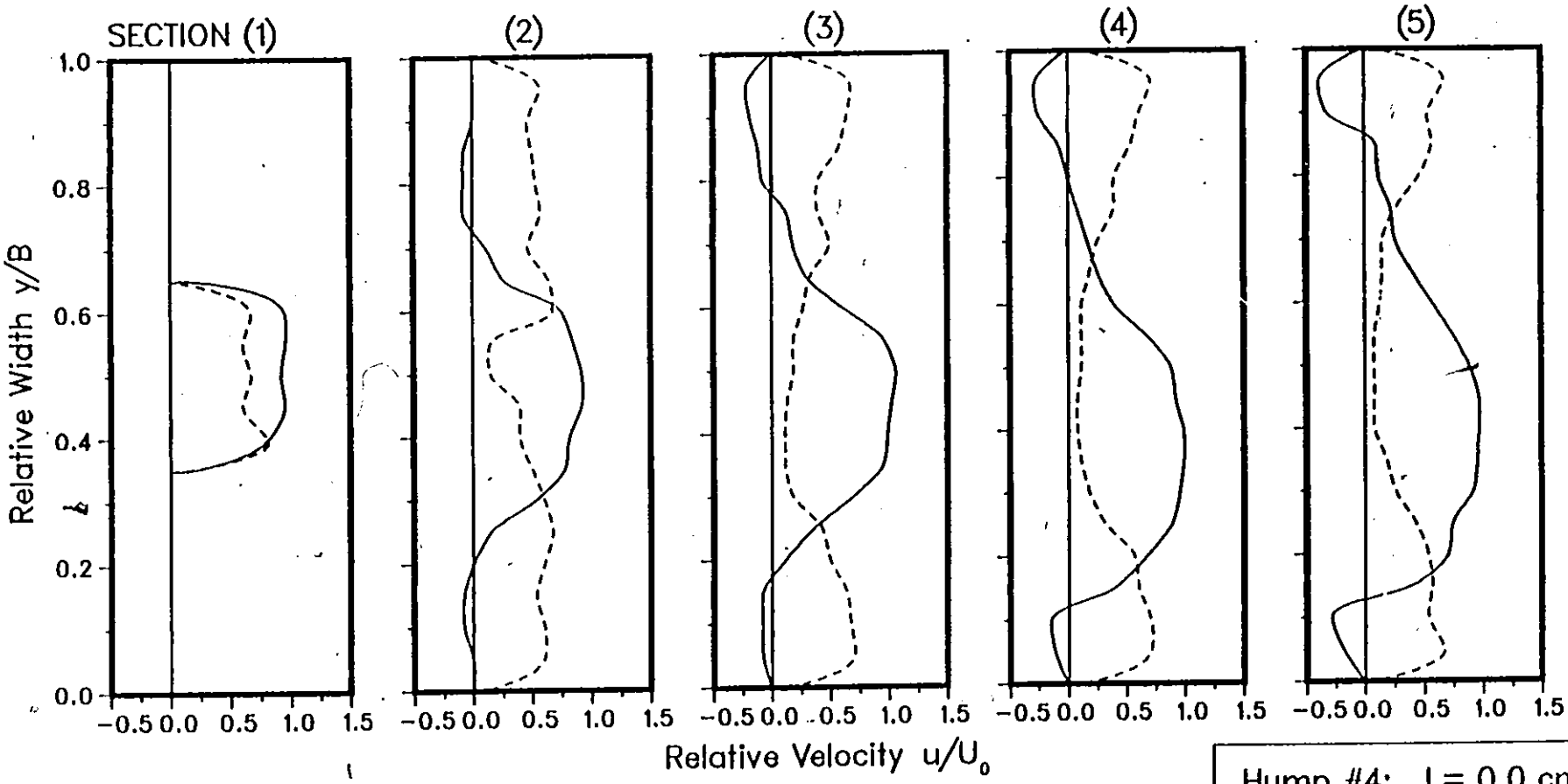

Fig.58: Comparison of Cross-Stream Distribution of Flow velocity at Five Stations Downstream of the Culvert Outlet.

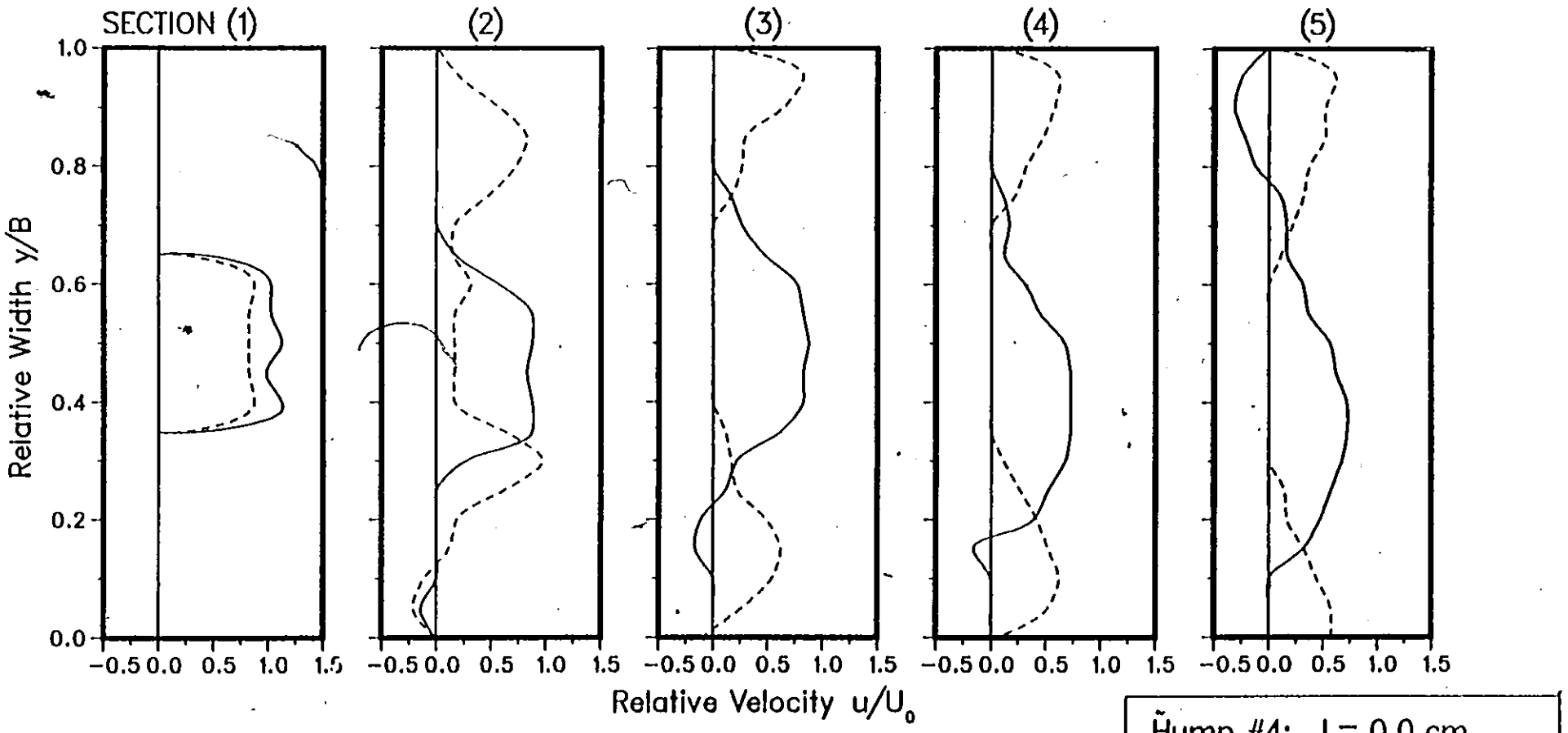

Fig.59: Comparison of Cross-Stream Distribution of Flow velocity at Five Stations Downstream of the Culvert Outlet.

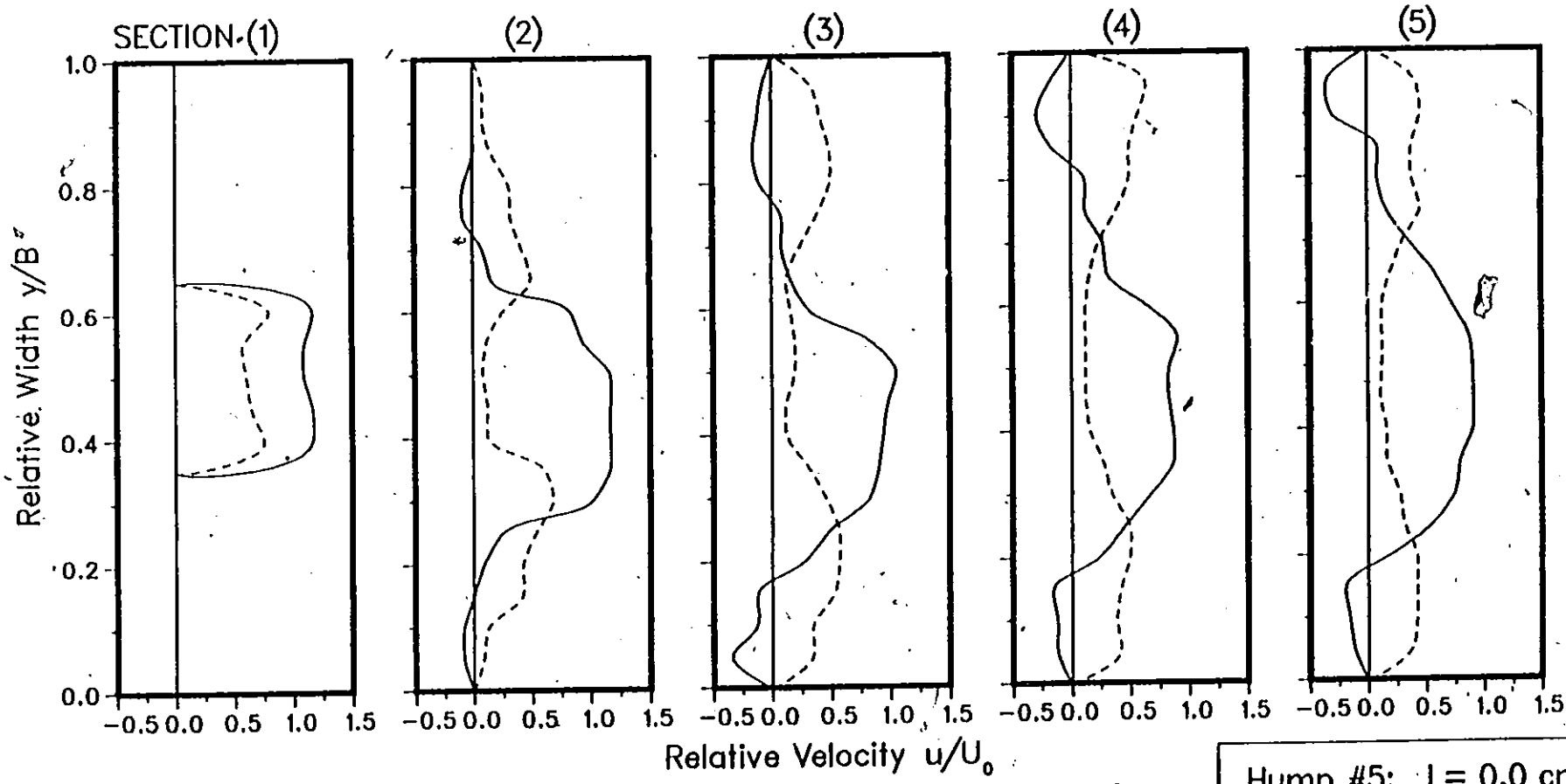

Fig.60: Comparison of Cross-Stream Distribution of Flow velocity at Five Stations Downstream of the Culvert Outlet.

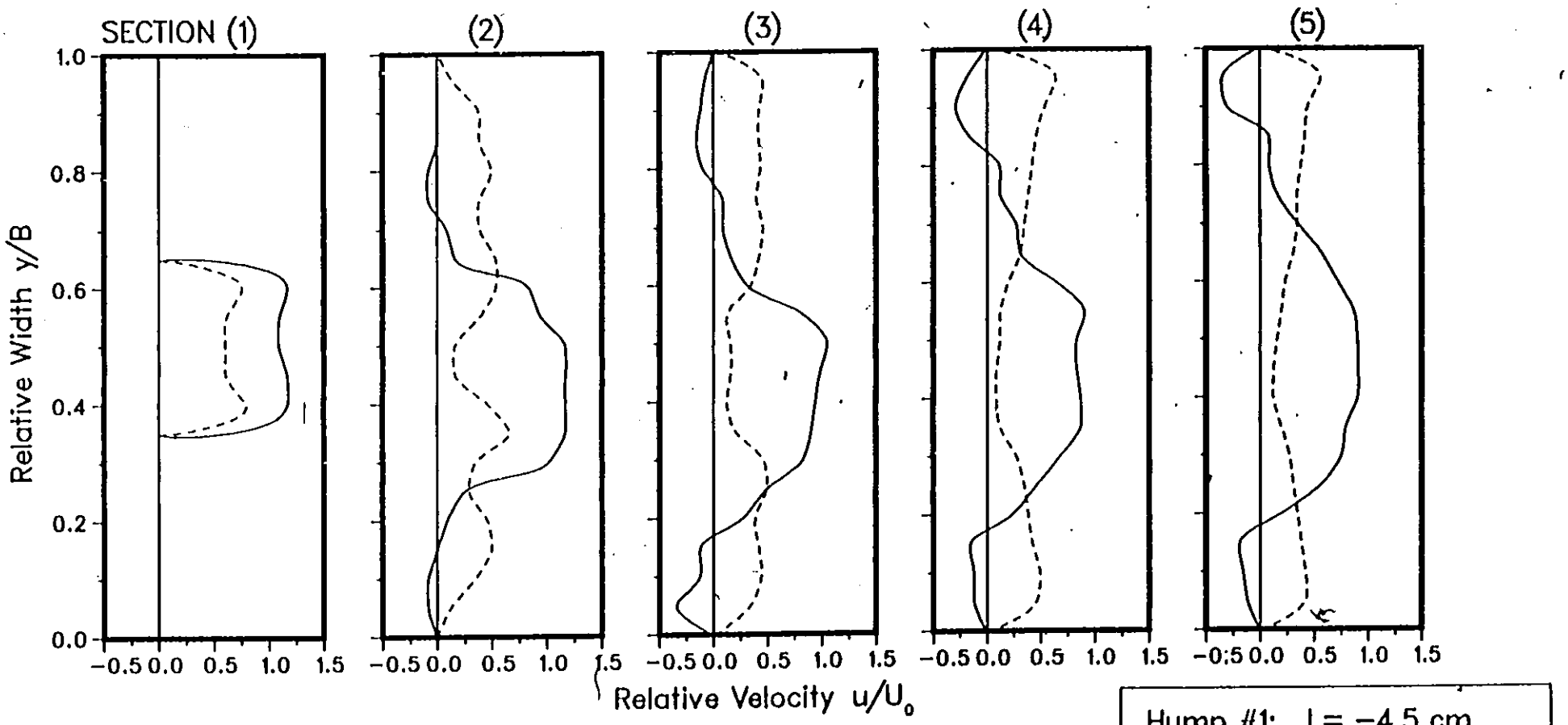

Fig.61: Comparison of Cross-Stream Distribution of Flow velocity at Five Stations Downstream of the Culvert Outlet.

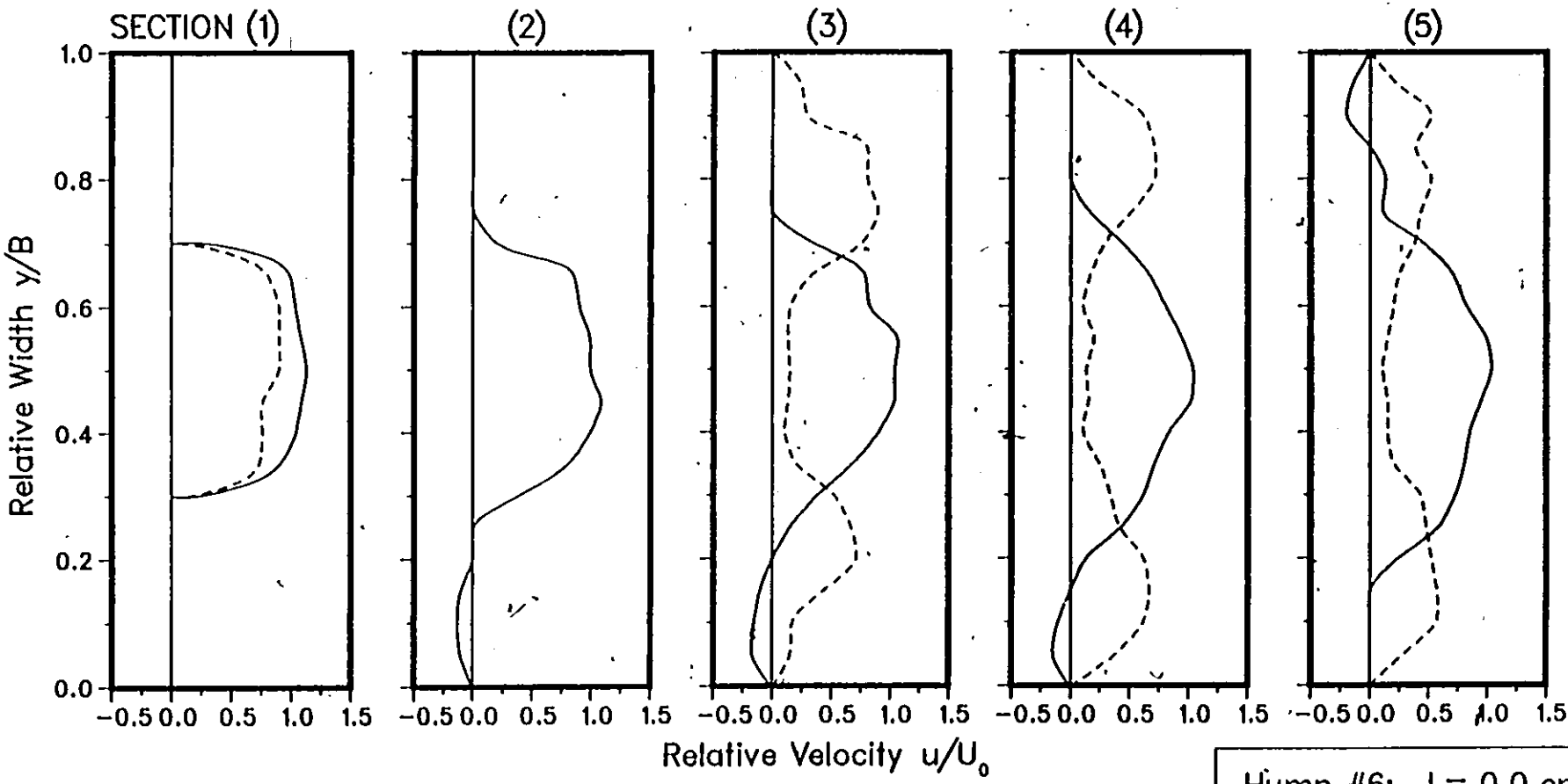

Fig.62: Comparison of Cross-Stream Distribution of Flow velocity at Five Stations Downstream of the Culvert Outlet.

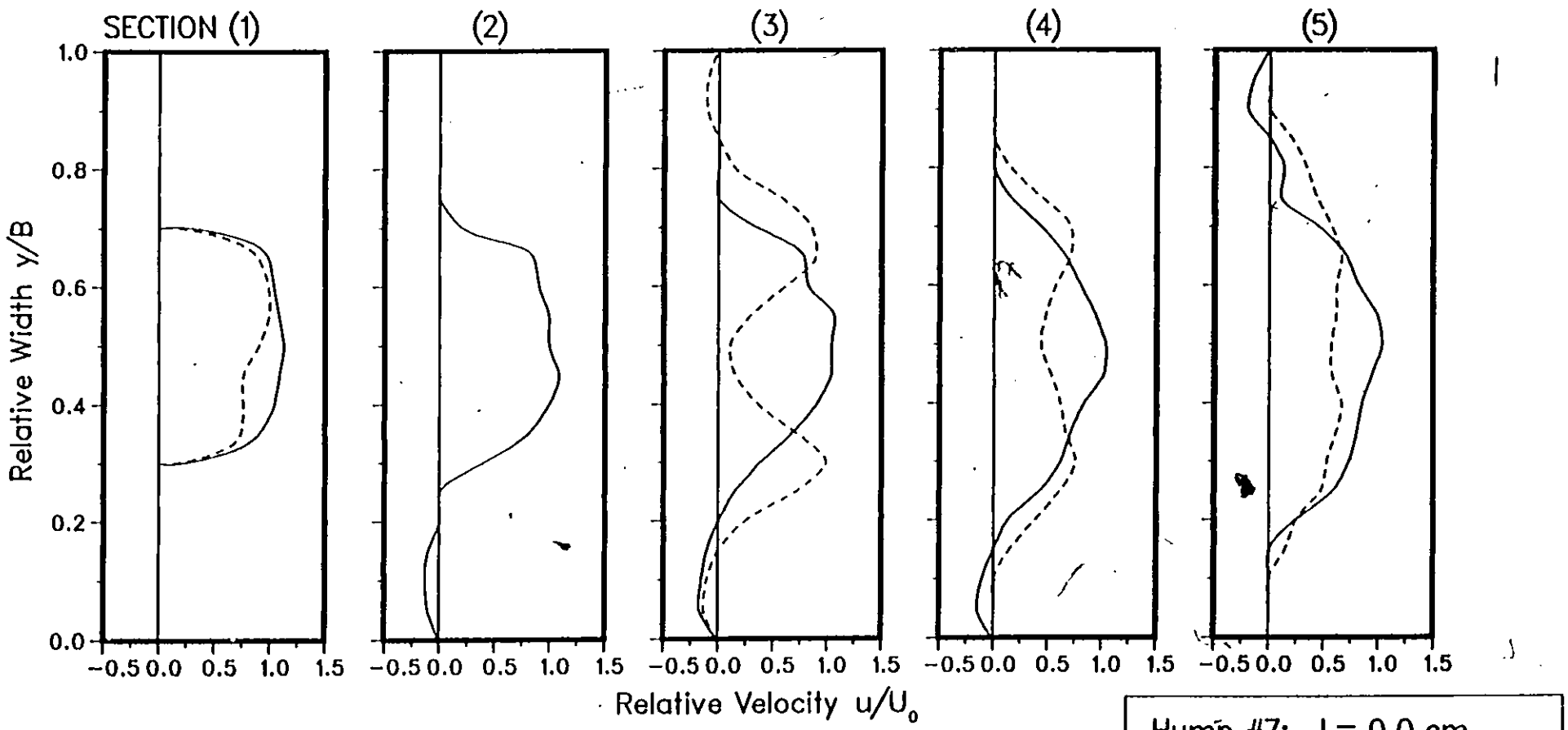

Fig.63: Comparison of Cross-Stream Distribution of Flow velocity at Five Stations Downstream of the Culvert Outlet.

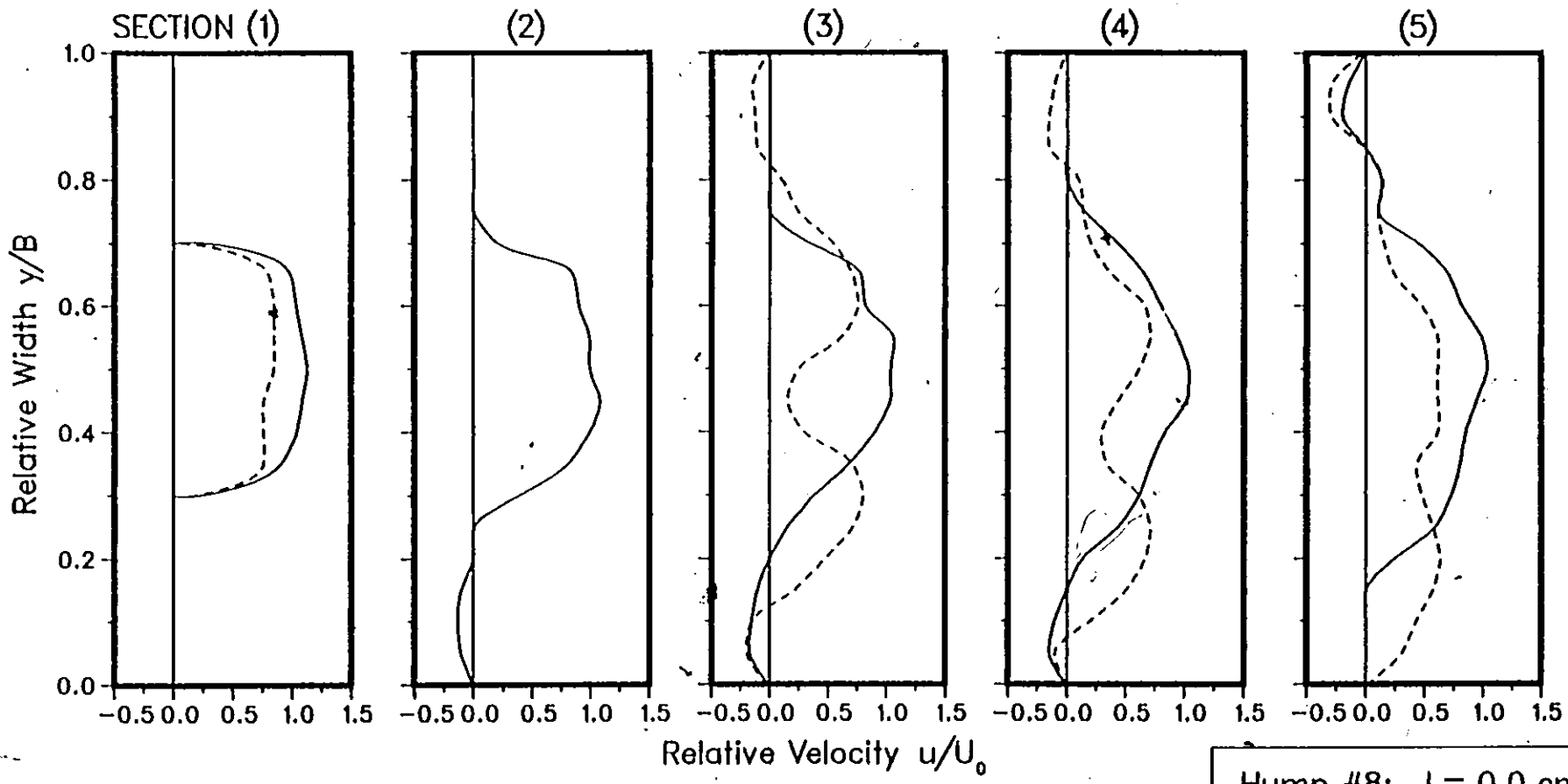

Fig.64: Comparison of Cross-Stream Distribution of Flow velocity at Five Stations Downstream of the Culvert Outlet.

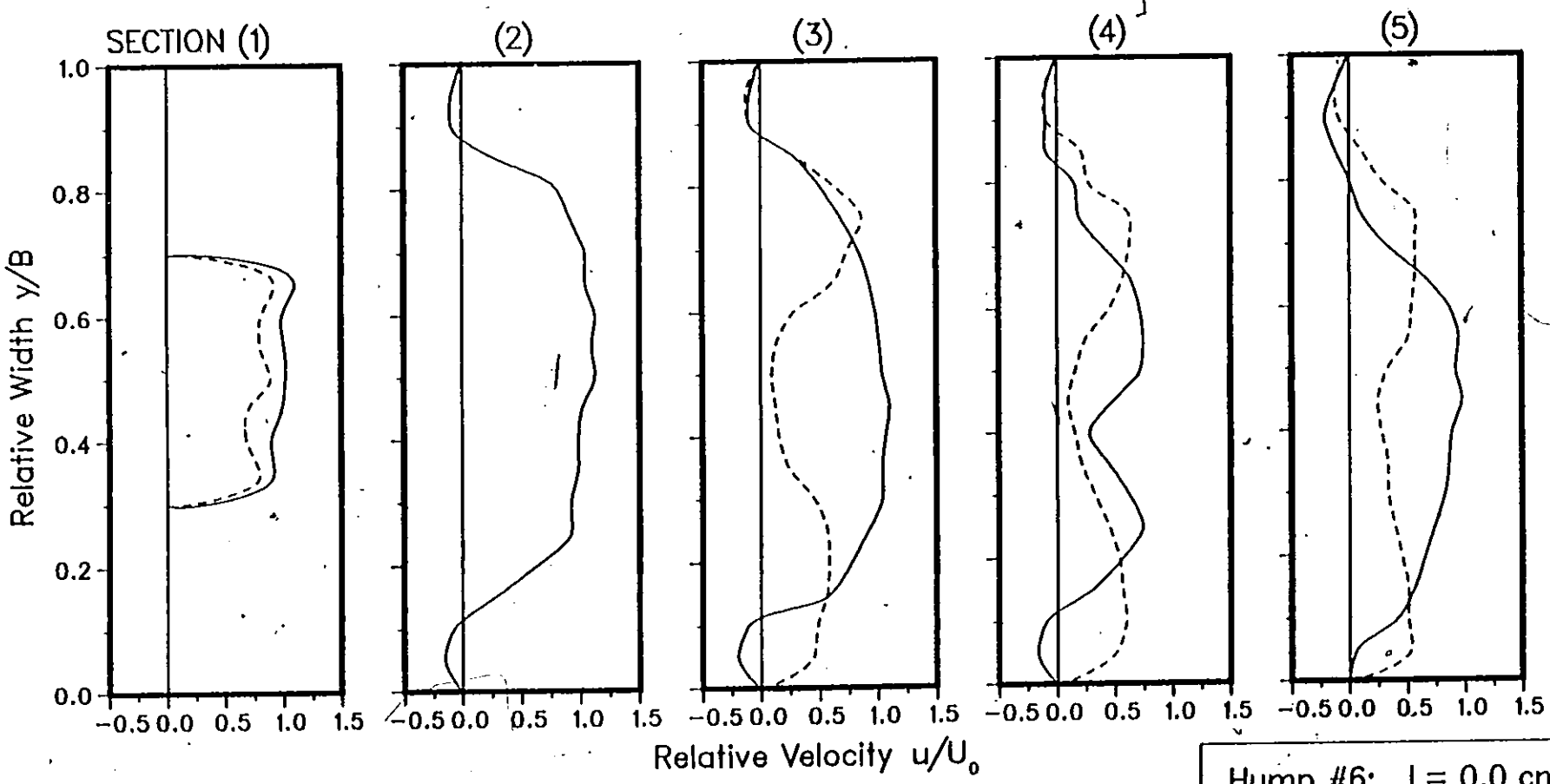

Fig.65: Comparison of Cross-Stream Distribution of Flow velocity at Five Stations Downstream of the Culvert Outlet.

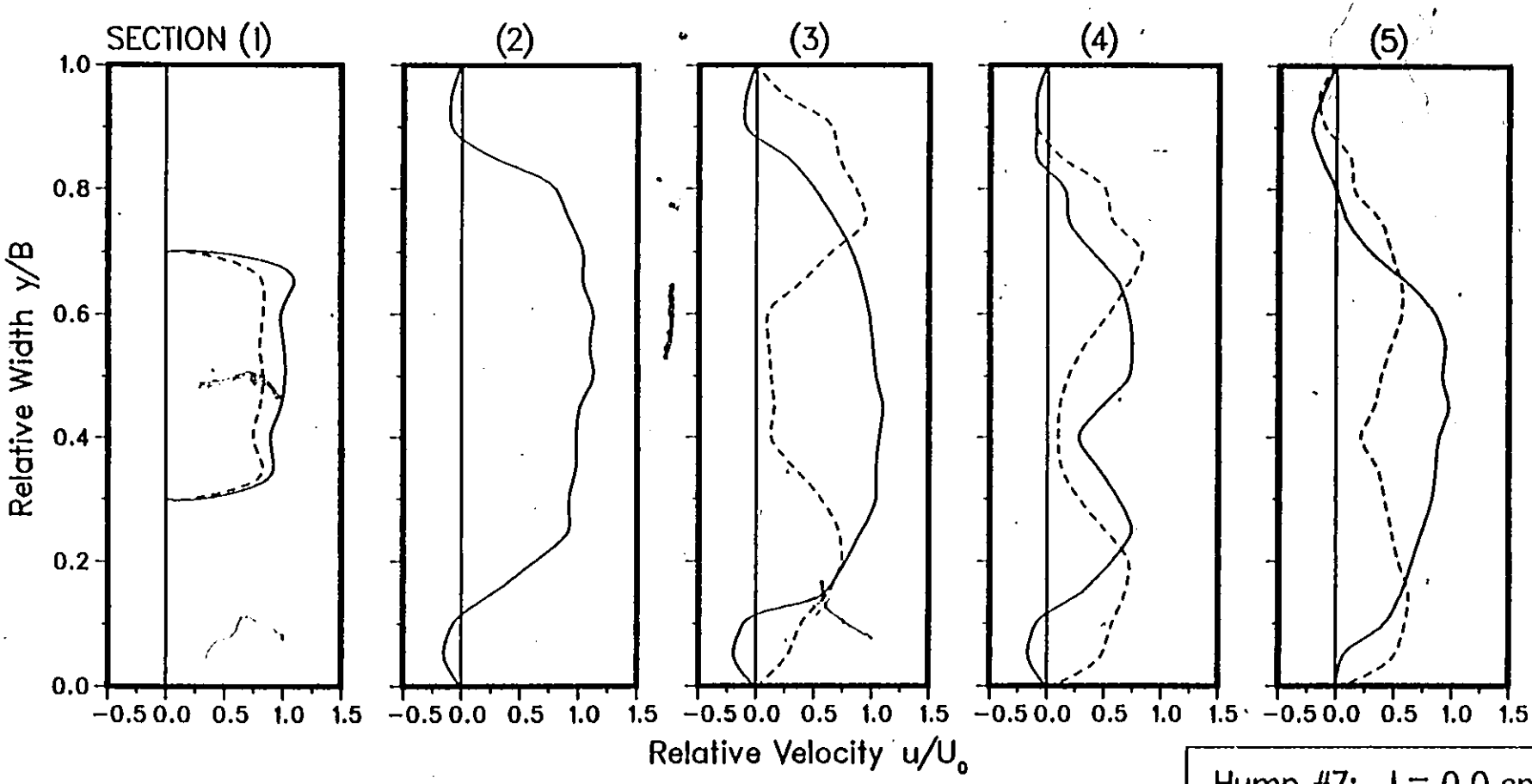

Fig.66: Comparison of Cross-Stream Distribution of Flow velocity at Five Stations Downstream of the Culvert Outlet.

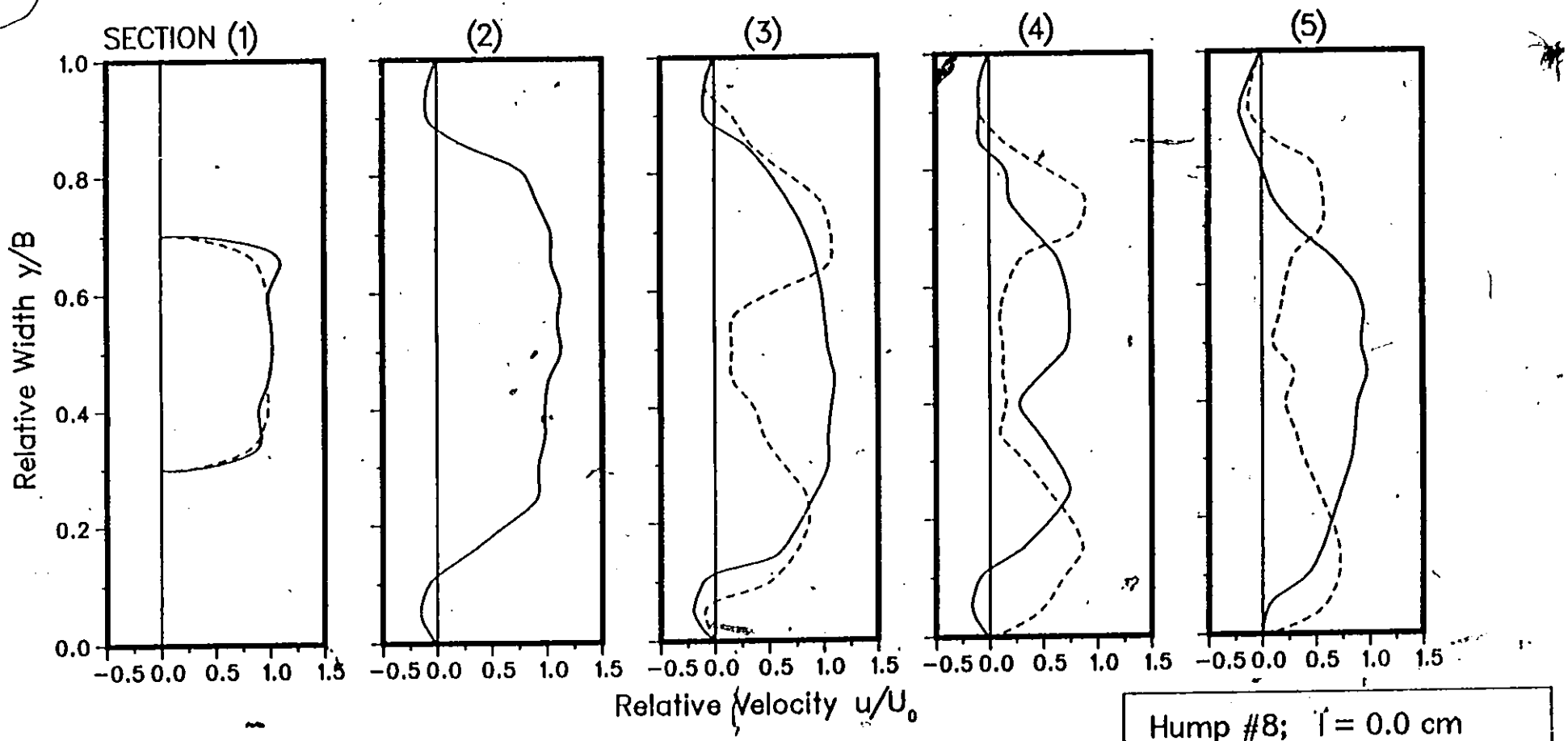

Fig.67: Comparison of Cross-Stream Distribution of Flow velocity at Five Stations Downstream of the Culvert Outlet.

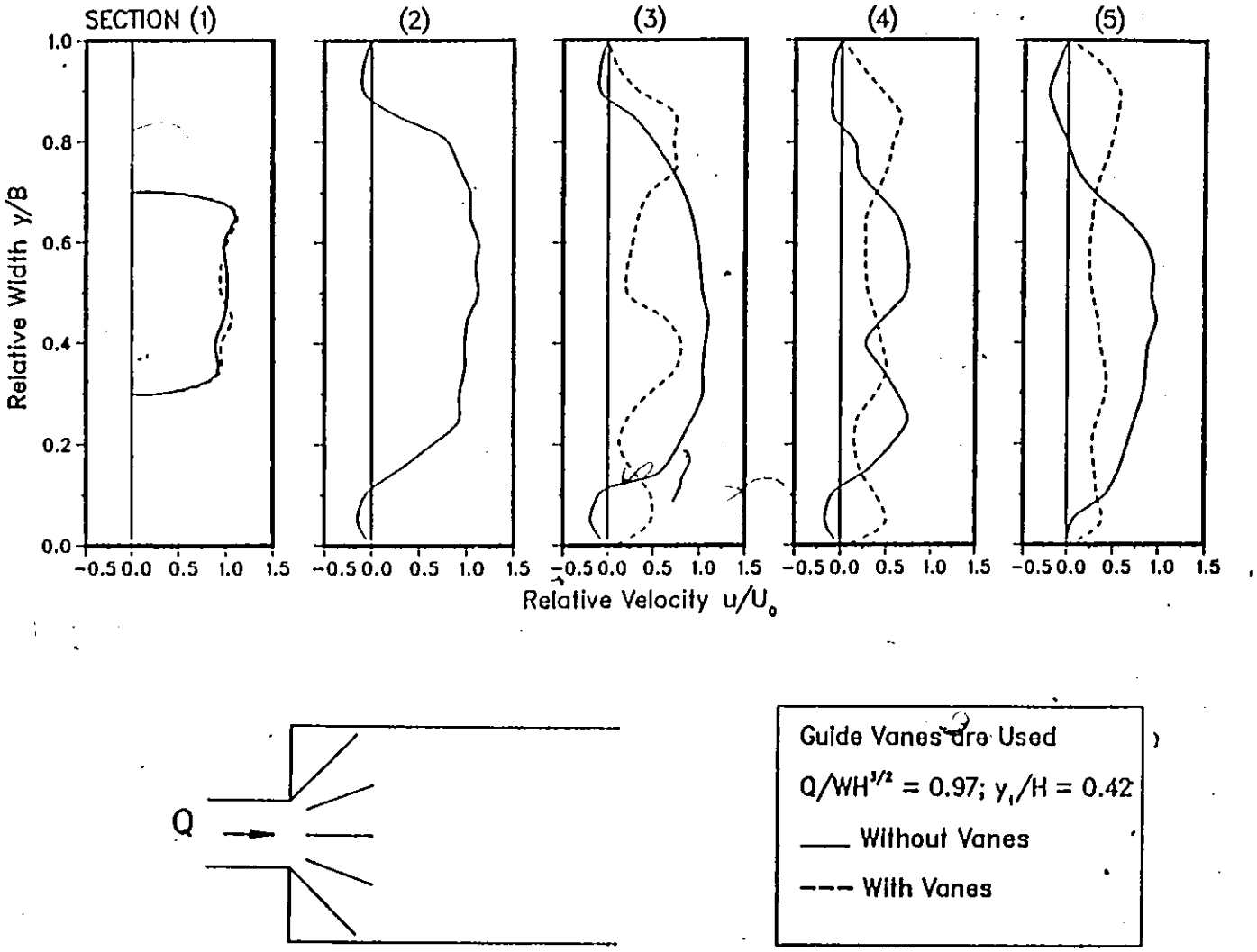

Fig.68: Comparison of Cross-Stream Distribution of Flow velocity at Five Stations Downstream of the Culvert Outlet.

APPENDIX C: NUMERICAL EXAMPLE

Numerical Example

1. Data:

Culvert width	W	=	2.0 m
Downstream channel width	B	=	6.0 m
Culvert height	H	=	2.0 m
Length of barrel	L	=	20.0 m
Discharge	Q	=	5.0 m^3/s
Tailwater depth	y_t	=	1.0 m
Slope	s	=	0.005
Effective grain size	d_m	=	0.5 mm

2. Assumptions:

- Outlet control
- Flow is subcritical

3. Scour depth computation

Use the equation developed in this study to predict scour depth in sand beds:

$$\frac{d_s}{H} = \left(\exp\left(\frac{F_r - 2}{2.03}\right) - 0.373\right)\left(\frac{d_m}{H}\right)^{-0.275} \qquad (0.1)$$

where $F_r = \frac{U_0}{\sqrt{gy_t}}$.

Velocity at culvert outlet $U_0 = \frac{Q}{Wy_t} = 2.5m/s$. Therefore $F_r = \frac{2.5}{\sqrt{9.811.0}} = 0.8$ and $\frac{d_s}{H} = 1.75$.

Note that almost the same value can also be obtained using Fig. 10 by interpolation where $\frac{Q}{wH^{\frac{5}{2}}} = 0.88$ and $\frac{y_t}{H} = 0.5$. Thus the scour depth is $d_s = 2 \times 1.75 = 3.5m$. This would imply that severe scour hole development occurs because of the concentrated jet-type flow issuing from the culvert structure. Scour control measures are therefore required in order to minimize the severity of scour. 4. Hump design:

- Hump height $h = 0.8 \times y_t = 0.8m$
- Take hump width = culvert width $= 2.0m$
- Hump location: For optimum hydraulic performance the hump should be placed immediately downstream of the culvert barrel (i.e $l = 0$).
- Hump leading length: Based on the experimental data, hump # 5 performed best when placed immediately downstream of the culvert barrel. This hump had an $\frac{h}{a_1}$ slope of 1V : 2H.

Since the hump height $h = 0.8m$, then $a_1 = 2 \times h = 1.6m$. Take a total hump length of $2 \times a_1 = 3.2m$. 5. Summary of design

- Hump height $h = 0.8m$.

- Hump width $w_h = 2.0m$.
- Hump leading length $a_1 = 1.6m$.
- Hump location: immediately downstream of the culvert barrel.

6. Cost First cost estimation of the common rip rap protection (without hump) will be performed and this will then be compared with the corresponding cos with the hump in place.

The design of "rip-rap" protection is based on the Ontario Ministry of Transport and Communication (1982).

the rip-rap median grain size :

$$d_50 = \left(\frac{0.035H^2}{y_t}\right)\left(\frac{Q}{WH^{1.5}}\right)^{1.333} = 0.12m \qquad (0.2)$$

Rip rap thickness is $2 \times d_50 = 0.24m$ say $0.25m$.

Length of "rip-rap" $L_r = 5 \times H = 10.0m$

Volume of rip-rap required on the channel bed is therefore: $10 \times 6 \times 0.25 = 15m^3$.

"Rip-rap" protection at channel banks : $2\left(\frac{H \times L_r}{2}\right) \times 0.25 = 5.0m^3$.

Thus, the total amount of rip-rap required is $15.0 + 5.0 = 20m^3$.

An average cost of "rip-rap" material is assumed to be \$ 30/m^3, which yields a total cost of \$ 600.

Now, based on the hump geometric dimensions, the latter volume was found to be roughly 2.0m^3. As was mentioned earlier in this study, even with the hump in place, "rip-rap" protection of the region just downstream of the culvert barrel is still required. Therefore the total amount of "rip-rap" required (including the hump) is: $2.0 + (2 \times 2 \times 6)(0.25) = 13m^3$ and the total cost is approximately \$ 400.

This cost is lower than that of the traditional "rip-rap" protection provided the hump is formed of stone material rather than concrete which is very expensive.